June 1982

MTR8701

George Berk
Paul N. Jean
Ersch Rotholz

Final Technical Report

On-Board Processing for Future Satellite Communications Systems: Comparison of FDM, TDM, and Hybrid Accessing Schemes

MITRE
Bedford, Massachusetts

June 1982

MTR8701

George Berk
Paul N. Jean
Ersch Rotholz

Final Technical Report

On-Board Processing for Future Satellite Communications Systems: Comparison of FDM, TDM, and Hybrid Accessing Schemes

CONTRACT SPONSOR NASA/LeRC
CONTRACT NO. F19628-82-C-0001
PROJECT NO. 8680
DEPT. D-97

MITRE
The MITRE Corporation
Bedford, Massachusetts

Department Approval: W. T. Brandon
R. Alan

MITRE Project Approval: W. T. Brandon
W. T. Brandon

1. Report No.	2. Government Accession No.	3. Recipient's Catalog No.
NASA/LeRC CR-167931		

4. Title and Subtitle	5. Report Date
FINAL TECHNICAL REPORT On Board Processing for Future Satellite Communications Systems: Comparison of FDM, TDM and Hybrid Accessing Schemes	June 1982
	6. Performing Organization Code
7. Author(s) George Berk, Paul N. Jean, Ersch Rotholz	8. Performing Organization Report No. MTR 8701
	10. Work Unit No.
9. Performing Organization Name and Address The MITRE Corporation P.O. Box 208 Bedford, MA 01730	11. Contract or Grant No. F19628-82-C-0001
	13. Type of Report and Period Covered Contractor Report
12. Sponsoring Agency Name and Address National Auronautics and Space ADM Lewis Research Center Cleveland, Ohio 44135	14. Sponsoring Agency Code

15. Supplementary Notes

Project Manager, David Culp, NASA Lewis Research Center, Cleveland, Ohio

16. Abstract

This report compares several satellite uplink and downlink accessing schemes for Customer Premises Service. Four conceptual system designs are presented: Satellite-Routed FDMA, Satellite-Switched TDMA, Processor-Routed TDMA, and Frequency-Routed TDMA, operating in the 30/20 GHz band. The designs are compared on the basis of estimated satellite weight, system capacity, power consumption, and cost. The systems are analyzed for fixed multibeam coverage of CONUS. Analysis shows that the system capacity is limited by the available satellite resources and by the terminal size and cost.

17. Key Words (Suggested by Author(s))	18. Distribution Statement
• Satellite Communications • 30/20 GHz EHF band • on-board processing • satellite routed FDMA • processor routed TDMA • frequency-rocked TDMA • satellite-switched TDMA	Unclassified - Unlimited

19. Security Classif. (of this report)	20. Security Classif. (of this page)	21. No. of Pages	22. Price*
Unclassified	Unclassified	193	

* For sale by the National Technical Information Service, Springfield, Virginia 22161

Page Intentionally Left Blank

TABLE OF CONTENTS

TABLE OF CONTENTS (Continued)

TABLE OF CONTENTS (Concluded)

LIST OF ILLUSTRATIONS

LIST OF ILLUSTRATIONS (Concluded)

LIST OF TABLES

LIST OF TABLES (Concluded)

SECTION 1

EXECUTIVE SUMMARY

Satellite communications systems for customer premise service (CPS) are compared. Certain baseline assumptions, common to all systems, are made. The systems use multiple fixed-beam coverage. These beams must cover most of continental United States (CONUS). In order to utilize the satellite DC power efficiently, the beams must have high gain. High-gain beams have limited coverage; therefore, a large number of beams are needed for CONUS coverage. To limit the number of beams and still furnish sufficient coverage, two beam sizes were selected. Twenty-two spot beams of 0.35° beamwidth illuminate the major metropolitan centers. Ten area beams of 0.7° beamwidth illuminate rural areas. Those CPS users that are in the 0.35° beams are called metropolitan CPS (or CPS_1) users and those that are in the 0.7° beams are called rural CPS (or CPS_2) users. It is assumed that the metropolitan traffic is uniformly distributed among the 22 metropolitan beams. Similarly, the rural traffic is uniformly distributed among the 10 rural beams. Although this assumption is not realistic, it is sufficient for a simple comparison between systems. It is assumed that technology restricts the weight and power consumption of the satellite to less than 5000 lb and 5000 W, respectively. To keep the terminal cost low and avoid expensive satellite tracking systems, the terminal antenna must not be larger than 3 m. For cost reasons, the terminal system noise temperature is set at 1000 K.

By definition, the satellite systems must operate in the 20/30 GHz band. Some key technology for the 20/30 GHz band is either in the development stage or does not exist. A survey of major United States manufacturers was conducted for this report. While antenna dishes are readily available, dual-frequency feed systems need further development. Space qualified traveling wave tube (TWT) and solid-state power amplifiers at 20 GHz are in the development stage. High-power (above 5 W) TWT and lower-power (above 2 W) solid-state amplifiers at 30 GHz (for earth terminal transmitters) are available only as laboratory models. Low-noise amplifiers at 30 GHz do not exist. Some laboratory models at 20 GHz have been developed. Modems for a bit rate exceeding 30 megabits per second (Mb/s) are not commercially manufactured in this country, although technology for the manufacture of such modems probably exists. The survey showed that, with current technology, the cost of radio frequency (RF) subsystems (transmitters, up- and down-converters, and antennas) at 30/20 GHz is very high.

The restrictions imposed by the baseline assumptions, like satellite DC power, antenna gain, terminal noise figure, and antenna size, limit the system capacity. Efficient utilization of the available resources depends on the accessing mode for the CPS and trunking services. The relation between satellite DC power and system throughput is derived for several combinations of accessing modes. Although certain combinations of accessing modes provide efficient utilization of the satellite DC power, they appear to involve a complex satellite design and for this reason are excluded from further considerations. Four representative access modes for CPS service are selected on the basis of feasibility and high throughput capacity: Satellite-Routed Frequency Division Multiple Access (SR-FDMA), Satellite-Switched Time Division Multiple Access (SS-TDMA), Processor-Routed TDMA (PR-TDMA), and Frequency-Routed TDMA (FR-TDMA). The preferred mode for the trunking service is Satellite-Switched TDMA (SS-TDMA).

In the SR-FDMA system, routing is accomplished by frequency assignment and filtering in the satellite with no on-board processing. This system employs low data rate and terminals of moderate complexity. However, it supports the lowest throughput, since the satellite TWT amplifier operates at backoff and the uplink noise adds to the downlink noise.

The SS-TDMA system requires a fairly complex satellite. Only those CPS_1 users that experience rain are processed and routed at baseband. Most of the CPS_1 users are switched to a destination beam and downlink carrier by means of a microwave matrix. All CPS_2 users are processed and then switched to their destination beams. In addition to processing, these users employ one-half the CPS_1 burst rate; therefore, they use the same terminal power as the CPS_1 users. Those CPS_2 users that experience rain attenuation are processed, decoded, and encoded in soft-decision demodulators. The SS-TDMA supports large throughput with less weight and satellite power than the other processing satellites.

The PR-TDMA system requires a very complex satellite. The routing is achieved in a baseband processor. This system supports the largest throughput; however, it employs the heaviest satellite and the most expensive terminals. Although the PR-TDMA system offers flexibility, full processing for all users, and adaptive coding, it is not economical for small users.

The FR-TDMA system uses 32 carriers for routing. The routing is straightforward and does not require memory or switching

matrices. The large number of carriers results in a very low burst rate and relatively low-cost earth terminals. However, the large number of carriers requires a very large number of processing devices. This system ranks second in cost efficiency.

To reduce the cost for the CPS users, a trunking transponder is placed on-board the CPS satellite. The trunking system employs a single carrier in every beam. The routing is provided by a microwave switching matrix. The trunking service uses some of the CPS_1 beams and consumes a small proportion of the satellite resources.

The system cost for the four CPS designs is estimated with a simple cost model. The trunking cost is not evaluated. In a cost-efficient system, the terminal cost per voice channel must be a fraction of the satellite cost per voice channel. The satellite cost per voice channel determines the number of voice channels that are supported economically by a terminal.

The SR-FDMA has the lowest system cost, but also the lowest throughput. The system cost per voice channel is the highest of the four systems.

The SS-TDMA is the most cost-efficient system per voice channel because of partial processing in the satellite (relatively low-cost satellite), coupled with a high system throughput.

The PR-TDMA is not cost efficient because of a complex full-processing satellite and high downlink burst rate (high terminal cost).

The FR-TDMA system has the lowest terminal cost, relatively high throughput, and a relatively low cost per voice channel.

Operation in the 20/30 GHz band (high rain margin, new technology) together with processing in the satellite and adaptive coding in the high-capacity systems results in complex and expensive designs.

The most cost efficient design is a satellite that provides processing only for those users that experience rain attenuation and a frequency hopping (frequency-routed) TDM system. This combination merits further study.

SECTION 2

INTRODUCTION

This study is one of several performed by the MITRE Corporation for National Aeronautical and Space Administration/Lewis Research Center (NASA/LeRC). Previous work included a study on processing satellite concepts and a study on frequency-routed FDMA systems.* Topics which were discussed in detail in those reports, e.g., efficient spectrum utilization, are omitted from this document.

The study reported here investigates satellite systems that provide cost-efficient communications capabilities to customer premise service (CPS) terminals. CPS terminals are small earth stations which are located on the customer premises and service a limited number of users (4 to 12). A unique feature of a CPS system is that thousands of terminals access the satellite directly. While several accessing schemes were considered, only four were selected and investigated in detail. Each system employs a different routing method in the satellite. These systems are described by the routing and the accessing mode as follows: Satellite-Routed Frequency Division Multiple Access (SR-FDMA), Satellite-Switched TDMA (SS-TDMA), Processor-Routed TDMA (PR-TDMA), and Frequency-Routed Time Division Multiple Access (FR-TDMA). Since a CPS system consists of thousands of earth terminals, the system cost can be reduced by reducing the terminal cost. This can be achieved by shifting the burden from the terminals to a high-performance satellite that uses multiple high-gain beams, processing, and high-power transmitters. However, a high-performance satellite is heavy, consumes a large amount of DC power, and may not be feasible. Realization that such systems are satellite-power limited led to an investigation of the relationship between DC power and system throughput.

Preliminary investigation indicated that the user cost in a CPS satellite system exceeds the cost of existing terrestrial links. Therefore, trunking service was included in the system in order to reduce the CPS user cost.

A brief description of the basic system assumptions is given in section 3. They include the number and size of antenna beams, the earth-terminal dish size, and receiver noise temperature.

*See bibliography p. 136.

In order to conserve orbital space and avoid future frequency congestion, NASA specified that the CPS system must operate in the 20/30 GHz band. This will also advance the state-of-the-art technology. Technology for this band is mostly in the development stage. An overview of currently available technology is presented in section 4. Information about present subsystem costs is used in the cost comparison of various systems. The survey also identifies areas for technology development

Four promising cases are discussed in detail. An SR-FDMA system is presented in section 5. The earth terminals transmit a multicarrier signal, one carrier for each active user. The routing in the satellite is provided by hard-wired filters.

An SS-TDMA is described in section 6. In order to reduce the satellite weight and power consumption, most of the traffic is routed by microwave switching matrices in non-processing transponders. A fraction of the traffic is routed and processed at baseband. Only a fraction of the users experience excessive rain attenuation and benefit from a processing gain.

In section 7, a PR-TDMA system is presented. All the routing is provided at baseband by microprocessors. The message bits of the entire uplink frame are stored in memory devices.

An FR-TDMA system is outlined in section 8. The earth terminals transmit a frequency hopping signal, one hop for each active user. The number of hop frequencies equals the number of downlink beams. This permits routing by hard-wired filters in the satellite. A baseband processor serves for reformatting the uplink frames into fewer downlink frames.

The design of the trunking transponders is described in section 9. Non-processing microwave switching matrices are used for routing. The weight and power consumption for the trunking services is a fraction of the CPS weight and power.

A cost-comparison study is discussed in section 10. The space-segment and terminal costs for the CPS service are estimated for the four conceptual designs. Section 11 summarizes the important findings of this report.

A bibliography is provided which lists related reports.

System throughput is calculated in the appendix for 13 different combinations of accessing modes for the CPS and trunking services.

SECTION 3

BASELINE ASSUMPTIONS

The satellite systems described in this report provide communications capabilities for relatively small earth terminals located at customer premises. Each terminal serves only a few users (4 to 12). The users generate two types of information: digital voice at 64 kilobits per second (kb/s) and data at 56 kb/s. Data transmission requires high link quality with a bit-error-rate of 10^{-6}.

The satellite operates in the 30/20 GHz band because the 6/4 GHz band is already overcrowded and the 14/11 GHz band soon will be. At the present time, the 30/20 GHz band is little used. High-gain antennas for this band have relatively small dimensions, a desirable feature, since space may be limited at the customer premises. Using high-gain antennas also reduces the terminal radio frequency (RF) power requirements and thereby reduces the overall terminal cost.

High-gain satellite antennas conserve the satellite DC power, which is the limiting factor in such communications systems. A solar cell array of reasonable size and weight that is compatible with present launch vehicle capabilities can deliver no more than 5000 W DC. Apportionment of this power among the satellite subsystems shows that only 1000 W DC can be allocated for the traveling wave tube (TWT) amplifiers in a processing satellite and this, in turn, determines the satellite throughput. The available bandwidth is not a limiting factor because multibeam operation allows frequency reuse of the 2.5 GHz bandwidth. Although high-gain antenna beams conserve satellite resources, they cover only a limited area. To cover most of continental United States (CONUS) with the satellite system, the number of spot beams must be very large; this results in a complicated satellite design of high power consumption and heavy weight. Limiting the number of antenna beams to 32 simplifies the transponder design. However, 32 high-gain spot beams cover only part of CONUS. The compromise solution adopted uses 22 spot-beams to illuminate the major metropolitan centers and 10 area-beams to cover less densely populated parts of CONUS; see figure 3-1. The area beams have lower gain, which reduces the system efficiency. The half-power beamwidth of the spot beams is 0.35°; this value is a compromise between the requirement for high gain and the difficulty of achieving accurate antenna pointing. In many cases, 0.35° beams will cover more than one major city; therefore, employing this beam size reduces the need for so many beams. The area beams have a 0.70° half-power

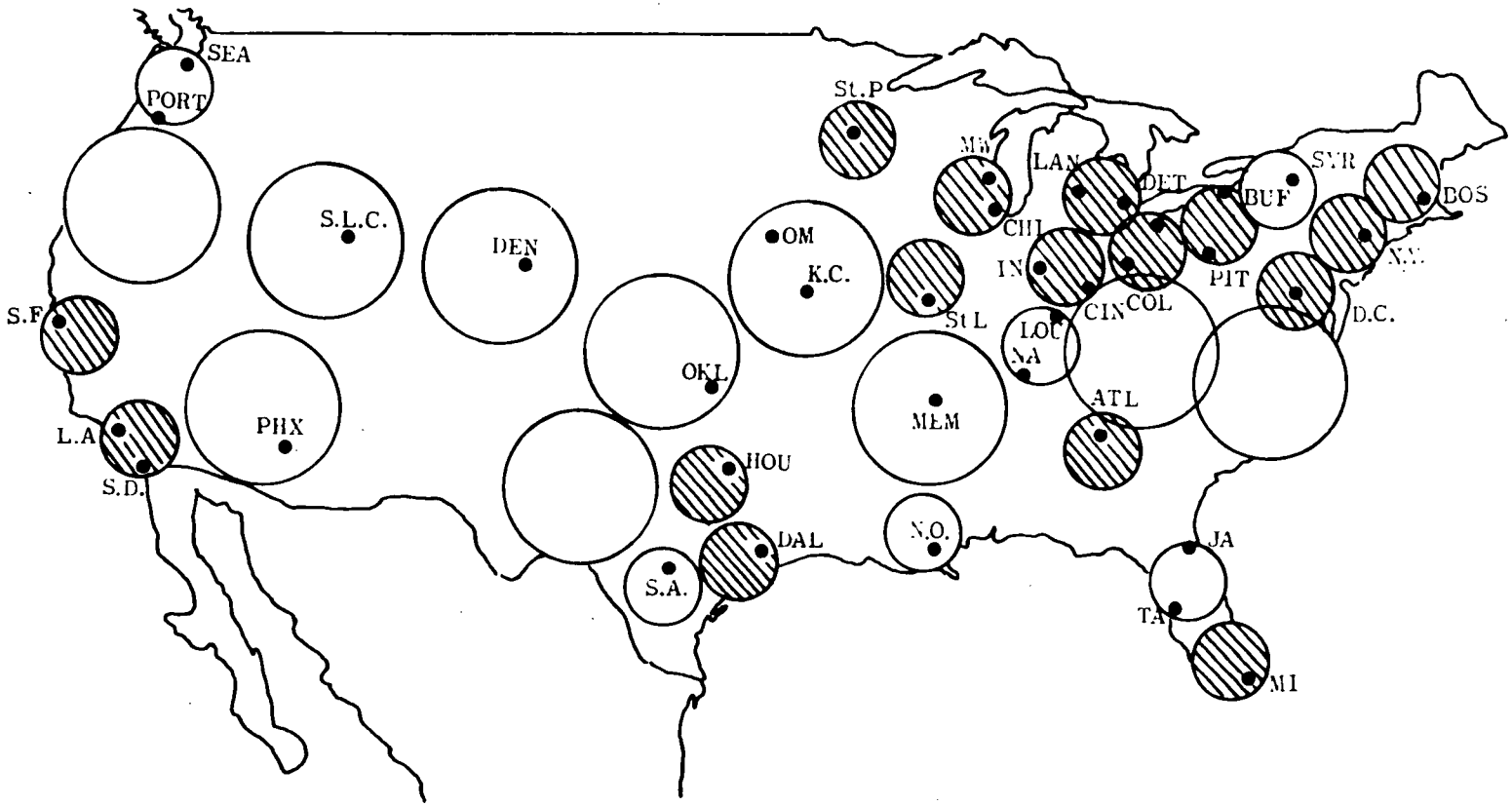

Figure 3-1. Beam Coverage of Continental United States
(Cross-Hatched Beams Also Carry Trunking Traffic)

beamwidth; this value is a compromise between complete CONUS coverage and the gain reduction associated with wide-beam coverage. The CPS terminals illuminated by the spot beams are termed "metropolitan CPS" and are denoted with the subscript 1. The CPS terminals covered by the area beams are termed "rural CPS" and are denoted with the subscript 2.

The number of earth terminals in a CPS system is very large; therefore, their cost must be minimal. To achieve this, it is assumed that the CPS terminals have a 3-m antenna dish; a larger antenna requires an expensive satellite-tracking mechanism. To maintain a reasonable terminal cost, the CPS system noise temperature assumed is 1000 K. Analysis shows that the cost of CPS operation (dollars per voice channel per year) exceeds the cost of similar terrestrial services. In order to reduce the cost, trunking service is included in the same satellite. The trunking service is very powerful: a trunking terminal can afford to use a tracking 6-m antenna and 500 K low-noise preamplifiers. Therefore, the trunking service demands little from the satellite resources. For example, if the trunking throughput is 50% of the CPS throughput, the trunking power consumption is only 15% of CPS power consumption and its weight is only 25% of CPS weight.

Trunking traffic can be expected only from some of the major metropolitan centers. Since the metropolitan centers are already covered with spot beams, the trunking service can utilize some of the 22 spot beams. Trunking coverage is provided by 16 spot beams. (See the cross-hatched beams in figure 3-1.) This number was selected because the switching matrix in the trunking transponder must have a size that is a power-of-2 for two of the three matrix architectures discussed later. This number of trunking beams also agrees quite closely with NASA projections for anticipated trunking centers. The data rate of the trunking terminals is assumed to be 12.6 megabits per second (Mb/s) and the quality of transmission corresponds to a bit-error-rate of 10^{-6}. System parameters pertaining to the trunking service are denoted with the subscript T.

Operation in the 30/20 GHz band involves problems that are specific for this frequency range. One problem is the availability of high-power amplifiers for this band. Another problem is the high propagation loss during rain storms. Rain margins of 10 dB in the uplink and 6 dB in the downlink yield a 99.5% link availability for most of CONUS. Florida and some areas in the southeast experience very heavy rain storms and require larger rain margins. The need to employ a 10 times more powerful amplifier in the earth station and a 4 times more powerful TWT amplifier in the satellite for combatting rain is a disadvantage particular to this frequency

band. Such an over-design can be reduced if the CPS terminals resort to coding during rain storms. Rate-1/2 coding gives about 5 dB coding gain. The rain margin for the downlink can be reduced from 6 dB to 1 dB. The rain margin for the uplink can be reduced from 10 dB to 5 dB if the satellite employs decoding/encoding. When rate-1/2 coding is applied to a data stream it doubles the symbol rate. In order to maintain a symbol rate of 64 kb/s, the data rate at the input of the encoder must be reduced to 32 kb/s when coding is used.

To facilitate the analysis, it is assumed that the traffic is uniformly distributed among beams. Since the purpose of this report is to compare various satellite systems, the results are not affected by this simplification.

SECTION 4

SURVEY OF 20/30 GHz TECHNOLOGY

This section presents a summary of current 20/30 GHz technology and an evaluation of specific developments.

4.1 IDENTIFICATION OF SYSTEM SUBASSEMBLIES

This general survey of several system subassemblies describes these items: antenna systems, solid-state and TWT-type high-power amplifiers, and frequency synthesizers. The scope of further technology development on the above subassemblies is identified as required.

4.1.1 Antenna Systems, Ground and Space Applications

Ground terminals for CPS should use dish sizes from 2 m to 3 m without electronic tracking. In general, the antenna size is a function of the terminal simultaneous voice channel capacity and satellite antenna gain. Trunking terminals use antennas from 4.5 m to 6.0 m in size with step tracking.

The effect of surface finish on antenna performance is directly measured by the RF loss in antenna gain and is calculated as follows:

$$\Delta G = -686 \left(\frac{\epsilon}{\lambda}\right)^2 \quad \text{dB}$$

where

ΔG = gain loss
ϵ = surface accuracy in inches (rms)
λ = free-space wavelength

Figure 4-1 shows the required surface accuracy for the different size antenna systems if the loss in antenna gain (due to surface finish) is limited to 1 to 1.5 dB. A ratio of $\lambda/32 = \epsilon$ corresponds to a 0.7 dB loss while a ratio of $\lambda/16$ produces a 2.6 dB surface loss.

Feed systems at 20/30 GHz can vary from a single feed horn to the more complex Cassegrain types. A downlink to uplink frequency separation ratio of 1.5 precludes the use of the same feed for both

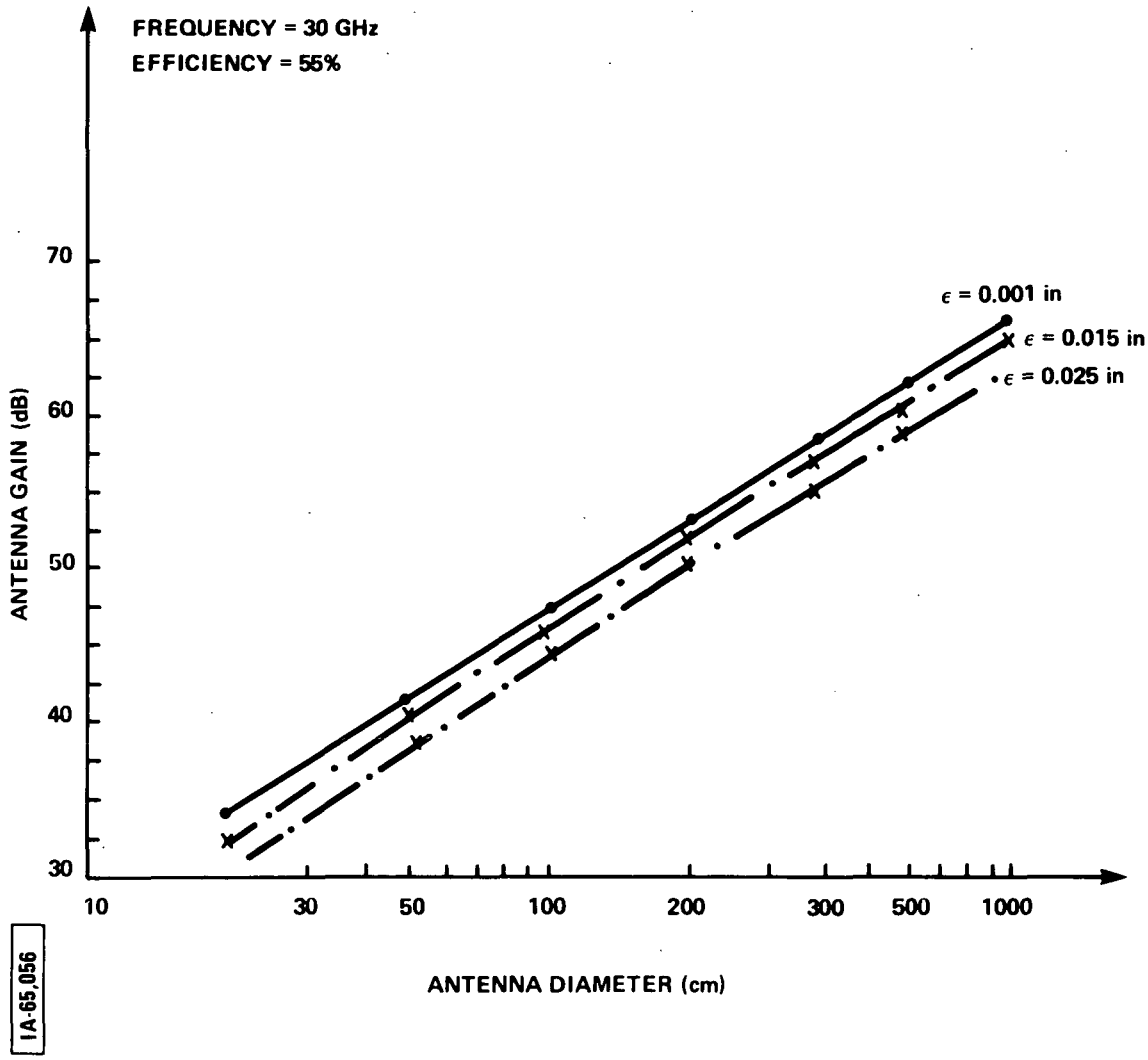

Figure 4-1. Gain Versus Antenna Diameter

transmit and receive frequencies. Feeds which cover either frequency band are available. Among them are the corrugated cylindrical horns and rectangular feed horns. However, feeds with dual-frequency capability need to be developed.

Feeds at 20/30 GHz are more complicated than those at 4/6 GHz or 7/8 GHz due to the waveguide structure. The tolerances on the feeds are very tight due to the high-performance requirement and the high-power level. These feeds will be different from those at the lower frequencies. Focusing feeds at 20/30 GHz is not easy because of the narrow beamwidth; however, a common feed system can be accomplished with large-size, corrugated, waveguide horns. The biggest problems are in the antenna assembly technique and alignments, not in manufacturing, according to Harris Co. The maximum usable antenna diameter, D_{max}, for a given tracking accuracy loss of 1.5 dB is:

$$D_{max} = \frac{42\,\lambda}{\Delta\theta}$$

where

$\Delta\theta$ = tracking accuracy in degrees

λ = free space wavelength

and

$$G_{max} = 38 + 10 \log (\eta) - 20 \log \Delta\theta$$

where

G_{max} is the maximum achievable antenna gain

η = antenna efficiency (approximately 55%)

The tracking methods depend on the antenna beamwidth. For a half-power beamwidth (HPBW), larger than $\theta_{HPBW} = 0.25^{o}$ and smaller than 0.5^{o}, a step-tracking system is recommended. If the terminal antenna beam is less than 0.25^{o}, monopulse tracking is required, with increased cost. The tracking error loss, Δ G, is expressed as

$$\Delta G = 12 \left(\frac{\Delta\theta}{\theta_{HPBW}} \right)^{2} \quad \text{dB}$$

The basic antenna types employed in the satellites are: earth coverage horns, paraboloid reflectors, shaped-beam reflectors, arrays, and multiple-beam antennas.

High-gain spot beams can be achieved by using either a phased array or a fixed multibeam antenna (MBA). The phased array with electronic steering capabilities offers some advantages, namely, lightweight microwave integrated circuit fabrication, and power-combining, low-power, solid-state, power amplifiers. However, this array requires a large number of phase shifters with weight and loss contributions that significantly out-balance the weight gain of the single antenna element.

The advantages of the phased array antenna system are:

1. Electronic steering (limited in azimuth)
2. Elimination of rotary joint and waveguide losses
3. Power combining of low-power, solid-state amplifiers

The capabilities of an MBA are numerous: beam steering, scanning, beam shaping, sidelobe control, etc. The MBA can be a reflector structure with multiple horns or a lens (metal or dielectric). The reflector type MBA, even with offset feed horns, has limited beam capacity, well suited for only a small number of beams. The lens provides comparable performance to a reflector MBA, but has a bandwidth limitation and a weight penalty. The smaller aperture required at 30 GHz might remove the weight problem related to the dielectric lens.

An MBA also requires a broadband, beam-forming network (BFN) with stringent performance characteristics. A recommended BFN would use variable power dividers and phase shifters. Technology development is required in both areas.

4.1.2 TWT Power Amplifiers, Space and Ground Segment

Low-power, helix, TWT amplifiers (1 to 2 W) at 30 and 20 GHz have been available for almost a decade. The permanent positional magnet (PPM) focused helix tubes can deliver (from analytical calculations) substantially higher power since thermal limitations start only at a power level of 25 to 50 W. Presently, several design efforts are on-going both at Hughes and Varian for 10 to 15 W helix-type TWTs at 35 and 45 GHz. For this type of structure, the way to increase the power level is to improve the helix power dissipation. Helix-type tubes provide wide bandwidths and high efficiency even at K-band.

For power levels higher than 30 W, coupled-cavity structures must be used. They can be PPM focused at the 100 W level or solenoid focused at the 1 to 2 kW level. Coupled-cavity tubes have been built in the last five years at 38 GHz and higher frequencies

and have delivered the predicted power. However, coupled-cavity tubes have lower efficiencies than the helix types and their bandwidths are limited to 10 to 30%. Bandwidths of octave (66%) and multi-octave band have been demonstrated for helix TWTs.

Power versus frequency performance limits are shown in figure 4-2 for both types of TWT structure (helix and coupled-cavity). The limits are based on measured and analytically predicted performance.

Potentially, the helix-type TWT can lead to a low-cost high-power amplifier (HPA), and consequently transmitter, due to the simplicity of its assembly structure. Coupled-cavity tubes require not only a large number of precision machined parts and careful assembly techniques, but a more complex high voltage (20 kV or even more) power supply. Therefore, the coupled-cavity tube is not a low-cost alternative even with the possible success of some new technologies described in the next section.

The continuous wave (CW) power capability of TWTs decreases with increasing frequencies. Frequency scaling of the helix design, wire diameter, and pitch at millimeter waves requires dimensions (beam and slow wave structure) which are significantly smaller than at 4/6 or 7/8 GHz.

At millimeter waves, the collector voltages and the beam current are higher while the RF power is lower; therefore, the power densities and the associated thermal effects and heat losses are very high. The available output power above 10 GHz is approximately inversely proportional to the square of frequency ($1/f^2$). The beam conversion efficiency also is degraded by increased RF losses at higher frequencies.

The power capability of helix tubes is primarily limited by three factors:

1. Upper level for beam voltage below backward wave oscillation

   V_{max} 10 kV

2. Helix current and operating temperature

   I_h 2 to 5 mA

   T_{max} 400°C

3. Helix support insulating material thermal gradient and heat transfer characteristics

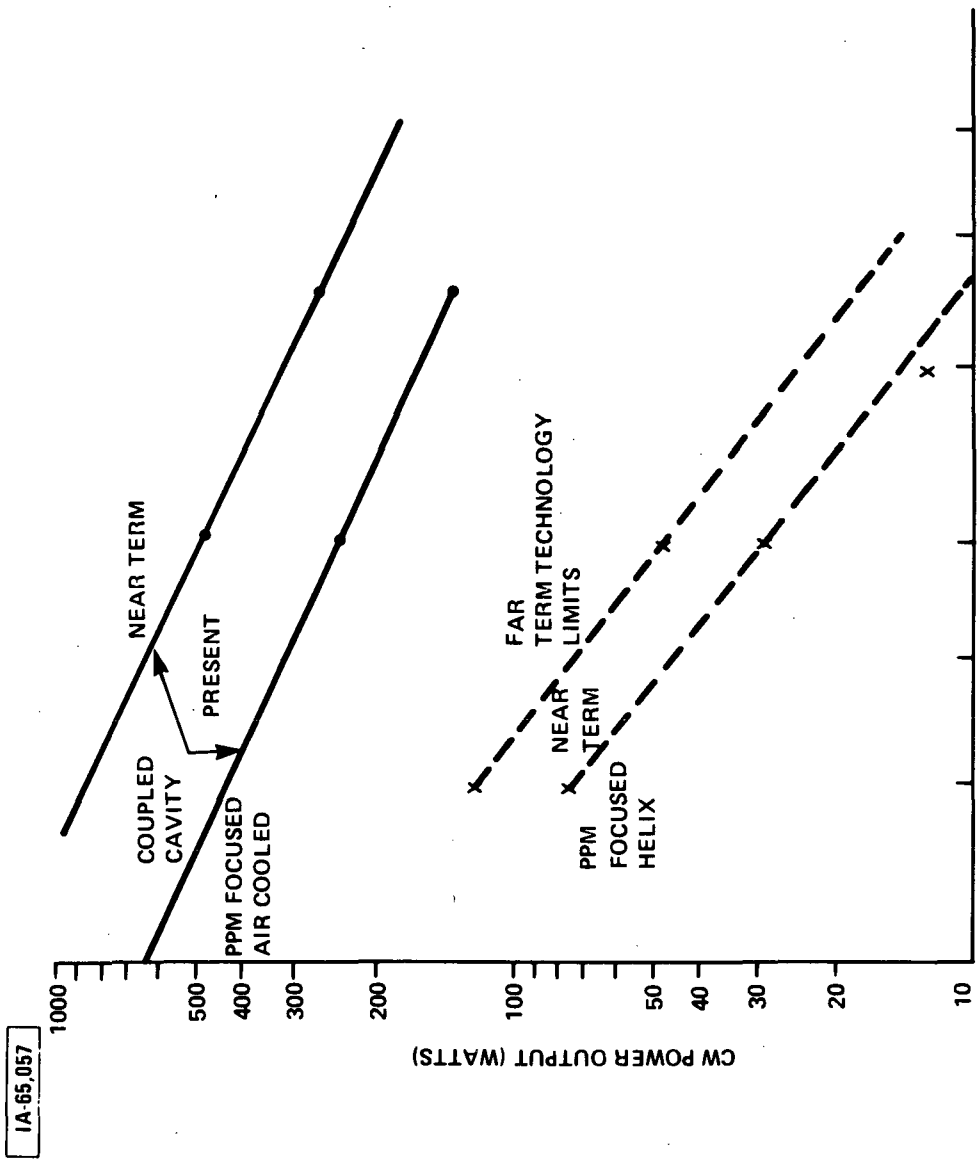

Figure 4-2. TWT Amplifier Power Versus Frequency

4.1.3 Solid-State Amplifiers

In the 1970s, 1 or 2 W RF power amplifiers at X-band were considered great achievements. Today, 10 W amplifiers at X-band have been demonstrated and 1 to 1.5 W power modules are available at 45 GHz. For transmitter use, Impatt amplifiers with 5 to 10 W RF output power are in the development stage at Hughes Electron Dynamics and elsewhere.

The transferred electron device type HPA has potentially wider bandwidth than the Impatt diode amplifier, but the available power is less, approximately 0.5 to 1 W maximum.

Solid-state amplifiers have the advantage of longer lifetime than TWTs, if an adequate heat sink is provided to the amplifiers. Solid-state amplifiers have a low DC-RF efficiency of 8 to 12%. The amplifier designs utilize several chips operating in parallel per module due to the low gain of the diode at the high-power level (0.5 to 1 W). The multiple-device amplifier operation ensures graceful degradation in case of failure; the transmitter continues to operate with reduced power. In a TWT amplifier, the same type of failure is catastrophic and the transmitter shuts down. If high-frequency semiconductor device yield is upgraded by new technology, solid-state amplifiers have promise for low-cost transmitters within their power limitations.

For small CPS terminals, solid-state power amplifiers of up to 5 W and 1 GHz bandwidth are most suitable. While solid-state amplifiers can be used up to 10 W, they are not a cost-effective alternative to TWTs; in fact, their bandwidth will be substantially reduced (approximately 500 MHz). Device technology, using gallium arsenide, silicon, as well as other new materials, needs to be improved for increased reliability, higher power output, and wider bandwidth. Power-combining techniques with reduced circuit losses also need to be developed and improved.

For the smaller CPS terminals, a 1 W RF solid-state power amplifier module is feasible and will be cost-effective in 1982. For higher RF power, higher efficiency and broader bandwidth, some further development is required.

Perhaps the greatest advantage of a solid-state transmitter is that it can be installed directly next to the antenna, including the power supply. This improves the overall performance by greatly reducing waveguide run and waveguide losses. The estimated reduction in system losses is about 2.0 dB relative to a TWT installation.

4.1.4 Low-Noise Receivers, Space and Ground Segment

Low-noise amplifiers (LNAs) at 20 and 30 GHz for space and ground receiver front-end applications can greatly enhance performance, reduce satellite DC and RF power requirements, and result in increased system capacity. The immediate and most significant impact of a space qualified 30 GHz LNA would be at least 5 dB improvement in satellite gain-to-noise temperature ratio (G/T). Low-noise, front-end amplifiers are not only important for increased capacity but required for additional gain compensation of RF front-end losses in a multibeam antenna system. Parametric amplifiers are too cumbersome to use in the spacecraft and are extremely sensitive to temperature and mechanical environment.

The only alternative to LNA and paramp is the image-enhanced, low-noise mixer (6 to 7 dB noise figure). Image-enhanced mixer design and technology at K-band frequencies is not straightforward and requires very careful selection of the Schottky-barrier mixer diodes. Bandwidths larger than 2 GHz might not be achievable. Therefore, for space and ground applications, the low-noise, front-end GaAs field-effect transistor (FET) amplifier development is critically important. Recently measured performance of some GaAs FET amplifiers at 20 GHz gives a 6 dB noise figure (T_{LNA} = 1000 K) with 8 dB gain, but there are indications that 4 dB noise figure can be achieved within the next two or three years. At this time, however, there is no 30 GHz LNA development for space applications that might require a greatly different and improved 0.3μ gate GaAs FET device.

4.1.5 Integrated Front End with Dual-Frequency Conversion

The impact of integrated front-end technology would be less labor-intensive assembly, wiring, and testing of subassemblies. Each functional subassembly may have less loss due to reduced size and integration into a single chip. Integration improves performance and results in a smaller, cheaper receiver. The same functional integration can be introduced at the transmitter for the low-level, up-converter module.

4.1.6 Frequency Synthesizers

Frequency synthesizers with analog frequency multipliers and dividers are well known and fully developed in manually adjustable and digitally controllable form. Synthesizers for commercial and military communications and radar applications are well developed at 4, 6, and 10 GHz. However, within the last few years, operating

frequencies for instrumentation synthesizers have been pushed up to 18 GHz and even beyond. These high-resolution, fast-switching, instrumentation-type synthesizers are too expensive for satellite terminal use, and there is no synthesizer on the market in the 30/20 GHz frequency band. Current commercial synthesizers generate L-band (1 to 2 GHz) frequencies directly and phase lock the signal source to a 100 MHz reference. This technique can be replaced in the future with direct multiply and divide, digital large scale integration (LSI) circuits that provide direct frequency multiplication and division up to 2 GHz. Using such circuits would result in higher resolution, lower phase noise, and a less expensive synthesizer. Current communications-type synthesizer resolution is in the 1 to 5 MHz range with an optional resolution to 100 kHz, at 2 to 4 GHz output frequencies. However, N-times multiplication from 2 to 30 GHz reduces the resolution N-times and increases the phase noise as N^2.

In an FDMA digital system, it is very important to operate with low phase noise, high resolution, and low-cost synthesizers (not compatible with current specifications). In a simultaneous multi-carrier operation, each up and down converter must have its own synthesizer and multiplier chain for appropriate frequency selection. That is not the case for TDMA operation where the terminal operates at a single carrier frequency. Therefore, the number of frequencies for carrier generation is very small, and high resolution is not required. Only high frequency stability, which is a function of the reference source, is needed.

4.2 STATUS ASSESSMENT OF SPECIFIC TECHNOLOGIES

In this section a detailed discussion is given of the specific technologies applied to system subassemblies. The reviewed subassemblies include antenna systems, medium and high-power TWT amplifiers, solid-state amplifiers, modems, and earth terminals. Status assessment is given for each item where advancement potential for improved technology can be identified.

4.2.1 Antenna Systems

Antennas with diameters of 2 m or less are single-piece reflectors; currently achievable surface accuracies are presented in table 4-1.

Table 4-1

Achievable Surface Accuracies

Surface Accuracy (inches)	Manufacturing Technique
0.025	Standard stamping or spinning Fiberglass
0.012	Precision spinning or molding Fiberglass
0.005	Mechanical casting or molding and machined surface

The most cost-effective antenna manufacturing process depends on quantity, size, and required tolerances; however, stamping and molding single-piece fiberglass is among the very promising techniques. Antennas over 3 m in diameter are typically fabricated from panels. Factors contributing to the operational antenna surface accuracy include:

- Panel fabrication technique (stamped or machined)
- Supporting structure
- Antenna assembly technique

Environmental factors affecting alignment and antenna gain are:

- Wind load
- Thermal gradients
- Gravity

The required surface accuracy (0.012 inch) for small terminal dish sizes up to 3 m can be realized with some refinement in the current manufacturing processes.

Fabrication technology for dishes up to 4 m in size would use a fiberglass, imbedded-wire-mesh structure as has been uniformly quoted by several industrial sources. Subreflectors from fiberglass (2 m size) are made currently for large Cassagrain feed antenna system (20/44 GHz) applications at Harris Corp.

Surface finish and tolerances of fiberglass are equivalent to metal, pressed-panel technology, as explained by Scientific Atlanta Co. representatives, and bounded by the structural size. The 2 m size subreflector has been built with 0.005-inch surface accuracy, which is excellent for 20/30 GHz applications.

Scientific Atlanta Co. is currently in the production phase of a 12/14 GHz Satellite Business System (SBS) 5 m size dish, antenna system comprising stamped metal reflector panels (24). They measure an overall surface accuracy of 0.020 to 0.025 inch (mostly due to the tooling effect). If dish sizes do not exceed 4 m, fiberglass antennas can be produced with surface tolerances of less than 0.012 inch, according to Scientific Atlanta. The 2 m size fiberglass dish can be made inexpensively with the same surface finish quoted above from a single-piece mold.

COMTECH Lab also reports that a 5 m dish at Ku-band fabricated from fiberglass does not present a problem. If it is scaled down to K-band, the fiberglass, imbedded-wire-mesh, low-cost antenna system is an appropriate choice at 20/30 GHz. On the subject of step tracking, COMTECH estimates that at C-band or SHF frequencies, step tracking with azimuth and elevation servo controls and a beacon receiver with two channels would cost approximately $10K. However, even a $5K-step track system can be realized if the beacon-receiver down converter is replaced by a pilot tone. Step-tracking system costs of $30 to 40K are extraordinarily high according to COMTECH.

On the antenna issue, Harris Corp. explained that, with today's technology, metal-bounded antenna construction has no disadvantages compared to fiberglass techniques, below a certain size dish. In other words, the metal structure rms surface finish is equal to that of fiberglass. Feeds at 20/44 GHz are more complicated and will not be readily available with current specifications and performance. Tolerances are very tight on the feed at high frequency and high-power levels. The design is not a simple scaling, but is different from the low-frequency application.

According to Scientific Atlanta, a 4.5 m dish is no longer moldable from fiberglass and should fabricated as a metal reflector-panel structure (this statement is confirmed by the Harris Corp.). Scientific Atlanta is producing a 5 m dish for SBS at 12/14 GHz; however, this method is expensive and cheaper techniques do exist. Currently, the SBS 12/14 GHz antenna sells for $20K, including the feed, dish, and mount, but not the tracking system. However, this antenna can be made more cheaply by a different technology. The 4.5 m metal dish operating at 20/30 GHz requires a tracking system. In single units this antenna system cost might be in the $100K range, but in production quantities the expected cost is around $20K including dish, feed, and pedestal. Antennas can be made economically in large production quantities. Fiberglass antennas can be produced with surface tolerances of about 0.012 inch if the size does not exceed 4 m. Therefore, the 4.5 m size is the breakover point to produce inexpensive antenna systems. A 2 m size dish can be made inexpensively from single-piece fiberglass

material, while the price quoted for a 4 m (0.012 inch rms) fiberglass antenna system without tracking is about $20K.

Dish sizes of less than 3 m do not require any automatic antenna steering and pointing; they need only manual tracking. The tracking loss for this size antenna system is anticipated to be less than 1.5 dB. Step-tracking electronics with 0.05° accuracy is available, fairly inexpensively, with current technology. The satellite, however, must be kept within a $\pm 0.05^{\circ}$ drift over a 24-hour period.

Concerning the tracking system, Scientific and Harris Corp. explained that step tracking is not necessarily the only cost-effective way. Several companies presently operate on a pilot-tone, direct-tracking system with a processor-controlled, open-loop system, provided the satellite has a relative slow motion (1°/day) in geosynchronous orbit. This pilot-tone system (which does not use a beacon receiver) could cost about $4 to 5K (this price was confirmed by COMTECH). At Scientific Atlanta, the cost of the most expensive step-tracking system is currently no more than $15 to 20K, including mechanical mount (two axis). The mount (pedestal) is the most expensive item due to the wind-loading-effect stabilization design.

The Rockwell-Collins Richardson Antenna Group is part of the Rockwell Company's Anaheim-Newport Beach operation. They have developed a 20/45 GHz antenna, circular-mode waveguide polarizer, orthomode transducer (OMT), and rotary joint. The antenna reflector is a shaped, Cassagrain, offset-feed parabola with a 1-foot dish. The expected efficiency is 65%, verified by tests on the antenna while the first sidelobe was below the 26 to 28 dB level. The complete feed is made from electro-formed, corrugated waveguide with a low-cost manufacturing technology. The antenna is designed for a three-axis, stabilized, shipborne platform with an open-loop pointing system (tracking) and a gyro-package, attitude stabilizer. Tracking accuracy with this system is expected to be within 0.4° to 0.5° and actual tracking loss is less than 1.5 dB.

Cross-polarization isolation measured on the above antenna is about 30 dB; the axial ratio expected is 1 dB.

Rockwell agrees with other experts that fiberglass, wire-mesh, antenna-fabrication techniques could provide 0.010-inch surface tolerances. The technology limit for fiberglass antennas is a 3.5 to 4 m dish, as quoted by Rockwell.

4.2.2 Medium and High-Power TWT Amplifiers

It is generally accepted that high-power, high-frequency amplifiers cannot be scaled down directly. Demonstrated technology at higher or lower frequencies does not preclude the need for substantial development at 30/20 GHz.

4.2.2.1 Helix Tubes (Low and Medium Power)

Hughes has developed high power (250 W) Ku-band TWT amplifiers for SBS satellites. At this time, the tube operates only in the CW mode for time division multiplex (TDM); however, plans for future pulsed-mode operation have been disclosed, with the pulse width varying from 100 μs to 1 μs, and less than 10% duty cycle.

At Hughes, a 35 GHz, wideband, helix-type, pulsed TWT operating at 35 GHz with 30% duty cycle is under developoment. The expected power output is about 20 W. The specified bandwidth is 2 to 3 GHz; however, 5 to 6 GHz can be achieved. This program was started recently and will be completed in 20 months. This tube will be available at 30 GHz also. According to Hughes, the passband ripple of this helix TWT might be a problem (as high as 2 dB). This tube is really a scaled-down version of the SBS tube described earlier. The output power of a helix TWT is limited to about 50 W at 30 GHz, even with a significant ($500K) research and development (R&D) effort. However, a 10 to 25 W helix TWT at 30 GHz is feasible and not difficult. RF power levels, above 50 W at 30 GHz or higher frequencies, can be achieved only with coupled-cavity designs. Similar information was obtained from Varian in regard to helix tubes where a 10 W TWT at 44 GHz is near completion with the possibility of obtaining 25 W with 40 dB gain and 20% maximum efficiency at 30 GHz. At Varian, several different technologies are currently being investigated for high-frequency high-power TWT amplifiers.

Helix tubes with high-power cathode structures exhibit definite temperature limitations. Gain flatness and low amplitude modulation/phase modulation (AM/PM) conversion are achievable only in a narrow band (100 MHz). Group delay and AM/PM conversion will suffer some degradation in a bandwidth of 1 GHz.

4.2.2.2 Coupled-Cavity Tubes (Medium and High Power)

At the present time, two "low" cost, coupled-cavity TWT design efforts for 45 GHz operation are in progress at Hughes: (1) the ferruleless cavities that have lower tolerance requirements, are less critical in assembly in exchange for bandwidth (BW) reduction (3 to 5%) due to the impedence matching problem, and (2) the diamond-turned cavities that produce wide bandwidth and the same output power as the ferruleless design, but require rather close

machined tolerances. Diamond-turned cavities can be made to very close tolerances but require a more labor intensive process.

The circuit design with the ferruleless cavities does not require high precision machining. Projected costs in the next five years are $2 to $3 per cavity. There are about 150 cavities expected in a coupled-cavity TWT assembly. The ferruleless design, however, is limited to 60 GHz maximum operating frequency by the gain/cavity and has less overall efficiency. The ferruleless and diamond-turned cavity techniques approach each other in cost. For quantities of 100 and over, the expected tube cost is about $50K. For coupled-cavity tubes, power requirements of 50 W or 250 W make no difference in cost; the same tube operates at 250 W. The expected bandwidth for the coupled-cavity TWT will be around 1.0 GHz initially and expand later to 2.0 GHz at 200 W CW output power. By the end of 1981, a ferruleless structure will be demonstrated. By the end of 1983, the broadband version of a 200 W CW power, coupled-cavity TWT will be available. Both diamond-turned and ferruleless techniques lead to "low" cost tube design. The same technique described for the 45 GHz tube can be applied for 30 GHz with similar cost effectiveness.

In summary, the basic differences between the two technologies for coupled-cavity TWTs are that the diamond-turned technique is applicable up to 90 GHz while the ferruleless approach is useful only up to 60 GHz; the bandwidth is expected to be 3 to 5% for the ferruleless, and at 30% for the diamond-cavity TWT. Finally, the ferruleless structure can be broadbanded, perhaps up to 7% bandwidth.

The ferruleless structure has typically 1.5 to 2.0 times the number of cavities of the diamond-turned cavity tube; therefore, the tubes are longer, weigh more, and require more prime power. A typical coupled-cavity structure TWT requires 20 kV beam and cathode voltage (while the helix type has 10 kV). If we take the basic $50K tube cost and multiply by 1.3 (the power supply cost), the complete 50 W to 250 W transmitter cost is approximately $115 to $120K. The expected cost reduction between quantities of 100 and 1000 may be in the order of 10% or less. The current estimated cost of a single TWT alone is $100K to $150K per tube. The lifetime is approximately 10,000 hours. The expected RF-DC efficiency is 20 to 25% with a depressed collector. The forecast cost of a 10 W helix tube at 30 GHz after two years of R&D effort is in the $20K to $25K range in lots of 25 to 50; a quantity 10% discount is available for 100. However, this tube cost may go down to $10K to $15K if large quantities (1000) are ordered. The yield, the parts cost, the assembly, etc., make coupled-cavity tube cost high and much more cost reduction cannot be expected.

4.2.2.3 Helix TWT Technology Assessment and Recommended Improvements

To increase power level, improvement of the helix structure and its heat dissipation is necessary. The thermal limitations of the helix are the following: (1) The heat must be transferred across several interface boundaries to reach the heat sink. (2) The thermal conductivity of the dielectric helix support rod is relatively low. (3) There is little heat transfer from helix wire to dielectric support rod.

All three problems are under investigation with some successful methods for solution, such as diamond supported helices for improved thermal conductivity, and continuous dielectric support.

Additional support by beryllium-oxide, heat-conductive, dielectric material is being investigated. Recent improvements in multistage depressed collector designs at 12 to 14 GHz have resulted in dramatically higher efficiencies (from 25-30% to 40-45%) in helix type TWTs. However, at higher frequencies, efficiencies as well as power output levels are expected to fall off fairly rapidly. The unique application of communication type TWTs requires further development from the tube technology experts in several areas such as:

1. Long life dispenser type cathodes
2. Velocity tapered helices
3. Multistage depressed collector operation
4. Improved electron gun design
5. Improvements in production, yield, and reliability

4.2.2.5 Coupled-Cavity TWT Technology Assessment

The coupled-cavity tube is capable of producing high peak and CW power in the order of several kilowatts to several hundred watts, respectively, at K-band frequencies. For satellite communications it produces low distortion and high efficiency with high CW power. Bandwidth, even if it is significantly less (about 10-15%) than with helix tubes, is still adequate. However, coupled-cavity TWT does require more complex (20 kV) power supply, higher beam voltage, and costs more (two or three times) than the helix tube. Coupled-cavity tubes are not suitable for small CPS terminals (and might not even be needed) due to their complexity and cost. A high-power, coupled-cavity TWT typically consist of 150 small cavities with tolerances $< 5 \times 10^{-4}$ inches, at the limit of the current machining capability. The cost of a single cavity today is $100; therefore, for the cavities only, the material cost is $15K. New low-cost production technology at Hughes like diamond-turning and the

ferruleless circuit program sponsored by Naval Ocean Systems Center (NOSC) and Rome Air Development Center (RADC), respectively, could lead to $50 per cavity or even $20 per cavity, substantially reducing the tube cost. Phase II of the ferruleless program is currently in progress and results are expected in 1982.

4.2.3 Solid-State Power Amplifiers and Transmitters

Solid-state power amplifiers are being built with GaAs FET device technology, Impatt devices (Si or GaAs), or transferred electron devices. The best result (quoted by Texas Instruments) on GaAs FET technology is 0.25 to 0.3 W RF power per module at 30 GHz (expected by 1983-85). This in turn could generate approximately 2 W RF power by power combining eight or ten single (0.25 W) modules. While GaAs FET amplifiers for 20 GHz space applications are feasible, they are too complex and not cost-effective for ground terminals at 30 GHz.

Impatt diode high-power amplifiers and their related Si or GaAs technology are well developed today and have made steady progress in both frequency and power during the last decade.

LNR Corporation is actively pursuing solid-state power amplifiers and transmitters (Impatt) at mm-wave frequencies. Currently, the main concern is a solid-state amplifier which will replace the TWT at 20 GHz in the spacecraft. The power output is expected to be 10 W, and perhaps an ambitious 20 W, from numerous power-combined modules (1 to 2 W per module) with bandwidth of 1.0 GHz; single-module DC-RF efficiency of 14% has been measured.

Rockwell is working on the concept of active, solid-state apertures (phased array) and demonstrating these program designed, solid-state, power amplifiers. The solid-state HPA at Rockwell consists of three- or four-stage, low-gain, high-power modules (7 dB gain per stage) with driver amplifiers. The single-device, output power is 1 W at 44 GHz with 8% DC-RF efficiency, and the total power output of the four-stage modules is expected to be 5 W with 5% overall efficiency.

Hughes Impatt amplifier activities at 44 GHz that are currently in the laboratory have achieved 2.5 to 3 W per module, the best result reported so far. Each power module has 7 to 8 dB gain with two device chips per module. To produce the specified 10 W at 44.0 GHz, four 3 W modules will be combined.

Similarly, at 30 GHz, about two power modules and two driver stages can produce 5 W power with 30 dB gain. No effort is on-going

at Hughes at this time for any 30 GHz solid-state amplifiers. The expected life-time for solid-state amplifiers is 1,000,000 hours; however, when the maximum junction temperature is $T_{j,max}$ = 275 K, the operational junction temperature T_j of 225 K is too high to support the quoted lifetime.

A 30 GHz 1 W solid-state HPA would be much less expensive, about half of the 2 W module cost (since the 1 W HPA is a single device). For pulsed-mode operation, the same thermal and pulse conditions exist for solid-state amplifiers as for TWTs; a duty cycle less than 1%, a pulse width of 100 μs, and 20 W peak power can be obtained at 44 GHz. Hughes does not believe that any power breakthrough in GaAs technology will be forthcoming; only an improved RF efficiency can be expected.

All Hughes Impatt amplifiers are injection-locked, oscillator-type amplifiers. Injection locking ensures better thermal stability and lower noise. No attempt was made for direct amplification. Locking gain of 8 dB has been measured and a bandwidth of 500 MHz is currently available. In the next phase, a 2 GHz bandwidth amplifier will be designed for the same application. The efficiency of the double-drift Si Impatt devices is quoted at 7 to 8%; the GaAs Impatt device operates with an expected 10 to 12% efficiency.

The cost of a 30 GHz Impatt amplifier at the 5 W RF power level with several cascaded modules (to achieve 30 dB gain) could be less than $10K (in quantities of 100).

In summary, the choice between a solid-state power amplifier or a TWT amplifier depends strongly on satellite configuration, access mode, and terminal size and capacity. Both alternatives require competitive development; however, Impatt power amplifiers have the highest potential for low and medium power extremely high frequency (EHF) amplification. Devices with 1 W and 2 W power output at 40 GHz and efficiencies over 12% have been demonstrated by double-drift GaAs material. However, no design effort is being conducted at this time for 30 GHz solid-state power amplifiers. LNR has a very ambitious effort to produce a 20 W power-combined, solid-state transmitter at 20 GHz with 15 to 17% projected overall efficiency. A single device is expected to deliver as much as 2 W power with 18% efficiency.

The long-term, projected power capability of Impatt devices indicates about two to four times increase in output power relative to the currently available units under development. The future success of such devices is contingent upon Department of Defense (DOD) and NASA research funding, since commercial users have very

little interest in EHF solid-state devices for the next five to seven years. Particular areas for improvement in the Impatt device are:

1. Thermal design with diamond heat sinks
2. Increased efficiency with tailored doping profile
3. Integrated impedence matching network with circuit design
4. Higher-yield, lower-cost, fabrication technology
5. Higher reliability, longer life with lower junction operating temperature

GaAs FET power transistors have made great progress during the last five years. The power output at X-band exceeds several watts and 10 W GaAs FET amplifiers at X-band have been built in the laboratory. At Massachusetts Institute of Technology (MIT) Lincoln Laboratory, 20 GHz 1 W amplifiers are in the planning stage. At Texas Instruments, 0.5 W power at 20 GHz from a single device has become a reality. The interest in developing FET amplifiers, despite their lack of power relative to the Impatt devices, is related to:

1. Much more linear amplification for multicarrier operation
2. Higher overall efficiency
3. Wider bandwidth
4. Relative ease of power combining

Further development requires fabrication and implementation technology improvements; innovative device design concepts; a lower thermal-resistance design; reduction in parasitics for broader bandwidth; more uniform drain, current distribution; and impedance-matching, circuit techniques for large-gate, high-power devices.

4.2.4 Power Combining Technology

The terminal power limitation due to power-limited, solid-state devices can be improved by several power-combining techniques including combined chips in a single package, external circuit combinings, and spatial or radial combinings by phased array antenna.

In package combinings, paralleling a limited number of GaAs FET devices has not yet been pursued in the past and research is strongly recommended. Impatt devices are very difficult to use for parallel chip combining due to their inherent low-impedence level. Spatial combining either GaAs FET or Impatt devices promises a great potential (80 or 90% combining efficiency) but no actual R&D effort

has been pursued at this time for feasibility, amplitude and phase error study, and evaluation.

External circuit, conventional, power-combining techniques, resonant (cavity) or non-resonant type (3 dB hybrid) have been used in the last decade to increase power. The prime disadvantage of this technique is the greatly increased weight and RF losses. However, the thermally-passive, non-resonant mode power combining provides more distributed heat load, higher reliability, and graceful degradation. Development of appropriate power-combining technology in view of the finite thermally-limited power capabilities of all solid-state devices is essential for high-power, solid-state transmitters in future satellite or terminal applications.

4.2.5 Burst Modem Technology

Linkabit Corp. currently has an outstanding design for aggregate converters (low data rate to high data rate). The SBS system operates at 48 Mb/s nominal input data rate per single transponder. Some terminals in that system operate with four modems, for a total of 4 x 48 = 192 Mb/s symbol rate as input to the data aggregator.

Current modems in production are operating at 5 to 10 Mb/s data rate either in quaternary phase shift keying (QPSK) or binary phase shift keying (BPSK) form and this current design, if there is a market, can be extended to 25 to 30 Mb/s rates. However, according to Linkabit representatives, this is the highest rate that today's existing technology can achieve. Modems at Linkabit are built with coder-decoder (CODEC) equipment either at 1/2 or 3/4 rate. Convolutional coding techniques at 45 Mb/s data rate are not available today.

The highest rate BPSK/QPSK modem ever produced at Linkabit operates at 30 Mb/s with digital phase lock loop (PLL) and is priced at $50 to $60K in small quantities. Current, state-of-the-art, high-rate modems are built almost exclusively by Japanese manufacturers like NEC or Fujitsu, except for those build by Harris Co. and AYDIN Corp.

As an example, the Digital Communication Corp. TDMA terminal 1004 series also has Japanese-built modems. The cost for a modem operating at 60 Mb/s burst rate as quoted by Linkabit, is $20K in-full scale production of quantities over 100, provided that substantial R&D money has already been recovered. The cost breakover point, according to Linkabit, is a modem at a burst rate of about 10 M/bs.

Most of the high cost of the modem (about 80%) is related to the complexity of the demodulator part. The receiver needs rapid acquisition of the preamble, burst synchronization, automatic gain control, and unique word alignment, all of which present problems at high-speed rates.

Only the aggregate rate converter-demodulators that operate at a high burst rate promise low-cost modems. According to Linkabit, a T_1 rate (1.544 Mb/s) is the highest data rate for a cost-effective terminal. The cost of the aggregate modem in production might be approximately $50K to $60K.

For this phase of development, a vigorous R&D program is needed, including high-speed logic and buffer-memory systems. The key components to high-speed modems are: high-speed quantizers, and sampling processors, followed by buffer memory with nanosecond storage, access control, and sampling time.

The two-phase R&D program suggested by Linkabit for high burst rate modem development is:

1. Control engineering functions design
2. High-speed quantizer technology development

Motorola and TRW currently have this technology (100 Mb/s quantizers); however, according to Linkabit, only a 30 Mb/s modem including forward error correction (FEC) decoder can be built by 1985 at low cost. The current 48 Mb/s modem with the aggregate-rate-converter (4 x 48 = 192 Mb/s) front end sells for $120K for the aggregate converter alone and approximately $30K for the single modem. Without the aid of an aggregate converter, the cost of a 256 Mb/s modem could be $1.0M.

The rate-1/2 CODEC equipment alone at 10 Mb/s symbol rate (the best available today) sells for $20K in small quantities.

At Digital Communications Corp, (DCC), modems are built with rates from 1.2 kb/s to 60 Mb/s for single channel per carrier (SCPC) and other data communication links, and TDMA terminals (baseband only) are built with rates up to 250 Mb/s for Intelsat. The company's lowest-cost modem sells for less than $10K in quantities over 50. The modem data rate is 2 Mb/s maximum and has a built-in, rate 3/4, soft-decision CODEC. The TDMA terminal model 1004 to 1005 price ranges from $30K to $300K for a full-capacity model. The full-capacity model 1004 has a 28 T_1 channel, fully-redundant, burst modem with an automatic switch-over (standby), a full-size memory, and a superframe synchronization function. The burst rate is Rb = 64 Mb/s with an acquisition time of 1 to 2 s. The largest capacity

equipment built at DCC is the model 1020, for Intelsat (with some Japanese-made parts). This unit provides SS-TDMA operation with 256 Mb/s total capacity, and its cost in small quantities is approximately $1.0M for the modem and baseband terminal alone.

In the opinion of DCC engineers, earth terminals with up to 50 voice channels are more cost-effective in the SCPC FDMA mode than in TDMA. In the TDMA system, terminal capacity of over 50 voice channels, with around 60 Mb/s burst rate, appears more economical. For low-cost modems, the cost breakover point with respect to burst rate is around 5 to 10 Mb/s, according to DCC. Above 20 Mb/s, a change in technology is required to achieve 30 or 64 Mb/s burst rates. To date, only a few 256 Mb/s burst-rate demodulators have been built. Engineers at DCC expect that the production cost of full modulator-demodulator, 256 Mb/s burst-rate, modem equipment (using an aggregate-rate converter) will be in the vicinity of $100K ($75K for the demodulator, $25K for the modulator) when it is available.

4.2.6 Terminal Technology

At Ford Aerospace, the current, small-terminal activities are at C-band and SHF band with 5-m and 8-ft special single-channel transponder (SCT) terminals. All major sub-assemblies like the HPA, LNA, and modems are built by in-house efforts. The cost of this fully-redundant, small-capacity terminal is around $400K, including modems, but no terminal equipment was built or designed for 20/30 GHz operation. In the opinion of Ford, to achieve a low-cost terminal, a low-cost modem is essential. Although TDMA has several distinct advantages, it is not cost-effective and only LSI technology can reduce this cost disadvantage. Ford Aerospace is actively engaged in monolithic microwave integrated circuit (MMIC) technology through company-funded, in-house efforts, for example, 12 GHz silicon-on-sapphire chips for direct demodulation at microwave frequencies. Another MMIC effort at Ford is a complete 20 GHz front end (LNA - mixer - IF plus broadband amplifier) all in chip form and eventually on a single substrate. The expectation from LSI and MMIC technology is that modem chips up to 2 Mb/s rate will cost $200/chip with a similar cost for FEC CODEC chips. For the high, downlink, burst rate, a direct demodulator at microwave frequencies rather than aggregate modems could be a cost-effective answer. The pure TDMA approach, in contrast to the hybrid mode, will get a boost from technology, according to Ford, since 50 Mb/s chips are available and implemented now, and chips for 250 Mb/s might be produced by 1985 to 1987.

Digital Communications Corp. developed a new system, the so-called DYNAC (dynamic bandwidth assignment) system. DYNAC is a complete RF-IF-baseband small satellite terminal for intercompany locations, customer-premise installation, and thin-route TDM/TDMA access mode within a star network configuration. The terminal operates in SCPC, FDMA/TDM, or TDMA modes at C-band. A selection of transmission symbol rates is available from 268 kb/s to 4.0 Mb/s (expandable to 6.0 Mb/s). Remote terminals operate in a TDMA mode to the central terminal while the central terminal broadcasts in TDM to remote users. Remote terminals always communicate to one another through the large central terminal. The central terminal supports network management, timing, synchronization, and burst-control loops. The terminal effective isotropic radiated power (EIRP) per carrier is 63 dBW, the G/T is 22 dB/K, and the modulation uses rate-1/2 soft or hard decision coding and decoding. The terminal TDMA frame length is selectable from 10 ms to 250 ms. In the non-redundant configuration, the terminal sells for approximately $100K in quantities less than 50.

SECTION 5

SR-FDMA/FDM SYSTEM

The SR-FDMA/FDM access mode is described in detail in a previous NASA report (MTR-8311). This section provides only a general description and operational concept.

The system covers CONUS with 32 beams, as shown in figure 3-1. The CPS users are divided into two groups: users in metropolitan areas (CPS_1) illuminated by 0.35^o beams, and users in rural areas (CPS_2) illuminated by 0.7^o beams. The satellite does not provide on-board processing and the traffic is collected and distributed on a beam-to-beam basis by means of bandpass (BP) filters. CONUS is divided into five regions of approximately equal traffic. The regions consist of six to eight beams which are either all 0.3^o beams or include some 0.7^o beams. The available bandwidth is divided into CPS and trunking subbands. The CPS subband is divided into five bands of about 300 MHz for each region. The bandwidths assigned to the beams correspond to their traffic. In the present design, for the sake of simplicity, all the beams in a region carry equal amounts of traffic. Routing to appropriate beams is achieved by band allocation and filtering in the satellite. Within a beam, individual terminals are addressed by specific frequency assignments. Destination and routing are accomplished by appropriate filtering in the satellite in the following manner.

The receive antenna horns are connected first to the low-noise amplifiers. Then the beams (horns) of a region are combined in hybrid combiners. The output of the hybrid combiners is fed into BP filters that separate the traffic destined for CPS_2 downlink beams from the traffic destined for CPS_1 beams. These filters are connected to RF multiplexers that split the traffic into five groups according to the regional destinations. A total of 10 RF multiplexers select the traffic for the five regions. The multiplexer outputs that have the same destination region are combined in (five-port) RF hybrid combiners, as shown in figure 5-1. The outputs of these hybrid combiners are down-converted to a convenient IF frequency (1 to 2 GHz). Intermediate frequency (IF) multiplexers separate the traffic to individual beam subbands that arrive from different regions. The subbands are combined in IF hybrid combiners destined for the same beam. These IF hybrids are followed by up-converters and TWT power amplifiers. The number of IF filters in this system is equal to the product of the number of regions and the number of beams: $5 \times 32 = 160$. This number is significantly lower than in a design that does not use the regional concept.

ORIGINAL PAGE IS
OF POOR QUALITY

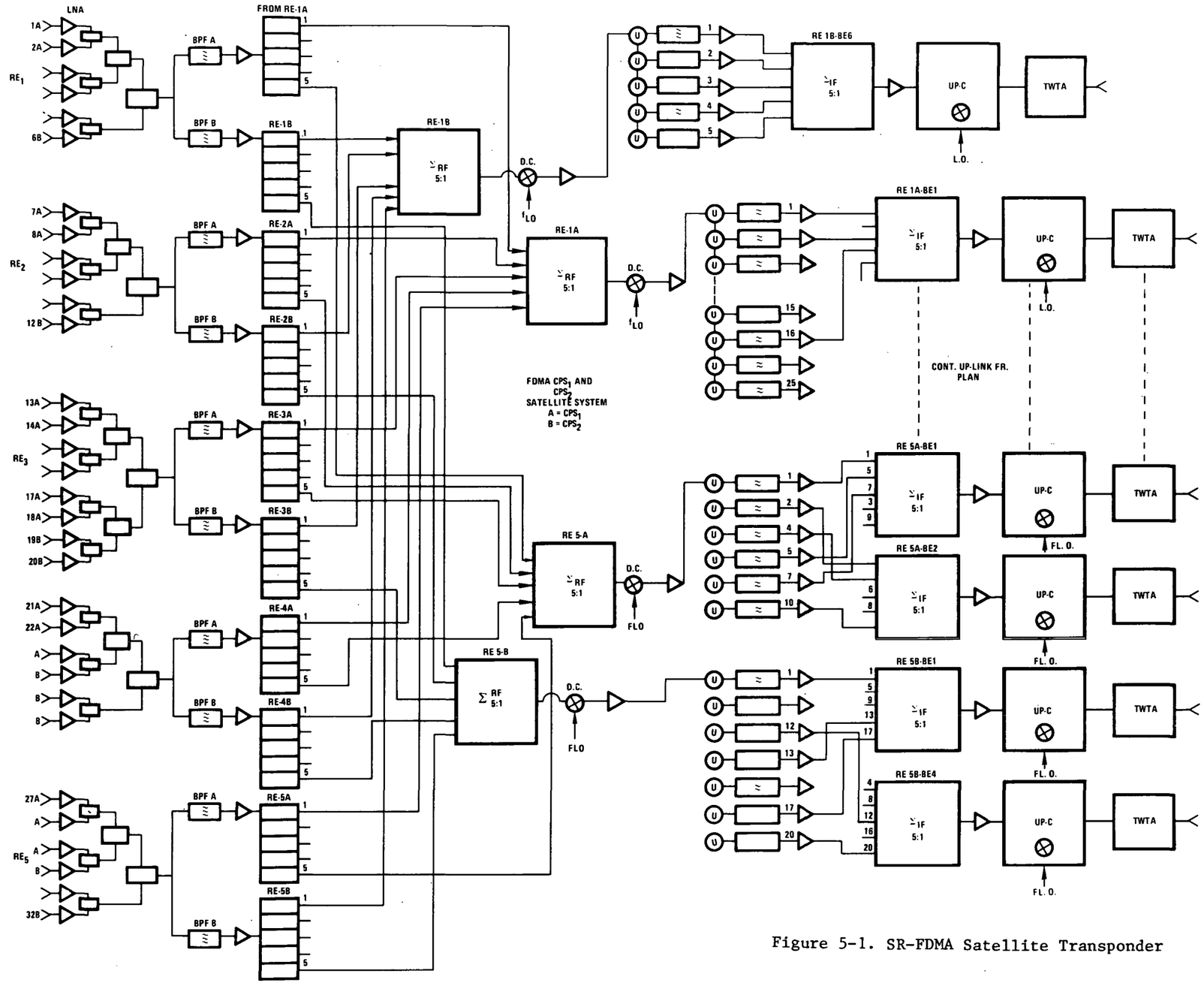

Figure 5-1. SR-FDMA Satellite Transponder

FOLDOUT FRAME

FOLDOUT FRAME

Page Intentionally Left Blank

In this system, no switching matrices are used. The system services 716 voice channels per beam for CPS_1 and 358 voice channels per beam for CPS_2 users (at 64 kb/s). The total capacity is 19,300 voice channels and the total throughput is 1.23 Gb/s. The satellite communications payload weight was calculated to include contributions of all major components and subassemblies by their weight and power. The total communications payload dry weight is estimated to be approximately 3200 lb without trunking transponders and 4600 W DC power is required, as shown in table 5-1.

The link budgets for a 3.0 m antenna CPS terminal are shown in tables 5-2 and 5-3. A relatively large margin of C/N_o is required (6 dB) to account for the additional uplink and downlink noise contribution and the large intermodulation noise due to FDMA operation. Multicarrier operation (FDM) requires a large backoff from the satellite TWT amplifier.

During rain, the CPS users switch to rate-1/2 convolutional coding-Viterbi decoding and improve their link performance by approximately 5.0 dB.

In summary, an SR-FDM/FDMA system is less cost effective than expected. This is due to the backoff mode of operation and the non-processing satellite. For a large number of small users this access mode has not only the lowest capacity, but also the highest cost per voice channel.

Table 5-1. SR-FDMA CPS_1 and CPS_2 Satellite Weight and Power

	Weight Unit (lb)	Total Weight (lb)	Power/DC Total (W)
Antenna System			
0.35^o	55	176	
0.70^o	37	80.5	
Transponder			
0.35^o / 0.70^o		2066.5	2014
Other Electronics & Battery		240	300
T.T. and Control		40	300
Structure			
Mech. - Therm.		200	---
Solar Array		312	158
Allowance at EOL		---	430
		3115	3202
Trunking		500	500
Communications Related Weight+		3615	3702

+Communications Related Weight includes the items listed and is a term defined for purposes of this report. It should not be confused with conventionally employed "communications payload" or "satellite dry weight".

Table 5-2. SR-FDMA CPS_1 and CPS_2 Users
Link Budget for 30 GHz Uplink

Parameter	CPS_1 8 ch x 64 kb/s	CPS_2 4 ch x 64 kb/s
Antenna Size (m)	3.0	3.0
Gain (dB)	56.5	56.5
Terminal $EIRP_{eff}$ (dBW)	58.5 (1.6 W)	61.5 (3.2 W)
Path Loss (dB)	-213.0	-213
Rain Loss (dB)	-10.0	-10
Miscellaneous RF Losses (dB)	-5.0	-5
Satellite Antenna $Gain_{eff}$ (dB)	49.0	44.0
Satellite Noise Temperature T_{sat} (K)	1500	1500
Satellite $(G/T)_{eff}$ (dB/K)	17.2	11.2
$(C/kT)_{UL}$ (dB-Hz)	76.3	73.3
Margin (dB)	19.3	19.3

Table 5-3. SR-FDMA CPS_1 and CPS_2 Users
Link Budget for 20 GHz Downlink

Parameter	CPS_1 8 ch x 64 kb/s	CPS_2 4 ch x 64 kb/s
Satellite Antenna $Gain_{eff}$ (dB)	49.0	43.0
Satellite $EIRP_{eff}$ (dBW)	43	40.0
P_{sat}/Beam (W)	18	
Atmospheric Loss (dB)	-2	-2.0
Miscellaneous RF Losses (dB)	-5	-5.0
Path - Loss (dB)	-210	-210.0
Terminal Noise T_{ET} (K)	1000	1000
$(G/T)_{ET}$ (dB/K)	23.0	23.0
$(C/KT)_{DL}$ (dB/Hz)	77.6	74.6
Margin (dB)	20.6	20.6
$(E_b/N_o)_{eff}$ (dB)	16.9	16.9

SECTION 6

SS-TDMA/TDM SYSTEM

A key feature of the SS-TDMA/TDM system is that the satellite provides adaptive rain compensation. Experimental data shows that less than 25% of CONUS experiences rain at any time; therefore, only a fraction of the CPS users need rain compensation. Rain attenuation can be compensated for with sufficient rain margin; 10 dB uplink and 5 dB downlink margins result in a 99.5% link availability for most of CONUS. The 10 dB uplink rain margin could be obtained by a 10 dB over-design of the terminal transmitter. Instead, this SS-TDMA system achieves a cost reduction by allocating only 5 dB to the terminal. The remaining 5 dB margin is obtained by processing in the satellite. Since only a fraction of the users (25%) may require rain compensation at any given time, processing for all users is not necessary and results in a complex, heavy, power-consuming satellite.

Those CPS_1 users that do not experience rain attenuation are not processed but switched to their destinations. The CPS_1 users that experience moderate rain attenuation are routed to hard-decision processors in the satellite which furnish a 5 dB margin. Finally, the CPS_1 users that experience heavy rain are routed to soft-decision processors (that include decoding/encoding) which furnish an 8 dB margin. The routing of an uplink signal to a processing or a switching transponder is achieved by appropriate frequency assignments.

The CPS_2 beams have a 6 dB lower gain than the CPS_1 beams. To offset this imbalance and use identical terminal transmitters, all CPS_2 terminals operate at half the CPS_1 uplink burst rate and use processing in the satellite. Those CPS_2 users that do not experience rain attenuation are routed to hard-decision processors, while those that experience rain are routed to soft-decision processors (which provide decoding/encoding). The routing to the processors is accomplished by means of a special frequency assignment in a beam.

Four simultaneous carriers for CPS_1 users in every uplink beam reduce the uplink burst rate and terminal cost. One of these carriers (the "special" carrier) is allocated for rain adaptation and processing, while the others route the users by switching matrices. Also, in the downlink beam four carrier frequencies are assigned for CPS_1 users. The CPS_1 uplink burst rate per carrier is 18 Mb/s, identical with the downlink.

The CPS_2 users operate with five simultaneous carriers in every uplink beam. Two of these carrier frequencies are multiplexed in pairs, while the fifth carrier supports those CPS_2 users who need soft-decision processing due to excessive rain attenuation and routes them to the processor. The CPS_2 users access the satellite with an uplink burst rate of 9 Mb/s per carrier, providing them with a 3 dB improvement in link performance. The CPS_2 downlink traffic is serviced by two carrier frequencies for each beam. In the processing transponder, the CPS_2 uplink TDMA frame is reformatted to be identical with the CPS_1 downlink frame in length, format, and burst rate.

6.1 SATELLITE DESIGN CONCEPTS

The satellite supports 86 switched RF channels for the three fixed CPS_1 carriers (22 beams) and the four CPS_2 carriers (10 beams). It also supports 32 processed RF channels; 24 channels operate with hard-decision demodulators and 8 channels use soft-decision demodulation with rate-1/2 decoding and reencoding on board the satellite. The signals received by the antenna horns are amplified by low noise amplifiers and are then down-converted to a convenient 2 to 4 GHz IF frequency. The down-converters are followed by a four-port IF multiplexer before switching. The switching is accomplished according to destination on a beam-to-beam principle by a 96 x 96 IF switch matrix which, for ease of fabrication, is realized by nine submatrices (32 x 32 each). The switching process is described in section 6.2. Since there are 32 beams, there are 32 horns, LNAs, down-converters, and IF multiplexers in the satellite. The IF multiplexer selects the four RF channels in the beam; f_{1i}, f_{2i}, and f_{3i} are connected to matrices S_1, S_2, and S_3 and are switched to the desired downlink beam and downlink frequencies, while f_{4i} is further down-converted to a second IF frequency (70 MHz). The 32 down-converted IF signals from f_{4i} (coming from 32 receive horns) are then switched by a 32 x 32 input IF_2 switch matrix to the processors, see figure 6-1. From this input, 24 channels selected by the network controller are processed in the hard-decision demodulator while the remaining eight IF channels are processed in the soft-decision demodulator/decoder. The CPS_2 users undergo a similar routing, except that a fifth carrier, f_{5i}, is used for rain adaptation. Significant satellite hardware savings can be achieved if a high-speed demodulator (18 Mb/s) is used for demodulating two carriers. The incoming carriers are multiplexed by means of a high-speed switch. This concept employs only 20 demodulators instead of 40 but requires a fifth carrier frequency for rain compensation. The complete SS-TDMA satellite block diagram is shown in figure 6-2.

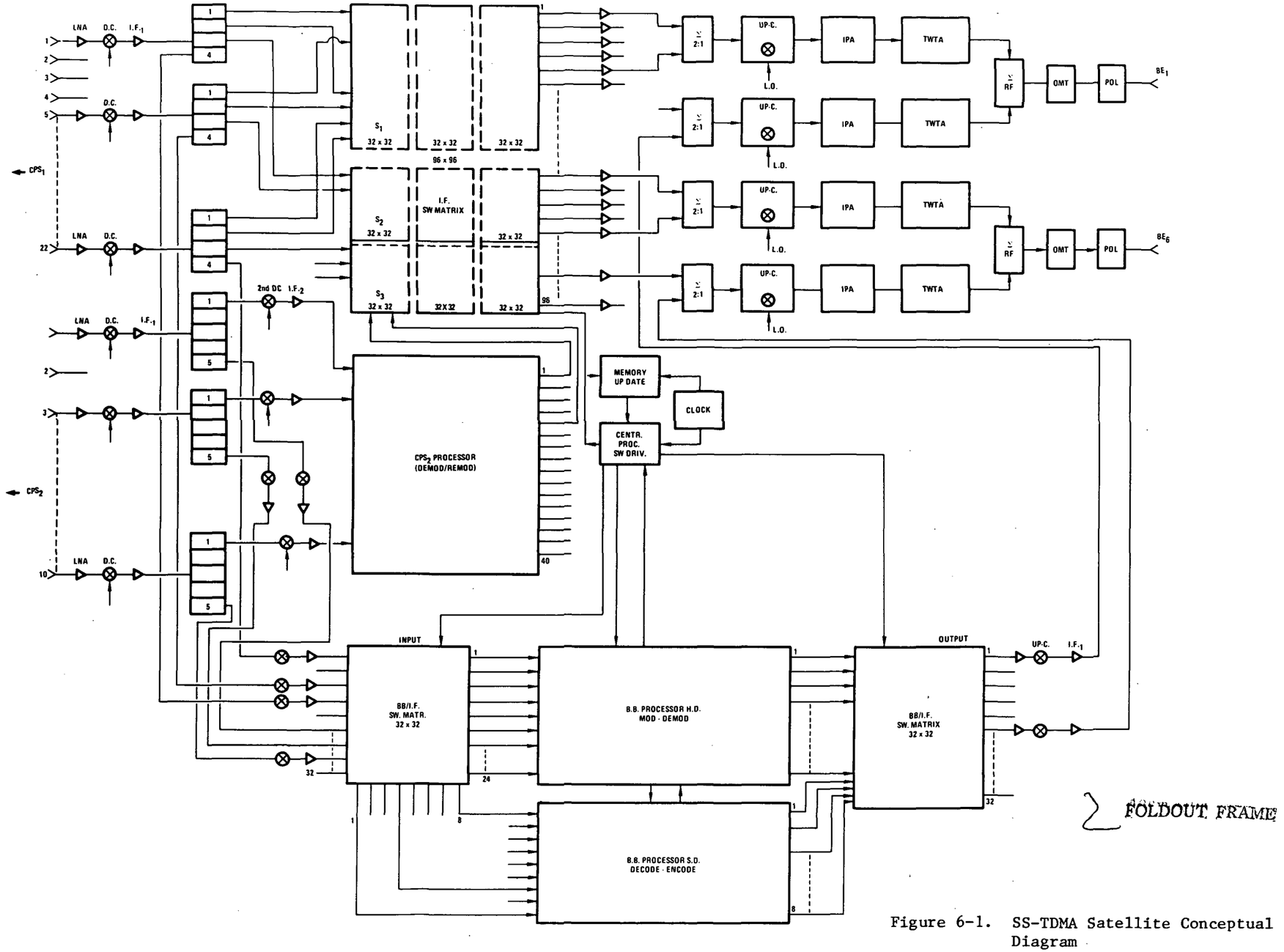

Figure 6-1. SS-TDMA Satellite Conceptual Diagram

ORIGINAL PAGE IS OF POOR QUALITY

Page Intentionally Left Blank

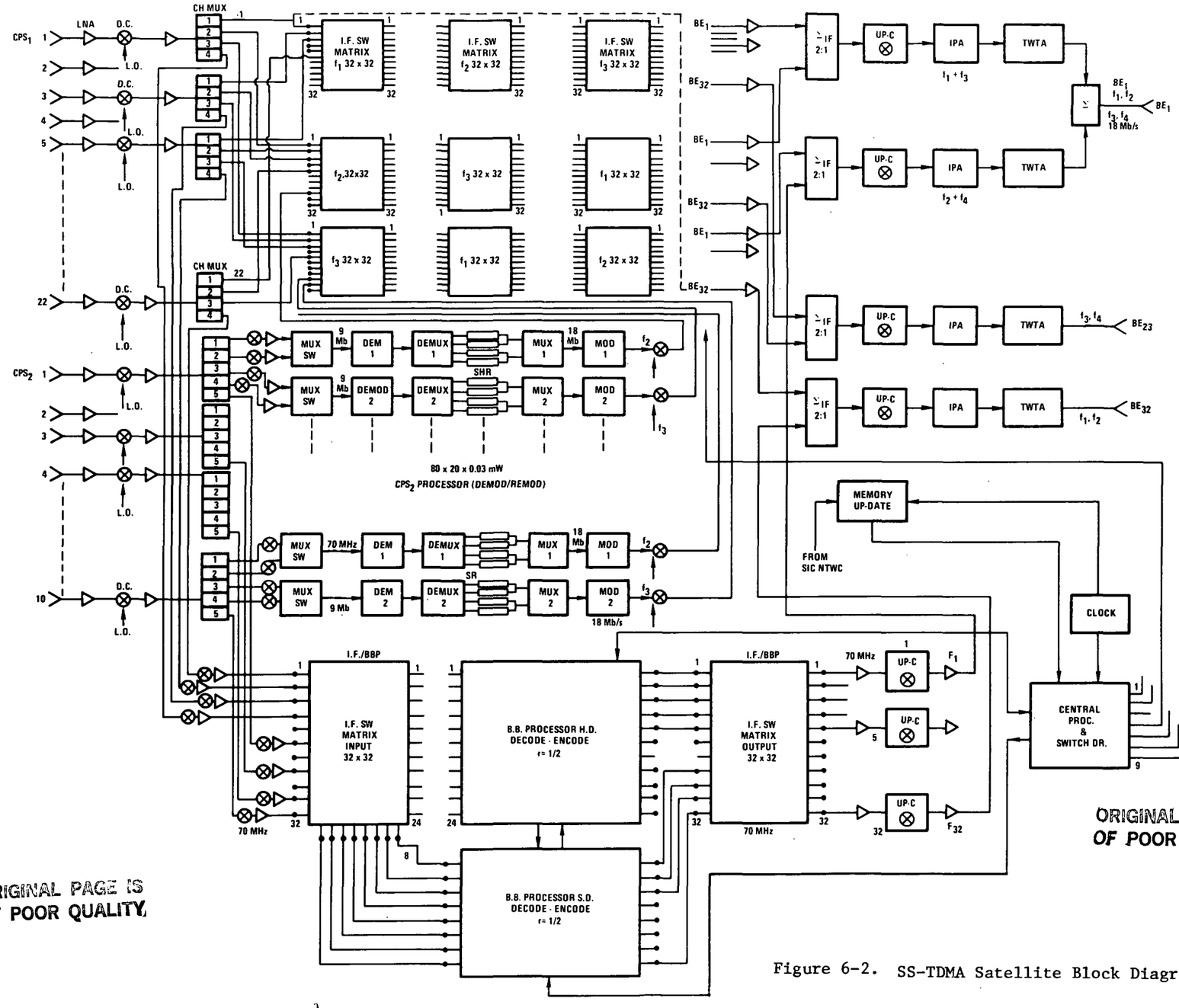

ORIGINAL PAGE IS
OF POOR QUALITY

Figure 6-2. SS-TDMA Satellite Block Diagram

FOLDOUT FRAME

The processor outputs, both hard-decision (24) and soft-decision (8), are switched by a 32 x 32 output IF switch matrix for further up-conversion. Subsequently they are combined with the switched-CPS_1 traffic and drive the 20 GHz TWT amplifiers. For each downlink beam, two 3 dB IF hybrid combiners are used. The hybrid combiner has two input signals, either from the switch or from the processor. The total number of IF hybrid combiners for CPS_1 is equal to $N_{beam} \times 2 = 22 \times 2 = 44$. The IF hybrid combiner is then followed by an up-converter to the 20 GHz band and a TWT amplifier. A single TWTA amplifies two carriers; therefore, it generates very low in-band intermodulation. The two TWTA outputs are then combined in a 3 dB power combiner and support a single downlink beam.

All CPS_2 users are converted to baseband and switched to their destination after remodulation except those who operate on the special rain frequency, f_5. The IF multiplexers separate the five uplink carriers. After down-conversion, the uplink will be demodulated and demultiplexed in pairs by a single demodulator (18 Mb/s). This is followed by a demultiplexer that feeds the four shift registers of appropriate size and speed. The outputs of the four shift registers are combined and drive the output multiplexer with a single input to the 18 Mb/s QPSK modulator. The modulator output at 70 MHz is up-converted to the first IF frequency band (2 to 4 GHz) and returns to the IF switch matrix, SW_1. For the CPS_2 users, there are 20 demodulators demultiplexers and 20 multiplexers and modulators (one for each downlink frequency) in the satellite processor. The frequency and beam addresses are stored in the satellite memory. A central processor controls the on-board memory and the switching sequence of the IF matrices. The switching system provides an equal path delay for all CPS channels, regardless of whether they are processed or switched. The CPS_2 users in rain transmit on the fifth frequency, f_{5i}, and are switched by a 32 x 32 IF switch matrix. The matrix is followed by a soft-decision processor (demod decode/mod/encode) for maximum rain margin.

6.2 OPERATIONAL CONCEPT OF THE 96 x 96 SWITCH MATRIX

In the CPS_1 portion of the satellite, each carrier frequency can have 32 beam destinations; therefore, a 32 x 32 matrix is required. Since the system uses three carrier frequencies, a 96 x 96 matrix can support all addressing alternatives. The demultiplexed incoming frequencies, f_{1i}, from the 32 IF multiplexers are connected to the input switch matrix (SW_{1i}). Similarly, the carrier frequencies, f_{2i} and f_{3i}, are connected to the SW_{2i} and SW_{3i} matrices, respectively. If the signal must be transmitted on carrier f_{1k} in a given downlink beam, the signal path will be from SW_{1i} to SW_{1j} and finally to SW_{1k}, as shown in figure 6-3. The SW_{1k}

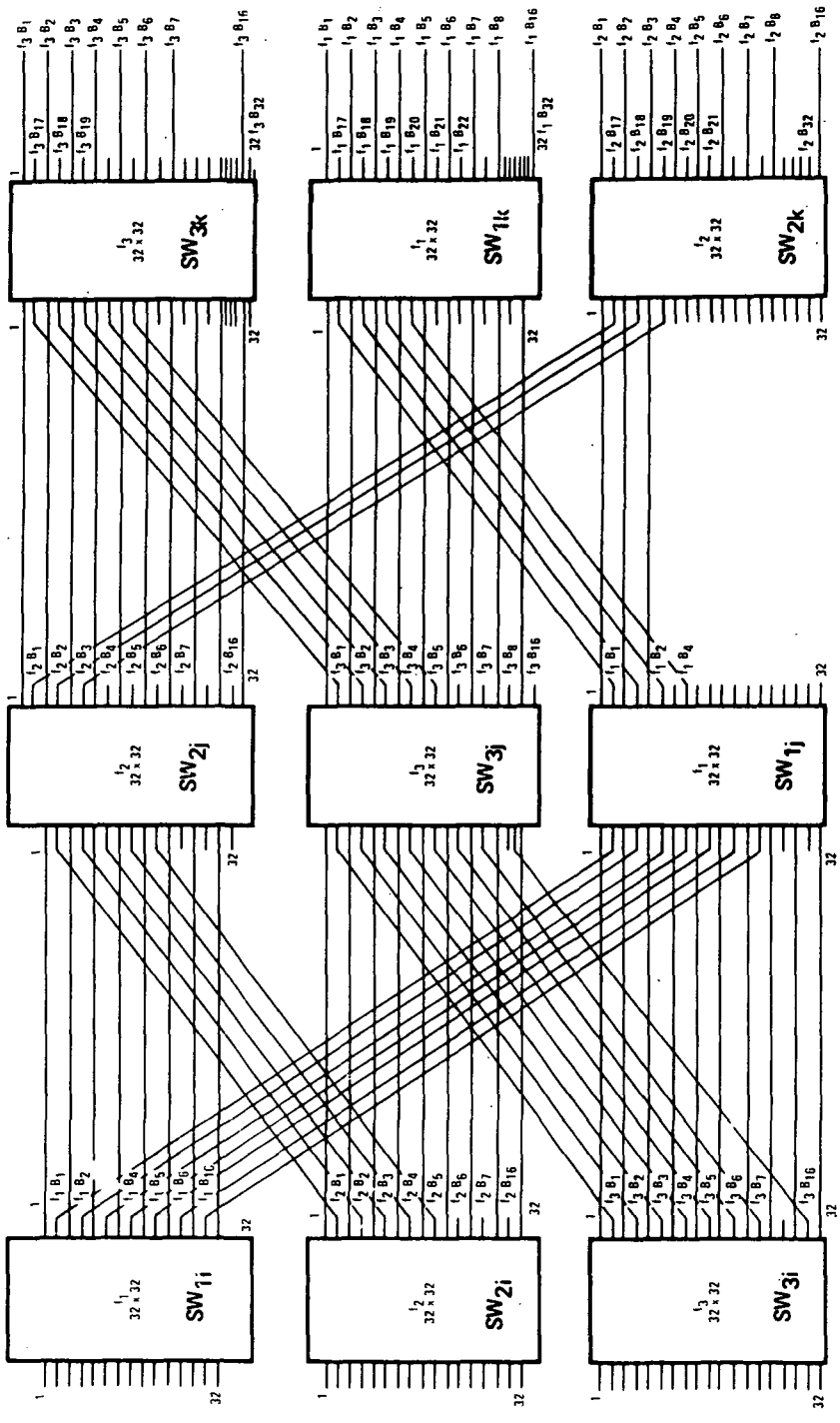

Figure 6-3. 96 x 96 IF Switch Matrix

switch matrix selects the appropriate beam for frequency f_{1k}. If the f_{1i} uplink user's address calls for the f_{2k} frequency in the downlink, the f_{1i} signal will not be switched by SW_{1i}, but will pass to switch matrix SW_{2j}. From here the path continues to SW_{2k} and finally to any of the 32 beams.

If the destination requires downlink frequency f_{3k}, the switch SW_{2j} passes the request to SW_{3k} for final beam selection addresses. The same logic and switching sequence is applied to input signal f_{2i}, which is switched to either f_{2k}, f_{1k}, or f_{3k} downlink frequencies for any of 32 beams. All incoming signals pass through three cross points before arriving at their final destination and all the signals have equal path length delay. The 1024 cross point per switch matrix design uses GaAs MESFET dual-gate, switch-amplifiers and crossbar switches. The anticipated DC power necessary to drive the switches is 5 V/5 mA per cross point and a total of 25.6 W per single 32 x 32 switch matrix. Therefore, the total power consumption, not including drivers, is 9 x 25.6 W = 230.4 W DC. The expected isolation between output ports exceeds 26 dB while total insertion loss is about 5 to 10 dB.

The required switching time is approximately 20 ns (1/10 of the 200 ns guard time) can be achieved with current technology. The switch reconfigures to its initial state at the end of a frame time (5 ms).

6.3 TDMA FRAME ORGANIZATION

The TDMA frame organization is shown in figure 6-4 for both CPS_1 and CPS_2 users. The selected frame time is 5 ms for CPS_1 and 10 ms for CPS_2 based on 18 Mb/s and 9 Mb/s uplink bursts rates, respectively.[2] The frame organization is common to both kinds of users. The number of preamble bits in a frame is 3600; therefore, the overall frame efficiency is 96%. The guard time between data slots is 0.4% of the total frame time (220 ns). The numbers of bits in a CPS_1 data slot is 320.

In the CPS_1 preamble, 220 bits are used for carrier/bit time recovery, 80 bits are used for unique word burst synchronization, and 20 bits for signaling bit error rate (BER) measurements. A single CPS_1 frame has 270 data slots and 30 signaling channel slots (64 bits each).

The common signaling channel in a frame, S_i, is used for bit synchronization, initial acquisition, orderwire, and future demand assignment multiple access (DAMA) control. The selected synchronization mode is open-loop and the terminal updates its

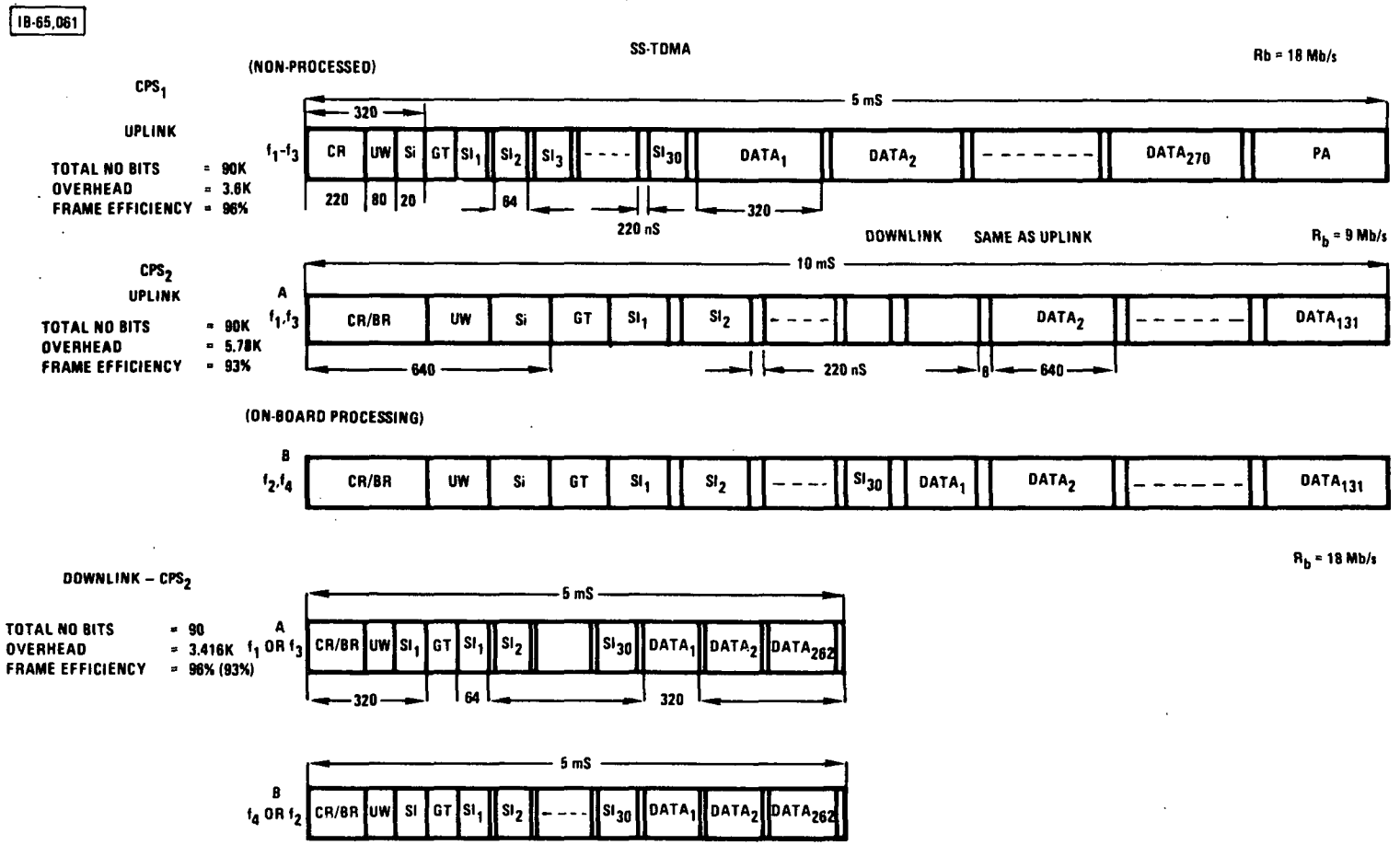

Figure 6-4. TDMA Frame Organization

timing reference via the common signaling channel in every ninth frame (or 45 ms) with the reference station which in turn locks itself to the satellite time and frequency standard.

The CPS_2 uplink frame consists of 131 data slots (640 bits each) and uses the same preamble and signaling channel organization as the CPS_1, but with twice as many bits. The length of the preamble is selected to be equal to a single data burst for flexibility. This organization makes it possible to slide the preamble into any position within the frame.

The downlink frame organization for CPS_1 is the same as the uplink. The CPS_2 frame is reformatted in the satellite so that the downlink frame is identical with the CPS_1 frame. The CPS_2 downlink uses two-carrier frequencies per beam due to the higher (2 x 9 Mb/s) burst rate.

6.4 LINK BUDGETS

The key feature of this system is allocating a minimum rain margin to the terminals and still achieving the 99.5% link availability. The remaining rain margin is applied adaptively in the satellite; therefore, the user is guaranteed satisfactory operation during rain. The proposed adaptive rain compensation budget is detailed in table 6-1. Initial rain margin is set to 5.0 dB without processing or coding. In case of moderate rain, the CPS_1 users are still routed through the non-processing part of the satellite, but use end-to-end, rate-1/2 coding. When this margin is exceeded, the users request a change in frequency and slot assignment. Then, through hard-decision processing, another 3 dB margin is gained. A soft-decision processor provides an additional 2 dB margin. The maximum rain margin available is 16 dB (5 dB terminal over-design, 3 dB from processing, 5 dB from coding, and 3 dB from a data rate reduction). CPS_2 users can only obtain 12 dB total rain margin. The on-board selection of coding decision and coding rate provides great flexibility in satellite bandwidths and power allocation between rainy and clear downlinks.

The link budgets for uplink and downlink are shown in table 6-2 and table 6-3, respectively. The CPS_1 terminal design is similar to the CPS_2 design (same uplink EIRP) with the exception that the CPS_1 terminal is designed for a nominal eight voice channel operation, while the CPS_2 terminal allows only four voice channels. Tables 6-2 and 6-3 indicate the operating link margin and C/N_o in clear weather for both users, and for users in the rain supported by processing. The downlink budget, after deducting rain losses,

Table 6-1. Uplink Adaptive Rain Compensation

	CPS_1	CPS_2
Initial Rain Margin Without CODEC or Processing	4.0 dB	4.0 dB
Rain Margin (End-to-End Coding r = 1/2)	9.0 dB	9.0 dB
Rain Margin (Processing and Coding r = 1/2)	12.0 dB	9.0 dB
Rate Change	3.0 dB	3.0 dB
Total Rain Margin	15.0 dB	12.0 dB
Soft Dec/Decode - Encode Demod - Remod	10%	20% Capacity
Demod/Remod	25%	100% Capacity

Downlink Adaptive Rain Compensation Steps

Not Processed - Not Coded
Coded but Not Processed
Processed but Not Coded
Processed and Coded r = 1/2
Processed and Coded r = 3/4

Table 6-2. SS-TDMA System
Link Budget for 30 GHz Uplink

	Terminal Type and Data Rate			
	8 x 64 kb/s CPS_1 in clear	4 x 64 kb/s CPS_2	CPS_1 in rain	CPS_2
	w/o CODEC	w/o CODEC	with CODEC	with CODEC
Antenna Size (m)	3.0	3.0	Same	Same
Antenna Gain (dB)	56.5	56.5	Same	Same
Terminal EIRP Eff (dBW)	66.4	66.4	Same	Same
Path Loss (dB)	-213.0	-213.0	Same	Same
Rain Loss (dB)	-4.0	-4.0	-12.0	-10.0
Misc. RF Loss (dB)	-5.0	-5.0	-5.0	-5.0
Edge of FOV Loss	-4.0	-4.0	-4.0	-4.0
S/C Antenna Gain (dB)	53.0	47.0	53.0	47.0
S/C Noise Ts (K)	1500	1500	Same	Same
S/C (G/T) eff (dB/K)	17.3	11.3	17.3	11.3
$(C/KT)_{UL}$ (dB/Hz)	89.3	83.3	86.3	83.3
R_b Burst Rate (Mb/s)	18.0	9.0	18.0	9.0
Margin (dB)	16.7	13.8	13.8	13.8
E_b/N_o Req. (dB) for BER = 10^{-6}	13.0	13.0	13.0	13.0

Table 6-3. SS-TDMA System
Link Budget for 20 GHz Downlink

	Terminal Type and Data Rate			
	8 x 64 kb/s		4 x 64 kb/s	
	CPS_1	in clear	CPS_2	CPS_1 in rain	CPS_2
S/C Antenna Gain Eff (dB)	49.0		43.0	Same	Same
S/C EIRP Eff (dBW)	55.4		52.4	55.4	Same
Rain Loss (dB)	-2.0		-2.0	-7.0	-7.0
Path Loss (dB)	-210.0		-210.0	-210.0	-210.0
Terminal Noise T_E (K)	1000		1000	Same	Same
$(G/T)_{ET}$ Eff (dB/K)	22.6		22.6	22.6	22.6
$(C/KT)_{DL}$ (dB/Hz)	89.6		86.6	86.6	86.6
Margin (dB)	17.1		14.1	14.1	14.1
Overall C/KT (dB/Hz)	85.9		86.6	86.6	86.6
(E_b/N_o) Eff (dB)	13.9		13.1	14.1	14.1
Net Link Margin (dB)	0.4		1.0	3.0	0.6

leaves about 3.0 dB overall margin for CPS_1 and 0.6 dB for CPS_2. The various losses are detailed in table 6-4.

6.5 SS-TDMA TERMINAL DESCRIPTION

The terminal operates with a dual-feed, 3.0 m dish antenna and a 10 W RF power TWT amplifier. The LNA front end with 400 K noise temperature is directly mounted on the antenna pedestal. The received signal from the LNA by an electromechanical switch and bandpass filter will pass either f_1 or f_4 (clear or rain mode operation) to the first RF down-converter. The down-converter local oscillator (LO) signal is supplied by a 1.44 GHz synthesizer and times-15 multiplier chain, see figure 6-5. The down-converters are followed by a second down-conversion for each RF frequency; then the 70 MHz IF signals are combined in a 70 MHz IF combiner. This combiner supplies the common input signal to the QPSK demodulator and the rate-1/2 decoder in the terminal. From the output buffer, the signal passes to the demultiplexer buffer, then to the digital to analog converter and finally to the analog data and voice output as shown on the complete block diagram of the terminal in figure 6-6.

Similarly, the digital input from the multiplexer buffer will go to the rate-1/2 encoder, then to the QPSK modulator, before being up-converted to RF signal for power amplification. In the transmitter section of the terminal, two uplink chains will be used: one for uplink frequency f_1, and another for frequency f_4, if needed.

The key terminal parameters are monitored and controlled by a processor terminal control unit. The terminal frequency synthesizer can be a separate design for the receiver or common with the transmitter synthesizer, as shown in figure 6-5.

6.6 SATELLITE WEIGHT AND POWER

The SS-TDMA satellite DC power allocation is shown in table 6-5. The satellite weight and power budget is shown in table 6-6. The antenna system accounts for 256 lb, the transponder calls for approximately 1865 lb, and the solar array is 312 lb. The total communication payload dry weight is approximately 3100 lb; to this the trunking transponders add another 520 lb. The satellite DC power requirement is approximately 1800 W for RF power generation, and 870 W for signal processing. The total DC power requirements are 4600 W, including approximately 500 W for trunking traffic support.

Table 6-4. Various Characteristics and Loss Summary

Terminal	CPS_1	CPS_2
Transmit Power (dBW-W)	10.0 (10.0W)	10.0 (10.0W)
Feed Loss (dB)	-0.5	-0.5
Antenna Gain (dB)	56.5	56.5
Eff. Radiated Power (dBW)	65.4	65.4
Antenna Pointing Error (dB)	-1.0	Same
Atmospheric Loss (dB)	-1.0	Same
Polarization Loss (dB)	-2.5	Same
Total RF Loss (dB)	-5.0	-5.0
Implementation Loss Max (dB)	-2.5	-2.5
Margin (dB)	+1.0	+1.0
Spacecraft		
Feed Loss + W. G. Loss (dB)	-2.0	-2.0
Antenna Gain (dB) Min at -4 dB Edge	49.0	43.0
Antenna Pointing Error (dB) $\pm 0.1^{o}$	-1.5	-1.5
Rec Carrier Power (dBW)	-104	-110

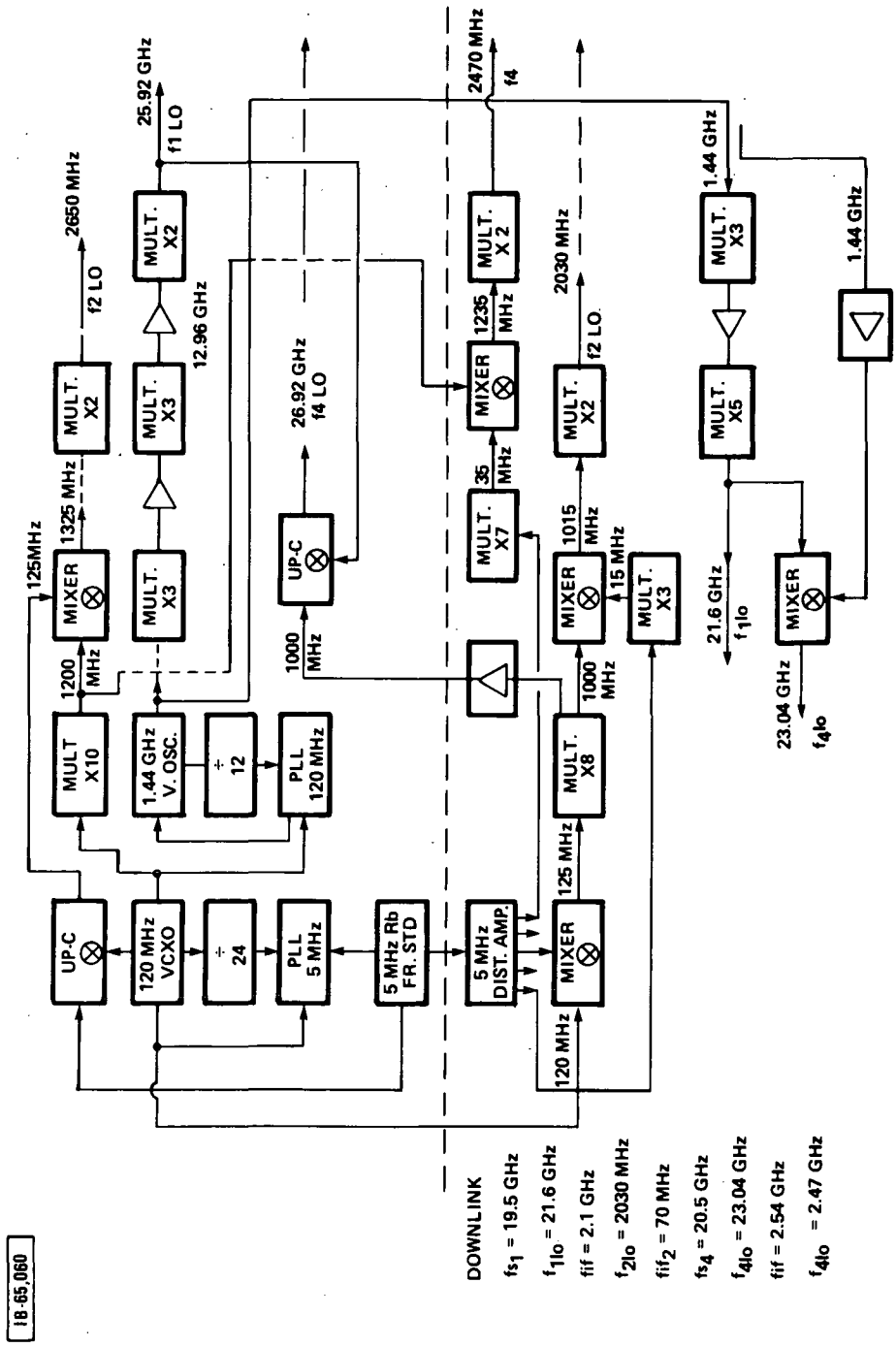

Figure 6-5. CPS_1 Terminal Dual Frequency Synthesizer

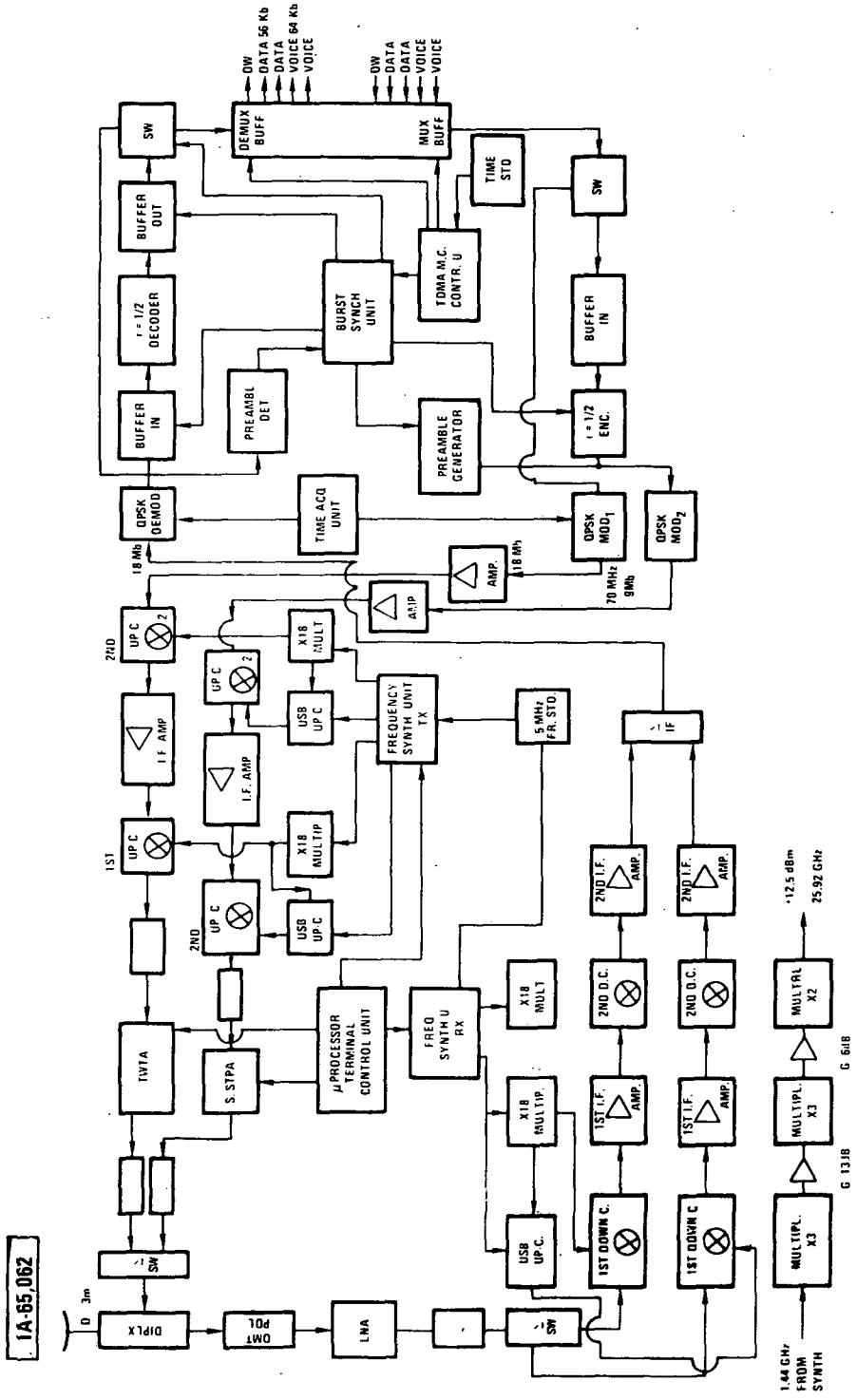

Figure 6-6. CPS_1 Terminal Block Diagram

Table 6-5. SS-TDMA Satellite DC Power Allocation

	CPS_1	CPS_2	Total	Trunking
$P_{RF}/N_C/N_B$	4.0 W	7.0 W	11.0 W	3.6 W
P_{RF} Total	352.0 W	140.0 W	492.0 W	58.0 W
P_{DC} Total	1035 W	412.0 W	1447.0 W	171.0 W
Overall Efficiency	34%	34%	34%	34%
Users (Throughput) (No. of Voice Channels)	23,670	5240	28,910 (1.85 Gb/s)	(1.0 Gb/s)

If CPS_1 use r = 1/2 coding at all times, then the DC power will be:

	CPS_1 (W)	CPS_2 (W)	Total (W)
$P_{RF}/N_C/N_B$	2.0	7.0	9.0
P_{RF} Total	176.0	140.0	316.0
P_{DC} Total	517.6	412.0	929.6

Table 6-6. SS-TDMA CPS_1 and CPS_2 Satellite Weight and Power

	Weight/Unit (lb)	Weight/Total (lb)	Power/DC Total (W)
Antenna System			
0.35^{o}	55	176	---
0.70^{o}	37	80.5	---
Transponder			
0.35^{o}			
0.70^{o}		1865.4	1795.0
IF Processor		223	870.0
Other Electronics and Battery		240	300.0
T. T. and Control		40	300.0
Structure Mech. - Therm.		200	---
Solar Array		312	158.0
Aollowance EOL		---	731.0
		3137.0	4154.0
Trunking		523.0	480.0
Communications Related Weight+		3600	4634.0

+Communications Related Weight includes the items listed and is a term defined for purposes of this report. It should not be confused with conventionally employed "communications payload" or "satellite dry weight".

SECTION 7

PR-TDMA/TDM SYSTEM

Two PR-TDMA exemplar system designs are presented in this section. Both systems employ four uplink carrier frequencies to reduce the terminal burst rate. However, one system uses a single downlink carrier in each beam (system 1) while the other uses two (system 2). System 1 requires a high burst rate, but its design results in lower satellite weight and power consumption. System 2 has a more complex satellite, but the burst rate is reduced. The burst rates of the CPS_2 terminals are specified to be one-half the burst rates of the CPS_1 terminals; this reduces the 6 dB link disadvantage of the CPS_2 users to 3 dB.

The satellite utilizes a baseband circuit switch, controlled by microprocessors, to route each of the 32 uplink beams to the appropriate downlink beams. Efficient and contention-free operation of the switch is ensured by a system-wide DAMA scheme. Users establish links to other users by sending a request to the satellite control center (SCC) which dynamically assigns specific transmit and receive time slots for each link. A network control station (NCS) in each beam provides local control functions.

In addition to baseband processing, the satellite also furnishes adaptive rain compensation by decoding and re-encoding user messages. One uplink carrier in each beam is reserved for this function. Every terminal operates on a preassigned carrier but is also capable of transmitting on this special carrier. On-board the satellite, the special carrier is routed to a coding-processor.

7.1 TDM FRAME ORGANIZATION

Since voice communications take place in real-time, the frame length must be kept reasonably short in order to avoid adding excessive delay to the round-trip propagation transmission time. Also, because each uplink frame is stored on-board the satellite before retransmission, a long frame requires very large memories. On the other hand, the frames cannot be too short or the system throughput efficiency will be low due to the TDM overhead. Also, the frames must provide sufficient signaling capacity, which is particularly important in DAMA systems.

The frame design must be flexible so that the CPS_1 and CPS_2 users, who have different burst rates and throughput capacities, can

be accommodated easily. Also, the frames must support encoded messages on an adaptive basis. Finally, the frame organization for CPS_1 and CPS_2 must allow exchange of traffic between the two services.

7.1.1 Uplink Frames

A 5 ms frame is a good compromise between throughput efficiency and additional transmission delays. The same frame duration is employed by CPS_1 and CPS_2 users. Cross-strapping of the CPS_1 and CPS_2 traffic is possible because their bursts contain the same number of message bits (regardless of the burst rate). Therefore, after demodulation in the satellite each burst can be processed, stored, and routed in the same fashion regardless of its source.

The uplink frame format for the uncoded CPS_1 traffic is shown in figure 7-1. The burst rate in this frame is 19.9 Mb/s. In every beam, preambles are transmitted by an NCS. The NCS must transmit four preambles simultaneously, one for every uplink carrier. The preamble contains synchronization and control data for use by the satellite. A guard time of 200 ns separates each burst in the frame.

A frame contains 30 signaling bursts. A signaling burst consists of 96 bits; 32 bits are for receiver synchronization and 64 bits carry useful information. Every user has access to the signaling network. A terminal must send a signaling burst for each active user. Since a frame contains 270 message bursts and 30 signaling bursts, the signaling burst for a particular user can be sent only once every nine frames. This results in a signaling data rate of 1.4 kb/s. All uplink signaling bursts are routed to the SCC.

The last group of bursts is for message transmission; 270 message bursts are sent in every frame. Each burst contains 352 bits; 32 bits for receiver synchronization and 320 bits of message data. (This number of message bits is determined by the 64 kb/s voice data rate.) Therefore, 270 individual voice channels can be handled by each uncoded uplink.

The end of a frame is marked by an end-of-frame guard time of 3.2 μs. This time period permits the satellite to complete its processing before the arrival of the next frame.

The uplink frames have an overhead of 13.2%. The large overhead is due to the use of synchronization bits in the individual

IA-64,809

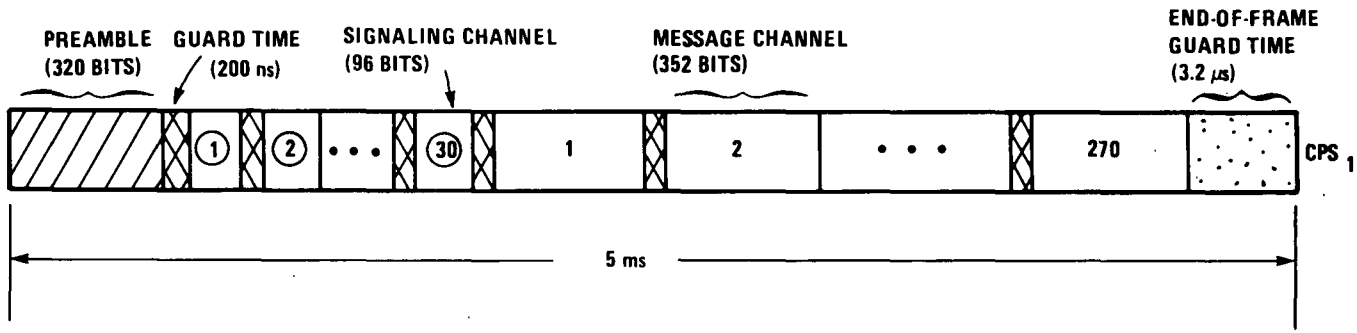

UPLINK BURST RATE = 19.9 Mb/s
FRAME DURATION = 5 ms
TOTAL NUMBER OF BITS PER FRAME = 99,504
TOTAL NUMBER OF OVERHEAD BITS = 13,104 (13.2% OVERHEAD)

1 PREAMBLE	320 BITS/FRAME
300 GUARD TIME SLOTS	1,200 BITS/FRAME
30 SIGNALING CHANNELS	1,920 BITS/FRAME + (960 BITS/FRAME FOR SYNC.)
270 MESSAGE CHANNELS	86,400 BITS/FRAME + (8640 BITS/FRAME FOR SYNC.)
1 END-OF-FRAME	64 BITS/FRAME

Figure 7-1. Uplink Frame Organization for Uncoded CPS_1

bursts. These synchronization bits are needed because the bursts that comprise a frame originate in different earth terminals.

The uplink frame format for the uncoded CPS_2 traffic is shown in figure 7-2. The burst rate in this frame is 9.9 Mb/s. The preamble, guard-time message bits, and end-of-frame marker in CPS_2 frames are identical to those in the CPS_1. However, due to the lower burst rate, the CPS_2 frame has a lower capacity: 15 signaling bursts and 135 message bursts. The overhead represents 13% of the CPS_2 frame.

The uplink frame organization for the CPS_1 and CPS_2 rain-compensation carriers is shown in figure 7-3. These frames provide access for coded message bursts on an adaptive basis. Coding is used to combat rain attenuation when the link rain margin is exceeded. Rate-1/2 coding is envisaged for this system.

Statistically, less than 25% of CONUS experiences rain at any time; therefore, only a fraction of the CPS users need to use coding. One uplink frame is allocated for rain compensation in every beam. Thus, as many as 25% of the users in a beam can simultaneously use the on-board coding processor to improve their link performance. A special frame is formatted to carry both coded and uncoded message data. In order to keep the frame simple, the uncoded and coded message bursts contain the same number of bits. This is possible because coding is coupled with a data-rate reduction at the encoder input. The frame design is flexible and allows the number of coded bursts to vary from zero to an entire frame (at the expense of the uncoded bursts). Each NCC transmits a special preamble the size of a message burst to separate the uncoded and coded bursts. Since this preamble has a standard size, it can be repositioned easily, in accordance with the demand for coded bursts. This preamble is always sent regardless of the number of coded message bursts. The satellite is constantly updated by the SCS in regard to the exact number of coded bursts in the special frame. Figure 7-3 depicts the situation in which one-third of the message bursts in the special frame are coded.

Although a fixed uplink carrier is assigned to every terminal, all the terminals can use the fourth uplink carrier (the rain-compensation carrier). Allocating time slots for the coded message bursts is a priority task; therefore, the uncoded bursts in the special frame will be preempted according to the demand.

IA-64,810

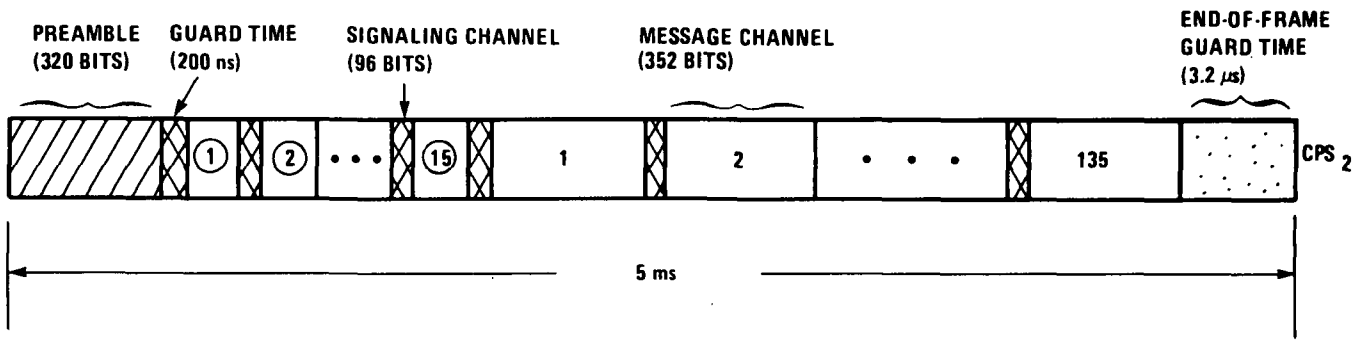

UPLINK BURST RATE = 9.9 Mb/s
FRAME DURATION = 5 ms
TOTAL NUMBER OF BITS PER FRAME = 49,644
TOTAL NUMBER OF OVERHEAD BITS PER FRAME = 6,444 (13.0% OVERHEAD)

1	PREAMBLE	320 BITS/FRAME
150	GUARD TIME SLOTS	300 BITS/FRAME
15	SIGNALING CHANNELS	960 BITS/FRAME + (480 BITS/FRAME FOR SYNC.)
135	MESSAGE CHANNELS	43,200 BITS/FRAME + (4320 BITS/FRAME FOR SYNC.)
1	END-OF-FRAME	64 BITS/FRAME

Figure 7-2. Uplink Frame Organization for Uncoded CPS_2

IA-64,811

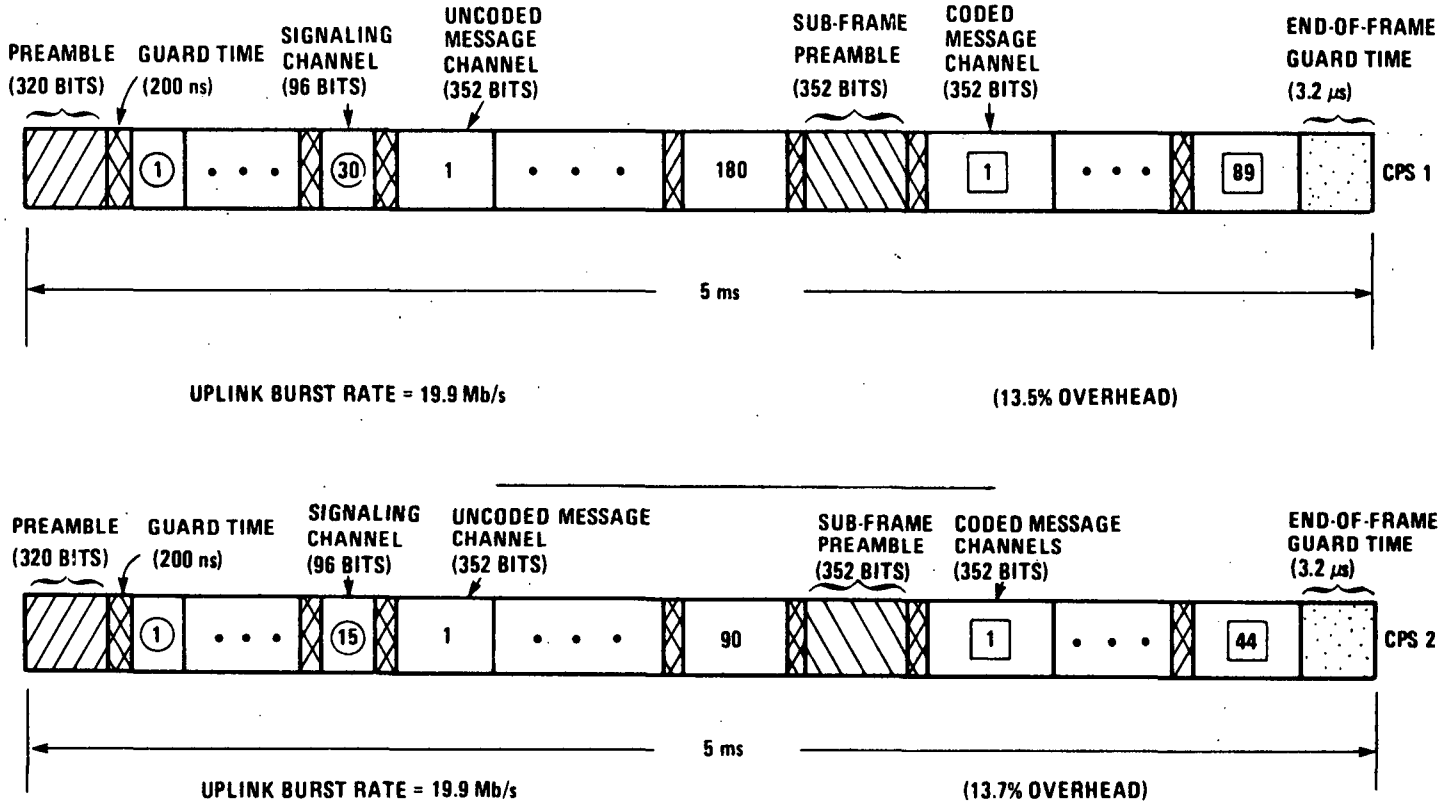

Figure 7-3. Uplink Frame Organization for Rain-Compensation CPS_1 and CPS_2

7.1.2 Downlink Frames

The CPS_1 and CPS_2 downlink frames are both 5 ms long. These frames consist of bursts that have been received by the satellite a frame time earlier. Since the bursts are retransmitted from one source (the satellite), there is no need for individual burst synchronization bits. The earth terminal receivers synchronize on the frame preamble. After frame synchronization, the earth terminal selects only the desired bursts. This greatly reduces the amount of frame overhead. A further reduction in overhead is achieved by using smaller guard times. Shorter guard times and higher burst rates in the downlink set additional requirements on the earth terminal receiver. The downlink frame for system 2 is similar to the frame for system 1. However, it has one-half the throughput capacity and one-half the burst rate of system 1.

Figure 7-4 shows the CPS_1 downlink frame for system 1. The frame contains a satellite-generated preamble that is used by the earth terminals for synchronization and control; the uplink preambles are not retransmitted. The guard times between frame bursts are composed of an 8-bit code. This unique code can be used as secondary synchronization information. The frame also contains the 120 signaling bursts that arrive at the satellite one frame time earlier from the SCC. Each frame contains 1079 message bursts. The odd number of message bursts is due to the special uplink preamble that is not transmitted in the downlink. These message bursts carry both uncoded and coded data. The coded bursts are not segregated in the downlinks as they are on the uplinks. Their positioning within the frame depends solely on their destination. There is no identification for the coded message blocks. Therefore, the receiving stations must be notified by the SCC or NCS whenever transmitting stations encode their messages. Each frame includes a 2.3 μs end-of-frame guard time that allows the satellite and the terminals to prepare for the next frame.

The CPS_1 downlink frames require a burst rate of 72.8 Mb/s. Approximately 5.1% of the frame bits is needed for overhead.

The TDM downlink frame organization for a CPS_2 beam is shown in figure 7-5. The frame contains a satellite-generated preamble, 4-bit guard times, 60 signaling bursts, 539 message bursts, and an end-of-frame guard time. This frame requires a burst rate of 36 Mb/s. About 4.2% of the frame bits are used for overhead functions.

IA-65,167

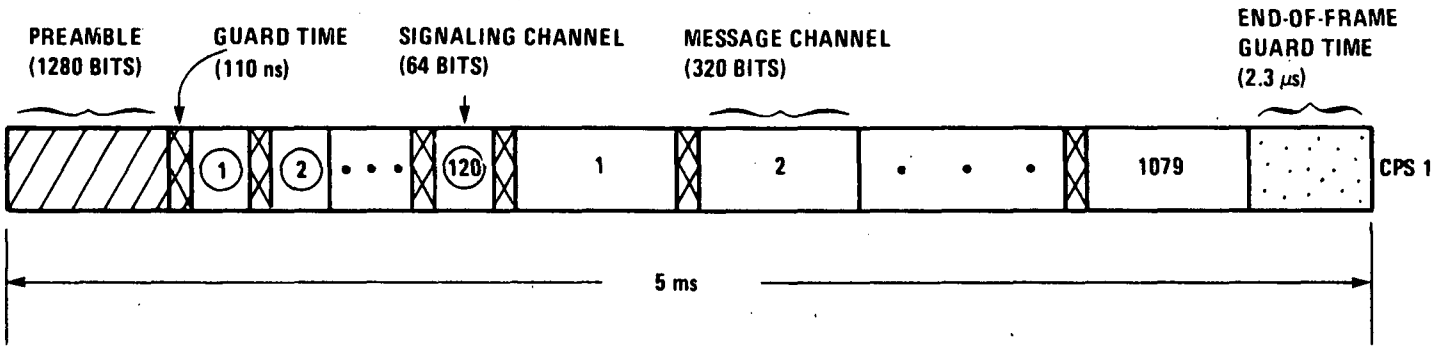

DOWNLINK BURST RATE = 72.8 Mb/s
FRAME DURATION = 5 ms
TOTAL NUMBER OF BITS PER FRAME = 364,000
TOTAL NUMBER OF OVERHEAD BITS PER FRAME = 18,720 (5.1% OVERHEAD)

1	PREAMBLE	1,280 BITS/FRAME
1199	GUARD TIME SLOTS	9,592 BITS/FRAME
120	SIGNALING CHANNELS	7,680 BITS/FRAME
1079	MESSAGE CHANNELS	345,280 BITS/FRAME
1	END-OF-FRAME	168 BITS/FRAME

Figure 7-4. Downlink Frame Organization for CPS_1

IA-64,812

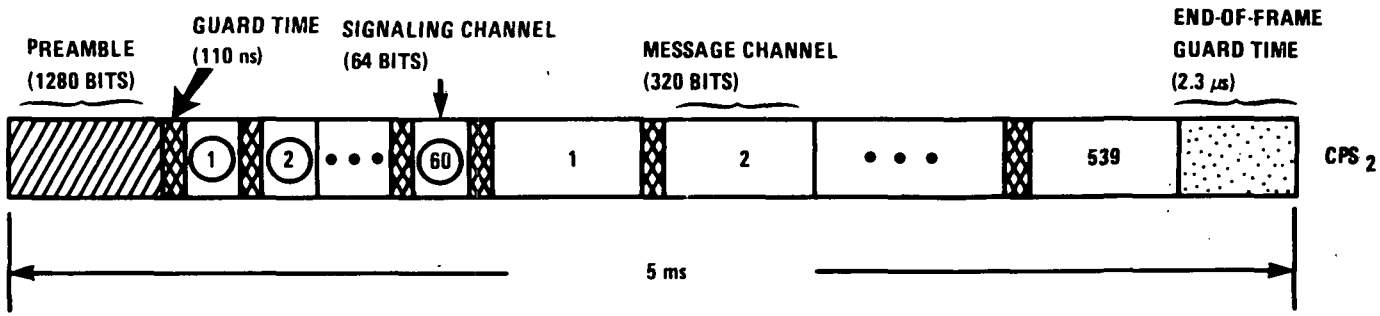

DOWNLINK BURST RATE = 36.0 Mb/s
FRAME DURATION = 5 ms
TOTAL NUMBER OF BITS PER FRAME = 180,080
TOTAL NUMBER OF OVERHEAD BITS PER FRAME = 7600 (4.2% OVERHEAD)

1	PREAMBLE	1,280 BITS/FRAME
599	GUARD TIME SLOTS	2,396 BITS/FRAME
60	SIGNALING CHANNELS	3,840 BITS/FRAME
540	MESSAGE CHANNELS	172,480 BITS/FRAME
1	END-OF-FRAME	84 BITS/FRAME

Figure 7-5. Downlink Frame Organization for CPS_2

7.1.3 Orderwire Frames

The orderwire uplink and downlink frames use the same burst rate. The frames are 5 ms long and require a burst rate of 45 Mb/s. The uplink frame contains 3240 signaling bursts from the SCC. They are sent via the satellite to the appropriate earth terminals by means of the CPS_1 and CPS_2 downlink carriers one frame later. The downlink frame contains 3240 signaling bursts sent to the SCC by the satellite. The satellite collects these bursts one frame period earlier from the CPS_1 and CPS_2 uplinks. About 7.8% of the frame bits is needed for overhead.

7.2 SYSTEM CAPACITY

The system includes 22 CPS_1 beams. Each of these beams supports 1079 voice channels. Thus, the system services a total of 23,738 voice channels, equivalent to a throughput of 1519 Mb/s for CPS_1. The system also includes 10 CPS_2 beams. Each of these beams supports 539 voice channels. The satellite services a total of 5390 CPS_2 voice channels or 345 Mb/s throughput. Including the 806 Mb/s of trunking throughput (see section 9), the total system throughput is 2.67 Gb/s.

7.3 PROCESSOR OPERATION

A simplified functional block diagram of the satellite CPS transponder is shown in figure 7-6. In every beam, the signals received in the satellite are amplified, downconverted, and demultiplexed into four separate channels. Then each channel is downconverted to 70 MHz and sent to a demodulator and input buffering subsystem. The frame preambles are used by the satellite for synchronization and control. The frame's signaling bursts are demodulated and sent to orderwire memories. These bursts are transmitted to the SCC via the orderwire downlink during the next frame period. Signaling bursts from the SCC arrive via the orderwire uplink and are sent to other orderwire memories where they are stored according to their destination. These bursts are distributed among the 32 downlink beams one frame time later.

The uncoded message bursts are demodulated by hard-decision demodulators and stored in message memories under the control of input microprocessors. The transponder contains 32 input microprocessors, one per uplink beam. The memory location in which a message block is stored depends on its downlink beam destination.

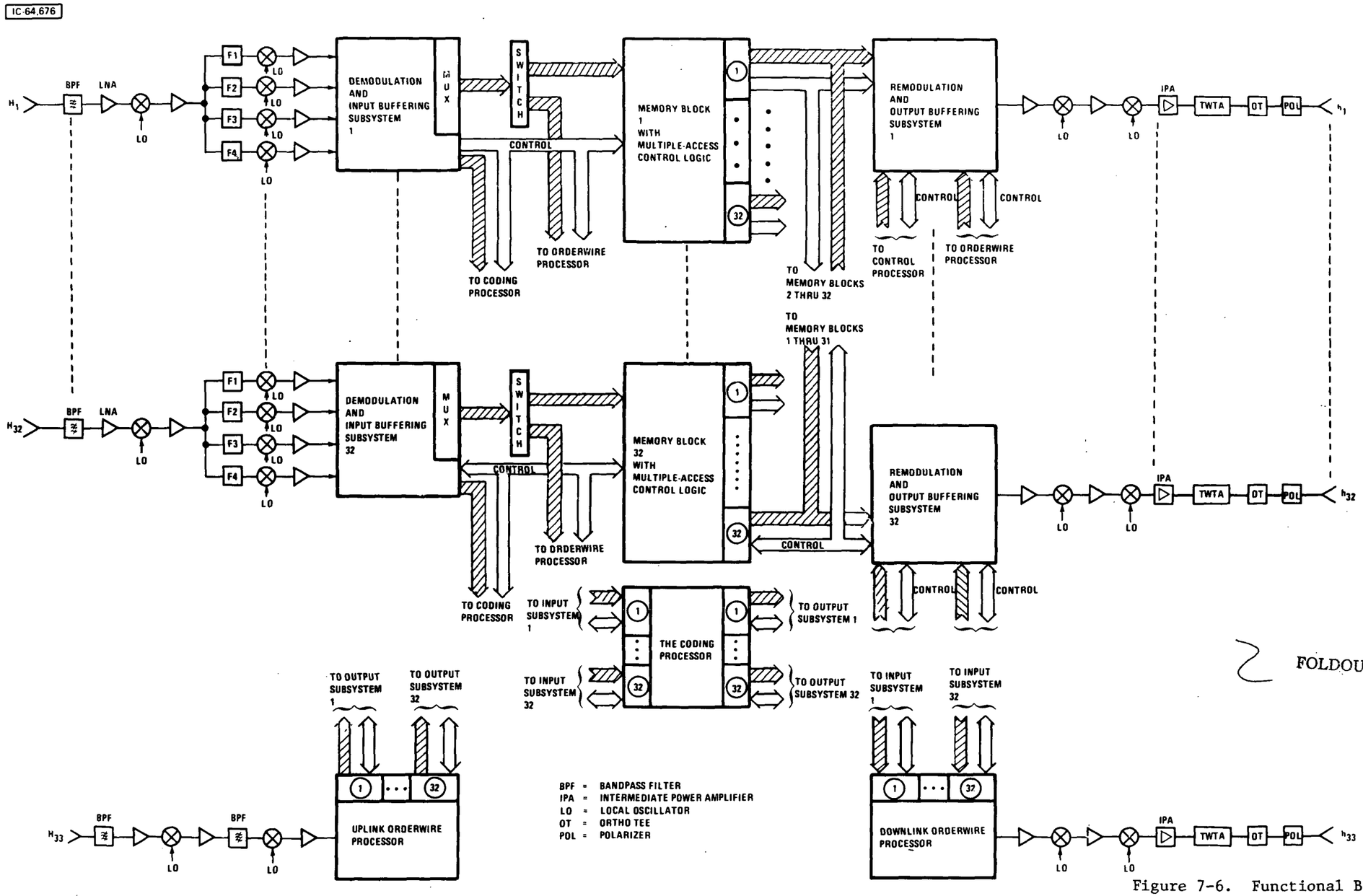

Figure 7-6. Functional Block Diagram of CPS Transponder

Page Intentionally Left Blank

The coded message bursts are routed to soft-decision demodulators and decoders. After demodulation and decoding, the message blocks are routed to the coding processor. There the message blocks are stored in coding memories according to their destinations.

After collecting the message bits of an entire frame in the various processor memories, 32 output microprocessors begin to assemble the downlink frames. First, each microprocessor constructs a frame preamble; then it fetches the signaling data from the orderwire memory. Finally, the microprocessor fetches the message data from the message memories and the coding memories. In order to ensure proper TDM routing, the data are fetched in a sequence specified (dynamically) by the SCC. Since the duration of a downlink frame is equal to the duration of an uplink frame, all messages are delayed by at least one frame period (in addition to the unavoidable propagation delay).

7.4 PROCESSOR ARCHITECTURE

The exemplar PR-TDMA satellite receives 128 uplink frames. System 1 supports 32 downlink frames while system 2 handles 64. The baseband processor is shown in the transponder block diagram, figure 7-6. Figure 7-7 shows a more detailed view of the subsystem that includes the demodulators and the input buffering. The three uplink carriers that serve only uncoded bursts are sent to hard-decision demodulators. The 32 overhead bits are stripped off the bursts and used for synchronization. The demodulated information bits are sent to double buffers for temporary storage. The fourth carrier (which can handle both coded and uncoded messages) is routed to a hard-decision demodulator (if the messages are uncoded) or to a soft-decision demodulator (if the messages are coded). The routing is provided by a switch which is updated by the SCC during the guard time between the last uncoded message burst and the special preamble. In the soft-decision processor, the demodulated information bits are sent to an FEC decoder. The decoded bits are sent to a double buffer for temporary storage.

The double buffers consist of two serial-to-parallel shift registers (SRs). The serial-to-parallel conversion is necessary because the processor uses conventional read/write memories (R/W) for data storage. The length of these shift registers is determined by several factors. One consideration is the access time of the R/W memories. Most R/W memories have an access time larger than 100 ns. If the length of the shift-registers is small, a fast memory access will be needed to accomplish the data transfers. Another consideration is satellite DC power; high-speed shift registers

consume a large amount of power, proportional to their length. In this system, a word length of 32 bits is used. Since the highest burst rate of the system is less than 80 Mb/s, the required memory access time is less than 400 ns. This accessing time is well within the limits of presently available technology. Another convenient feature of the 32-bit word is that it is a factor of both the signaling bursts (64 bits) and the message bursts (320 bits).

Double buffers are used to prevent loss of incoming bits while the previously collected word is being sent to the baseband processor. The uncoded data which are held in double registers are multiplexed onto a single bus and sent to a routing switch. This switch directs the signaling data to the downlink orderwire processor. The message data are routed to the baseband processor. The double buffers holding coded data are linked to the coding processor by a 32-bit bus.

The uncoded message data are stored in memory locations that correspond to their beam destinations; input microprocessors carry out this task. Each input microprocessor is responsible for servicing one uplink beam. The microprocessor has access to a routing table that contains the address of the memory location to be used for each incoming message burst. This table is updated by the SCC on a dynamic basis. As each set of new bursts arrives, the processor fetches the three or four addresses (depending on whether or not the fourth uplink is carrying coded data) that correspond to the current time slots. One address is sent to the memory access control system along with the 32-bit word to be stored. By using a TDM scheme, one data bus can serve the four uplinks. Each memory block serves one uplink beam. A memory block is organized into two sets of 32-bit R/W memories. One set is used to collect the arriving frame while the other holds the previous frame before its retransmission. The memory access control system permits the functions of each set to swap at the end of each frame period. Each individual R/W memory holds the traffic destined for one specific downlink beam (e.g., R/W 3 contains message data for downlink beam 3).

Coded message data are stored in memory locations (within the coding processor) that correspond to their beam destinations. A block diagram of the coding processor is shown in figure 7-8. Coding microprocessors control the storing operation. Eight such microprocessors are used, one for each group of four rain-compensation uplink carriers. Each microprocessor has access to a routing table. This table contains the address of the memory location to be used for storing the incoming message burst. The table is updated dynamically by the SCC. As the coded message data arrive, the microprocessors send the 32-bit words along with the

IC-64,170

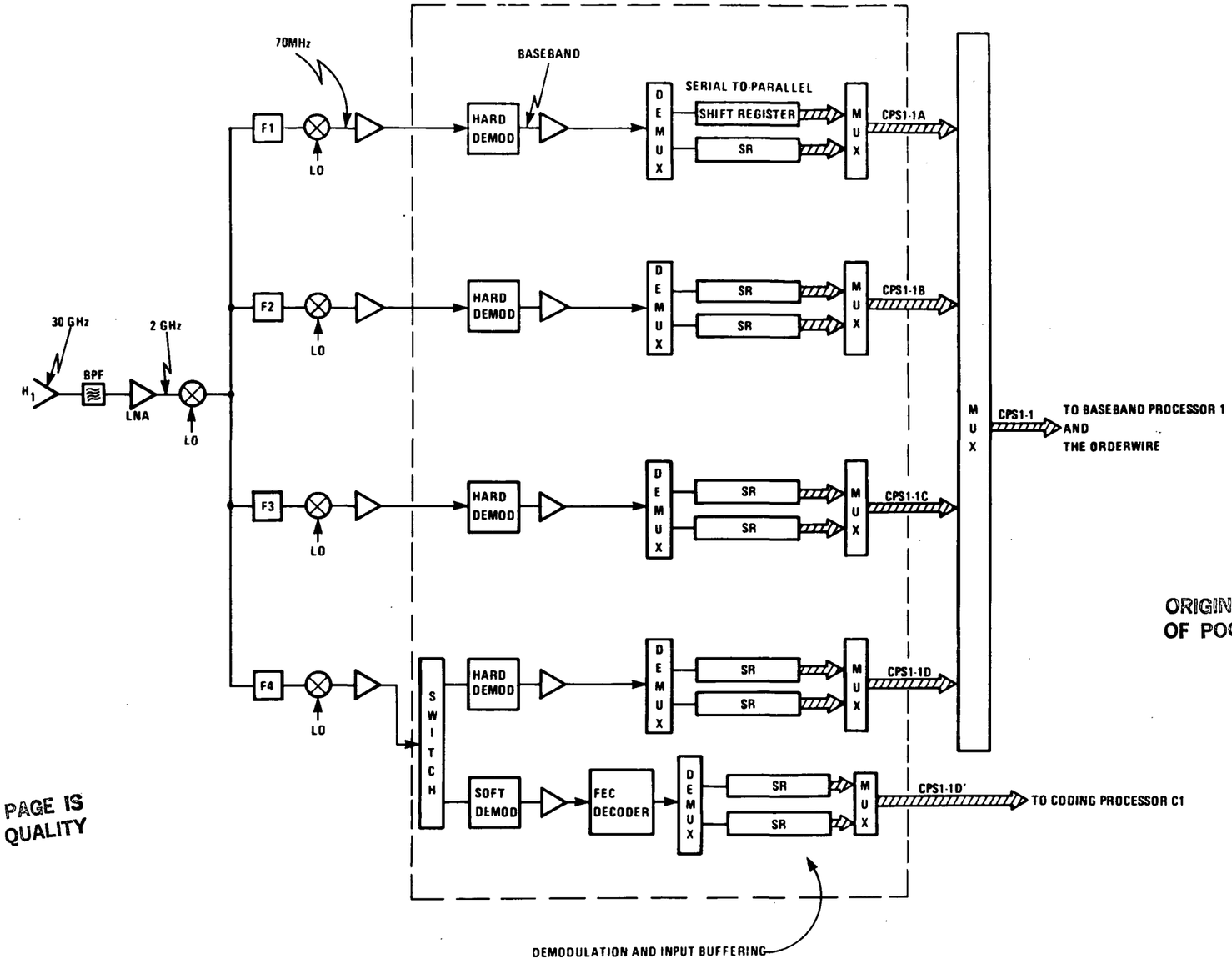

Figure 7-7. Demodulators and Input Buffering

Page Intentionally Left Blank

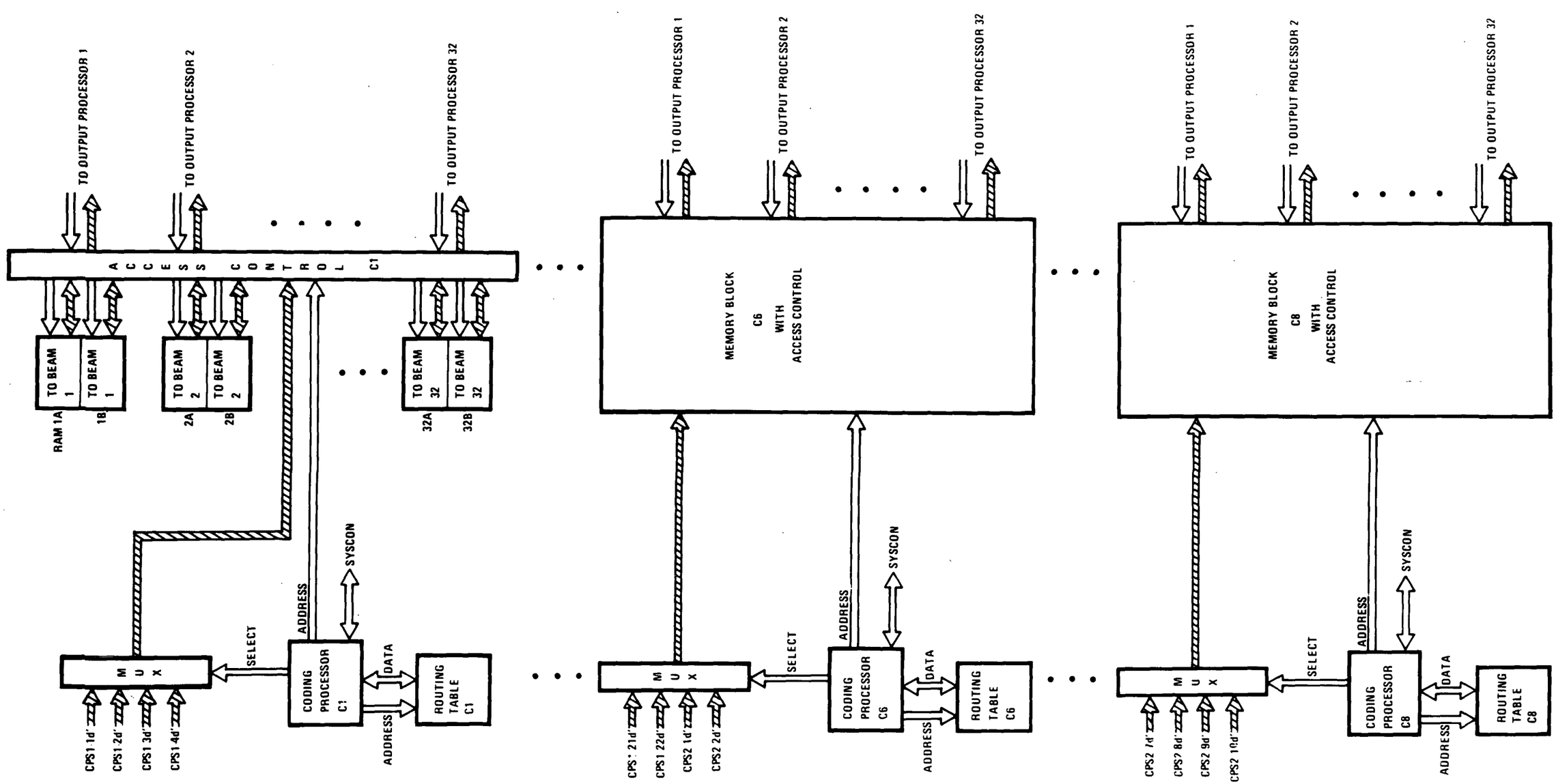

Figure 7-8. Block Diagram of the Coding Processor

IC-64,169

FOLDOUT FRAME

FOLDOUT FRAME

Page Intentionally Left Blank

proper address to the memory access control system. A single data bus can be used because the groups of uplink bursts are multiplexed before entering the processor. The memory modules, where the coded message data are stored, consist of two sets of 32 R/W memories; each R/W memory holds traffic destined for the same downlink beam. One set of R/W memories collects the incoming message data while the other holds the message data received during the previous frame.

Each uplink beam is serviced by an orderwire microprocessor. This microprocessor sequentially loads the incoming signaling data into a memory module that consists of two separate R/W memories. Figure 7-9 shows the downlink orderwire processor in which these memory modules are located. One R/W memory is filled with arriving signaling information while the other holds signaling data from the previous frame period for retransmission. The memory access control system swaps the function of R/W memories at the end of each frame.

On the output side of the downlink orderwire processor, a microprocessor constructs the downlink orderwire frame. First, it generates the frame preamble. Next, it collects the signaling data from the memory modules. These data are fetched sequentially from the R/W memories. Each 32-bit word is sent to a parallel-to-serial shift register that feeds a double buffer. The double buffer contains two burst-size (64 bits) shift registers; one register is filled while the other is emptied. The data leaving the double buffer are remodulated and transmitted to the SCC via the orderwire link.

The uplink orderwire frame from the SCC is sent to a demodulator. The frame preamble is used for receiver synchronization. The demodulated signaling bits are sent to a double buffer. In the double buffer, the serial bit streams are converted into 32-bit words. An orderwire microprocessor routes these signaling blocks to memory according to their downlink beam destination. The memory module is organized as two groups of 32 separate R/W memories. Each R/W memory holds the signaling information destined for the same beam. The uplink frame is organized so that all the signaling bursts can be stored sequentially as they arrive (all the signaling bursts destined for beam 1 arrive first, the bursts for beam 2 arrive second, and so on). Such an arrangement simplifies the R/W memory addressing procedure used by the microprocessor. As with the other memory systems, one set of R/W memories is being filled while the other is being emptied.

The downlink CPS frames are constructed by 32 output microprocessors. A block diagram of the TDM remodulation and output buffering system is shown in figure 7-10. The output microprocessors generate a frame preamble first. Next, the

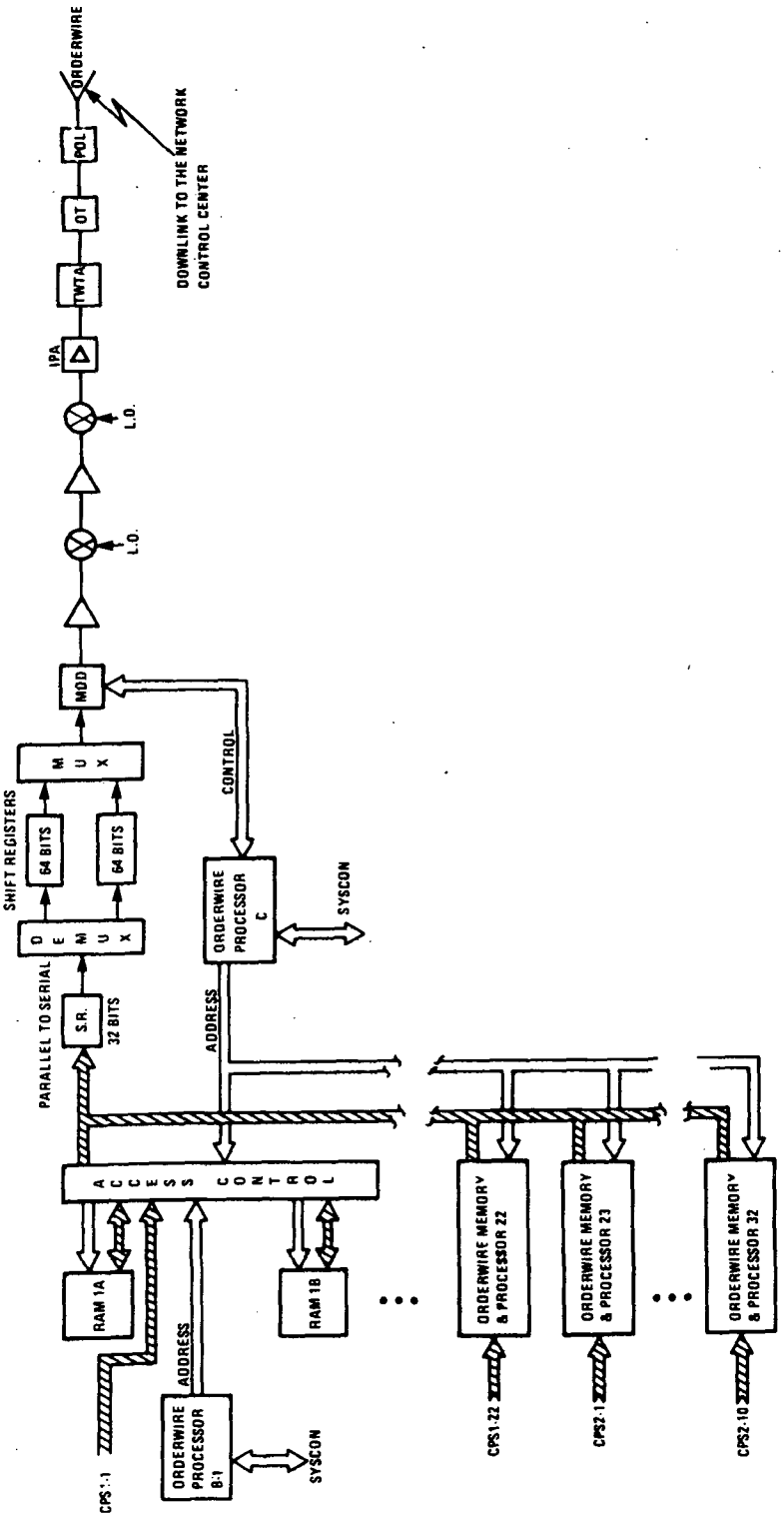

Figure 7-9. Simplified Block Diagram of the Downlink Portion of the Orderwire Processor

ORIGINAL PAGE IS
OF POOR QUALITY

IB-64,171

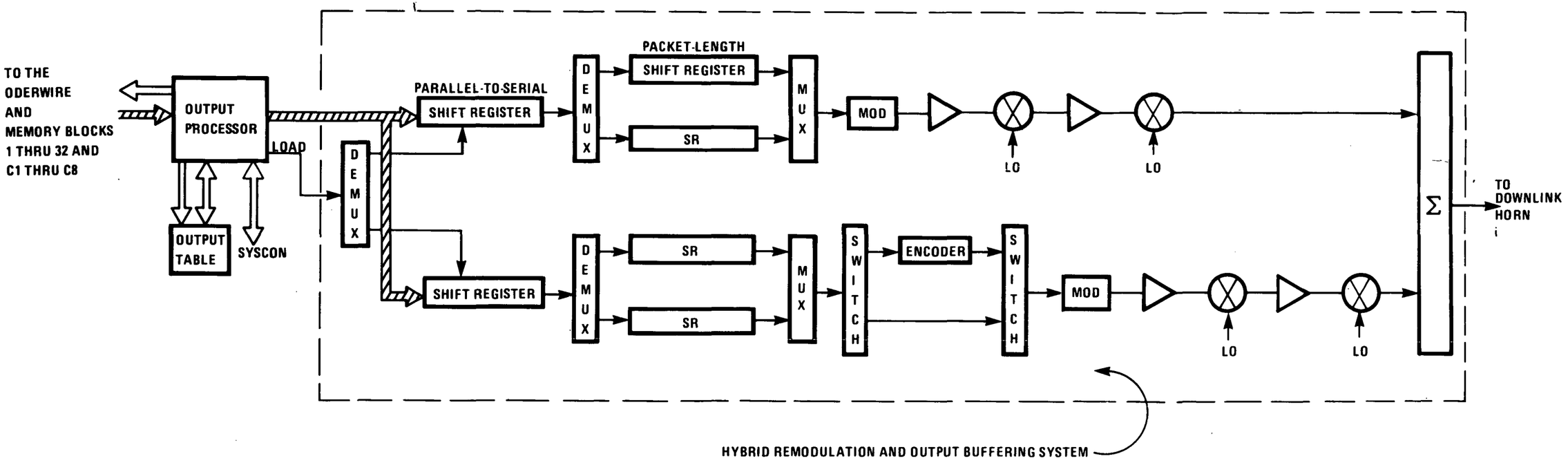

Figure 7-10. Block Diagram of Demodulators and Output Buffering for System-2

FOLDOUT FRAME

FOLDOUT FRAME

Page Intentionally Left Blank

microprocessors fetch the signaling data from the uplink orderwire processor. Since the orderwire memory is organized as 32 independent R/W memories, each microprocessor accesses directly the R/W memory which contains the signaling data destined for the downlink it is serving. If a single memory device were used, a TDM bus structure would be needed. This would require an extremely fast memory access speed as well as high-speed data buses.

Each R/W memory is filled in such a manner that emptying it sequentially provides the proper TDM sequence on the downlink. This simplifies some of the addressing tasks of the output microprocessors.

The output microprocessors send the 32-bit signaling words to a parallel-to-serial shift register. The serial output of this register is sent to a double buffer. This buffer consists of message-burst-size shift registers (320 bits). Each shift register holds five signaling bursts.

After all the signaling blocks are collected, the output microprocessor begins to fetch the message blocks. The message blocks are stored in the coding processor memory and the baseband processor memory. The exact location of each burst is stored in the output microprocessor output table. The microprocessor fetches one address at a time from the table in a sequential order. This table is updated by the SCC so that proper TDM routing can be maintained. As with the orderwire memory organization, the memory modules holding the message data are implemented with individual R/W memories. Each R/W memory contains message data from those uplink beams that have a common downlink beam destination. Thus, each output microprocessor can access the memory locations listed in the output table without contention. The cost of this freedom is inefficient memory utilization since each separate R/W memory must have additional locations held in reserve for traffic fluctuations as well as hardware failures. In addition, the memory access control systems required to allow simultaneous access as well as memory swapping (input function/output function) are quite complex and power consuming. However, without them, the system would require extremely high data rates and/or a reduction in system capacity.

The handling of uncoded message data is straightforward. The 32-bit words of each message are collected, converted into a serial bit stream, and sent to the double buffer. However, coded messages must receive special handling because they contain half as many bits (due to the mandatory data-rate reduction). Stuffing must be added to these messages so that they will be compatible with the output

system hardware. The expanded message can then be sent to the double buffer.

The output of the double buffer is sent to a switch. This switch routes data that do not require coding directly to the modulator. Data that require encoding are routed to a rate-1/2 FEC encoder which removes the stuffing bits and encodes the information bits. All modulated signals are upconverted and sent to a satellite transmitter.

The downlink burst rate can be reduced by using more carriers. Figure 7-10 shows a downlink system that uses two carriers. The burst rate is reduced by one-half, but the satellite weight and power consumption is increased. This system operates in much the same way as the previously described system. However, the 32 output microprocessors must construct two frames simultaneously. In order to reduce the number of components, only one downlink per beam is provided with an encoder. The coded messages must be transmitted on this downlink. This requires earth terminals that can receive two carriers.

A summary of the PR-TDMA system using a single downlink carrier is presented in table 7-1. Table 7-2 contains a summary of a PR-TDMA system with two downlink carriers per beam. For completeness, this information is used to derive the CPS_1 and CPS_2 transponder signal levels for the single downlink carrier system. The signal levels are shown in figures 7-11 and 7-12 for the CPS_1 and the CPS_2 transponders, respectively.

The estimated weight and power budgets for the two types of PR-TDMA satellite are given in tables 7-3 and 7-4. These budgets are derived from the designs presented above. The baseband processor weight and power estimates are based on an approximate chip count. The values used in determining the budgets are based on published data for commercially-available, high-speed, low-power, transistor-transistor logic (TTL), and complementary metal oxide silicon (CMOS) chips. These values may not represent state-of-the-art technology since some technology is never available on the open market. Therefore, the weight and power budgets presented here are conservative and can be considered an upper bound. The use of a single downlink carrier results in savings of about 125 lb and 54 W. These savings may not be significant; however, because of the reduced burst rate, the two-carrier system helps reduce the earth terminal cost which may result in a significant cost savings.

The PR-TDMA system supports the largest throughput; however, the satellite is the heaviest and most costly of the four satellites. In addition, the terminals are the most expensive of

Table 7-1. PR-TDMA System Description (Single Carrier Downlinks)

		CPS 1		CPS 2	
		Uplink	Downlink	Uplink	Downlink
Satellite					
Number of Beams		22	22	10	10
Beamwidth	(degrees)	0.35	0.35	0.7	0.7
Number of Carriers Per Beam		4	1	4	1
Noise Temperature	(K)	1500	--	1500	--
Power Amplifier Output	(W)	--	20.8	--	41.6
Output Backoff	(dB)	--	0	--	0
Earth Terminal					
Antenna Diameter	(m)	3	3	3	3
Noise Temperature	(K)	--	1000	--	1000
Power Amplifier Output	(W)	10	--	20	--
Output Backoff	(dB)	0	--	0	--
System Parameters					
Bit-Error-Rate		10^{-6}	10^{-6}	10^{-6}	10^{-6}
Required E_b/N_o*	(dB)	13.5	13.5	13.5	13.5
Burst Rate	(Mb/s)	19.9	72.8	9.9	36.1
Rain Margin	(dB)	15	6	15	6
Coding During Rain		YES**		YES**	
Processing in the Satellite		YES		YES	

*QPSK, including 3 dB implementation margin
**Up to 25% of the total users can use coding simultaneously

Table 7-2. PR-TDMA System Description (Two Carriers per Downlink Beam)

		CPS 1		CPS 2	
		Uplink	Downlink	Uplink	Downlink
Satellite					
Number of Beams		22	22	10	10
Beamwidth	(degrees)	0.35	0.35	0.7	0.7
Number of Carriers Per Beam		4	2	4	2
Noise Temperature	(K)	1500	--	1500	--
Power Amplifier Output	(W)	--	20.8	--	41.6
Output Backoff	(dB)	--	0	--	0
Earth Terminal					
Antenna Diameter	(m)	3	3	3	3
Noise Temperature	(K)	--	1000	--	1000
Power Amplifier Output	(W)	10	--	20	--
Output Backoff	(dB)	0	--	0	--
System Parameters					
Bit-Error-Rate		10^{-6}	10^{-6}	10^{-6}	10^{-6}
Required E_b/N_o*	(dB)	13.5	13.5	13.5	13.5
Burst Rate	(Mb/s)	19.9	36.0	9.0	18.0
Rain Margin	(dB)	15	6	15	6
Coding During Rain		YES**		YES**	
Processing in the Satellite		YES		YES	

*QPSK, including 3 dB implementation margin
**Up to 25% of the total users can use coding simultaneously

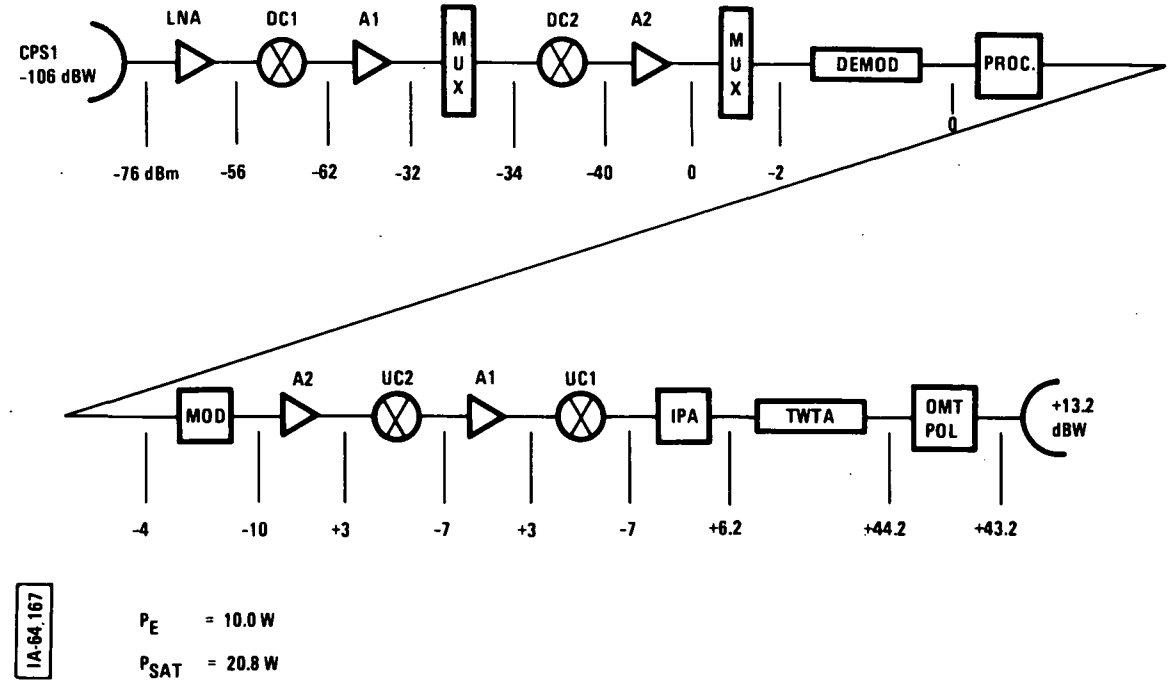

Figure 7-11. CPS_1 Transponder Signal Levels

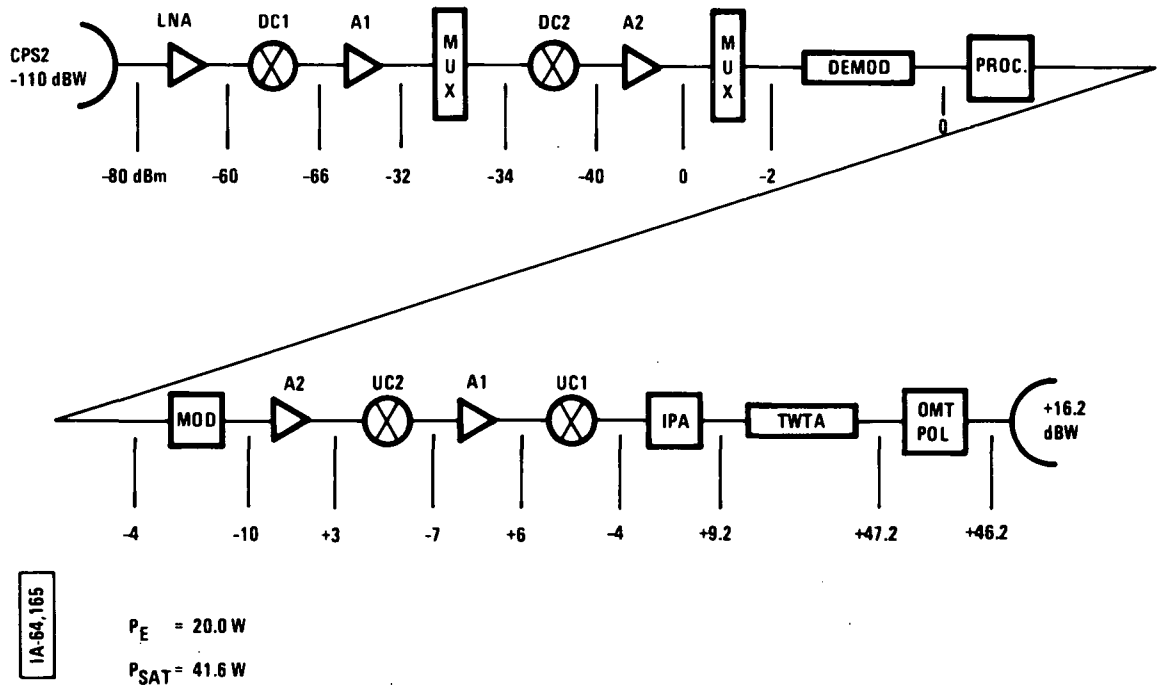

Figure 7-12. CPS_2 Transponder Signal Levels

Table 7-3. PR-TDMA Satellite Weight and Power Budget (Single Carrier Downlinks)

Item	Weight (lb)	Power (W)
Antenna System		
0.35^{o}	176	
0.70^{o}	80.5	
Transponder		
0.35^{o}	1016	797.5
0.70^{o}	538.5	571
Processor*	581	2955.5
Other Electronics and Battery	240	300
T. T. & C.	40	300
Structure	200	--
Solar Array	312	158 **
Allowance (EOL)	--	730
Trunking	523	480
Communications Related Weight+	3707	6292

*Includes the coding processor and orderwire processor

**Includes a 5% tolerance margin for the power generation

+Communications Related Weight includes the items listed and is a term defined for purposes of this report. It should not be confused with conventionally employed "communications payload" or "satellite dry weight".

Table 7-4. PR-TDMA Satellite Weight and Power Budget
(Two Carriers per Downlink Beam)

Item	Weight (lb)	Power (W)
Antenna System		
0.35^{o}	176	
0.70^{o}	80.5	
Transponder		
0.35^{o}	1085	800
0.70^{o}	570	570
Processor*	605.5	3008
Other Electronics and Battery	240	300
T. T. & C.	40	300
Structure	200	--
Solar Array	312	158**
Allowance (EOL)	--	730
Trunking	523	480
Communications Related Weight+	3832	6346

*Includes the coding processor and orderwire processor
**Includes a 5% tolerance margin for the power generation
+Communications Related Weight includes the items listed and is a term defined for purposes of this report. It should not be confused with conventionally employed "communications payload" or "satellite dry weight".

C-2

the four designs. Therefore, this system has the largest total system cost. On a voice channel cost basis, this is the most expensive processing system. The satellite complexity and the high downlink burst rate contribute significantly to the system cost. Although this system offers flexibility, full processing for all users, adaptive coding for 25% of the users, and a large throughput, it is not an economical solution for serving small CPS users.

SECTION 8

FR-TDMA/TDM SYSTEM

A pure-TDM system employs a single carrier for all users in a beam. It is characterized by a high burst rate and therefore requires high-power transmitters and fast modems. A hybrid TDM system employs several carriers. The users that operate in a given carrier are multiplexed in time. The lower burst rate of hybrid TDM requires lower power transmitters and slower modems.

Pure-TDM operation is desirable in a satellite downlink because of the limited satellite resources. Since pure TDM uses a single carrier, the TWT amplifiers can operate at saturation. The downlink burst rate is reduced in half by employing two carriers. The TWT amplifiers can still operate near saturation with little intermodulation interference.

A hybrid-TDM operation is preferable in a satellite uplink because of the terminal cost. Moderate-power transmitters and slower modems lower terminal cost substantially. A fixed carrier can be assigned to every earth station, thereby reducing its frequency synthesizer cost. In the system described here, the terminals do not operate on a single, preassigned frequency. Several carriers are used not only to reduce the burst rate but also to provide routing in the satellite. For this purpose, the number of carriers in the uplink equals the number of downlink beams. When a terminal transmits on a particular frequency, its signal is selected by a bandpass filter in the satellite and routed to the desired downlink beam. The users which have a common destination are multiplexed in time.

A satellite control center determines the time slot and carrier frequency, so that no more than one user in a beam occupies a particular time/frequency slot. The slot assignment is furnished on a dynamic basis in accordance with the needs of the moment. Figure 8-1 shows frequency and time relations in the FR-TDMA/TDM system.

8.1 EARTH TERMINAL OPERATION

An earth terminal services several users. Each user communicates with a different downlink beam; therefore, the terminal must be able to transmit on all 32 uplink carrier frequencies. The terminal sends one burst per user; the frequency of the burst

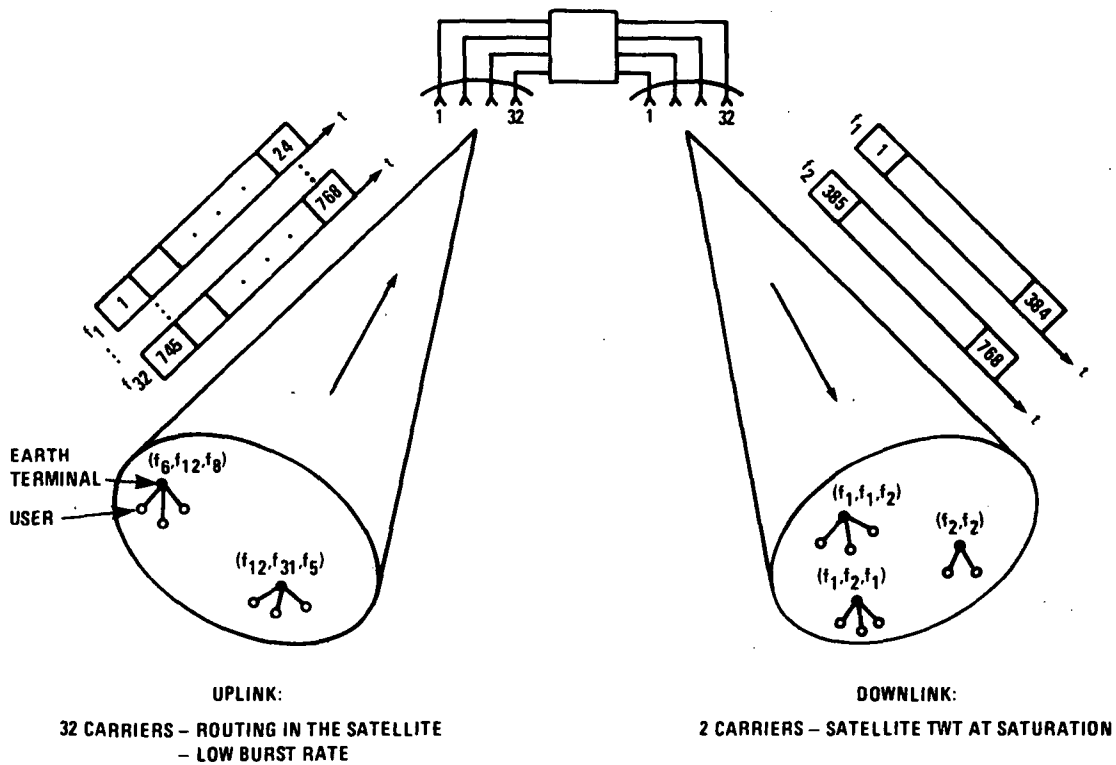

Figure 8-1. Time and Frequency Assignments in an FR-TDMA System

depends on the destination beam. Terminal design is improved if terminals are not allowed to send more than one burst at a time. The frequency synthesizer then needs to generate only one frequency at a time (see figure 8-2), which appears to be simpler and less expensive than generating several carriers simultaneously. The terminal power amplifier is driven by a single carrier at any given instant and can, therefore, operate at saturation.

The time slot in which a terminal sends a particular burst must be coordinated with the other terminals in the same beam so that no more than one user employs a given time/frequency slot. The satellite control center provides coordination by means of control signals that are transmitted over an orderwire channel. These signals determine the time slot and the carrier frequency for every burst. The terminal carrier frequency depends the on amount of frequency division in the synthesizer voltage-controlled oscillator (VCO) phase-locked loop; see figure 8-3.

An earth terminal may transmit several RF bursts in a frame. In the general case, each burst is at a different frequency, as in frequency hopping; see figure 8-2. Each burst consists of a number of synchronization bits followed by message bits.

8.2 SATELLITE OPERATION

The frequency spectrum received by a horn is divided into 32 subbands by means of bandpass filters. The outputs of these 32 filters are destined for the 32 transmit horns. This arrangement provides routing between receive and transmit horns. Analysis shows that the bandwidth of the bandpass filters is less than 10 MHz; therefore, they cannot be implemented at the receive 30 GHz band. For this reason, the receive spectrum is down-converted to a convenient IF frequency of 1 to 2 GHz where such filtering is feasible. The filtered subbands are then down-converted to a common IF of 70 MHz, which is the interface frequency with the demodulators/processors. The processor does not furnish any routing; it provides only frame reorganization by forming two downlink frames from the 32 uplink frames. In the processor, the 70 MHz signal is first demodulated. Then the bit stream is reshaped and collected in shift registers, which are loaded at the uplink burst rate and emptied at the downlink burst rate. The downlink bit stream is first modulated at 70 MHz, then up-converted to an IF of 1 to 2 GHz, and finally up-converted to the downlink frequency band of 20 GHz. Figure 8-4 shows the transponder block diagram.

The processor is quite simple; it consists of demodulators, shift registers, and modulators. The length of the shift registers

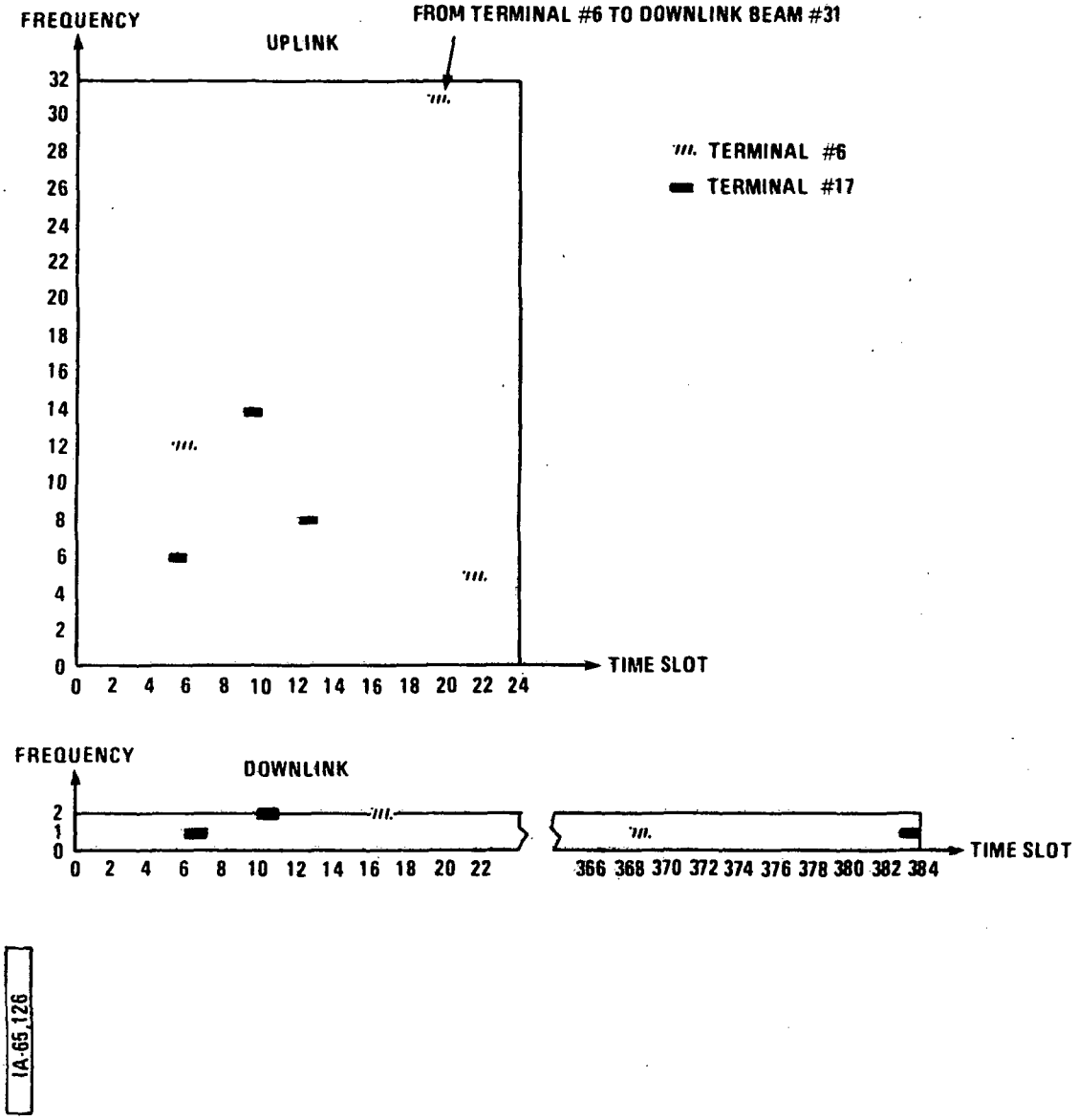

Figure 8-2. Time/Frequency Plots for the Uplink and Downlink

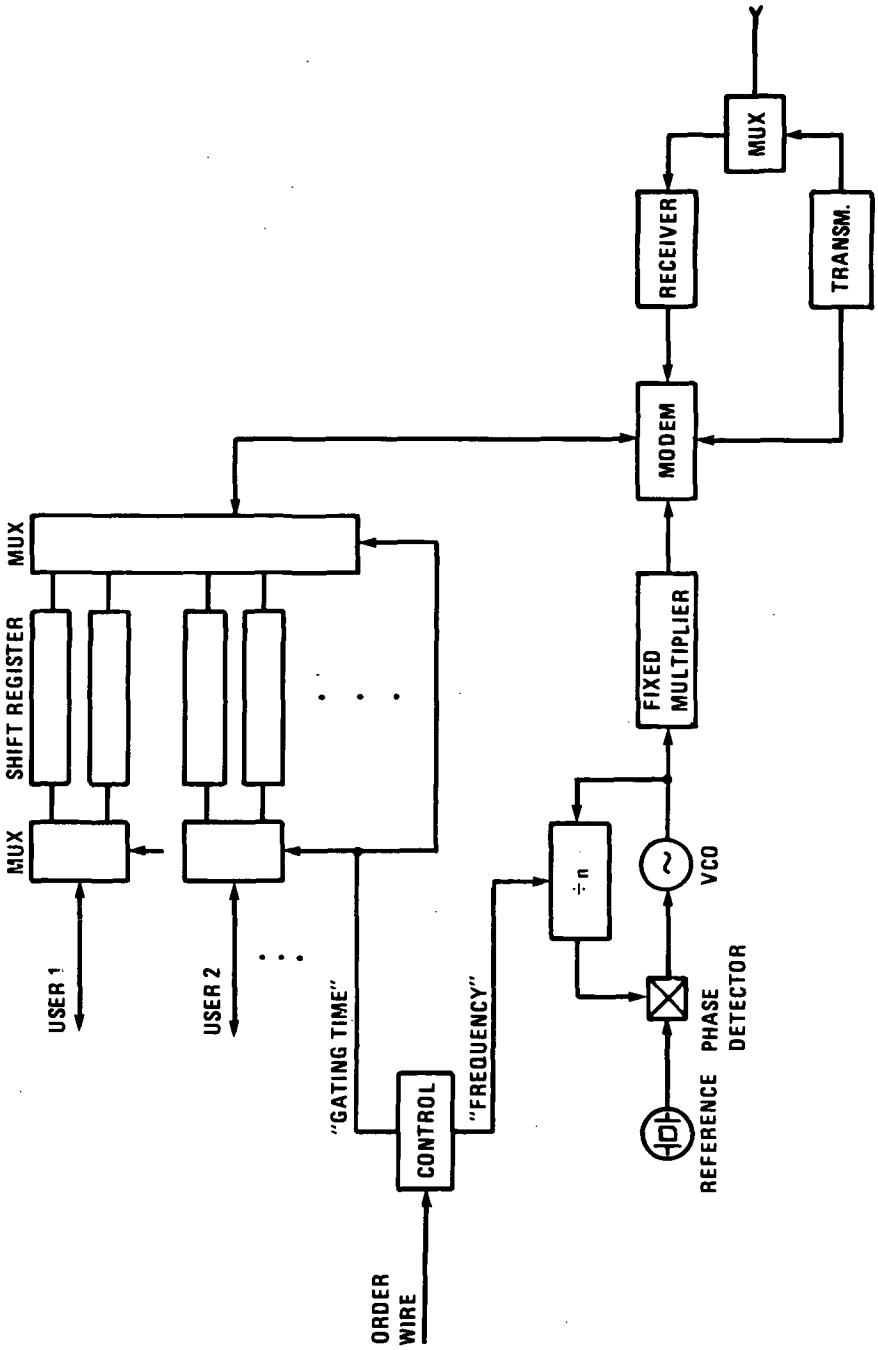

IA-65,131

Figure 8-3. Earth Terminal Block Diagram

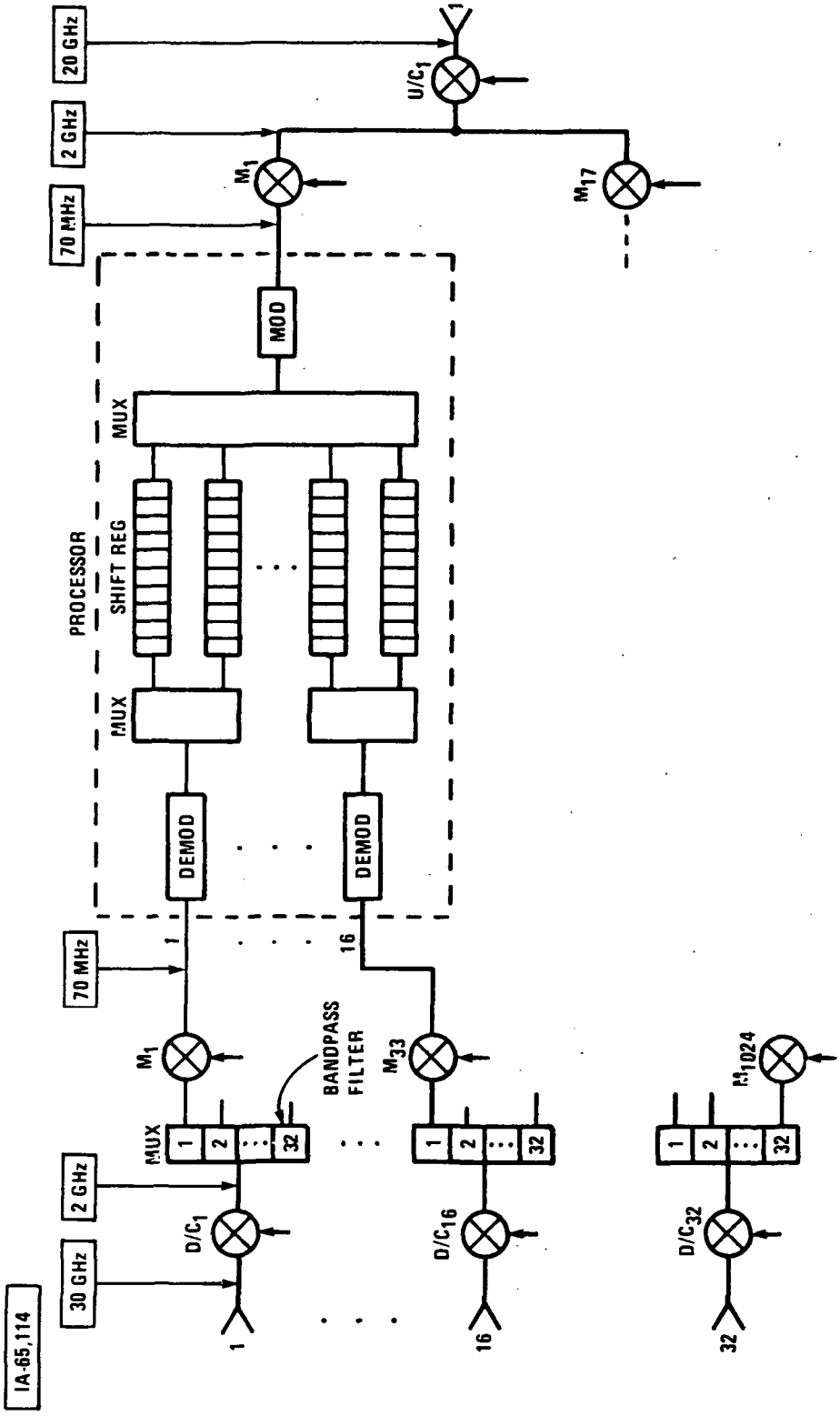

Figure 8-4. CPS Transponder Block Diagram

equals the number of message bits in a burst; the shift registers collect only the message content of a burst and not an entire frame. It is apparent from figure 8-4 that the number of demodulators is large, equal to the product of receive beams and uplink carriers per beam: 32 x 32 = 1024. The number of shift registers is twice as large. (Two shift registers are connected to each demodulator; while one is filling, the other is emptying.) The number of modulators is small, equal to the product of downlink beams and downlink carriers per beam, 32 x 2 = 64. The power consumption of all these processing devices is very large. If decoding/encoding is included in the transponder, the power consumed by the processor will exceed the 2000 W allocated to it. Thus, the transponder in this design is transparent to the signal coding which is used during rain storms.

The uplink system losses are:

$$L_{up} = L_{free\ space} + [L_{rain} - G_{coding}] + L_{edge} + L_{misc}$$

$$L_{up} = 213 + [10 - 0] + 4 + 5 = 232\ dB$$

The downlink system losses are reduced by the coding gain:

$$L_{down} = 210 + [6 - 5] + 4 + 5 = 220\ dB$$

The transponder block diagram (figure 8-4) shows a large number of down-converters (32 + 1024) and up-converters (64 + 32): Generating local oscillator frequencies for them is not a trivial task. A closer look shows that the number of distinct local oscillator frequencies is much smaller than the number of frequency converters. The down-converters D/C_1 through D/C_{32} merely translate the receive spectrum into the 1 (or 2) GHz band; see figure 8-5A. All these down-converters utilize a single local oscillator frequency. The mixers M_1 through M_{1024} convert the 1 (or 2) GHz spectrum into a common IF centered around 70 MHz. They need distinct local oscillator frequencies; the number of these frequencies equals the product of the number of transmit beams and the number of separate frequency bands used in the beam pattern. These separate, non-overlapping bands are referred to as colors. If there are four colors, then the number of distinct local oscillator frequencies is 32 x 4 = 128. The colors assigned to the beams are designated f_a, f_b, f_c, and f_d. LO frequency f_1 equals f_{129}, equals f_{257}, etc. Eight mixers use the same LO frequency; thus they are supplied from the same multiplier chain by means of an eight-way power splitter. Similar arguments can be applied to the up-converters.

IA-65,129

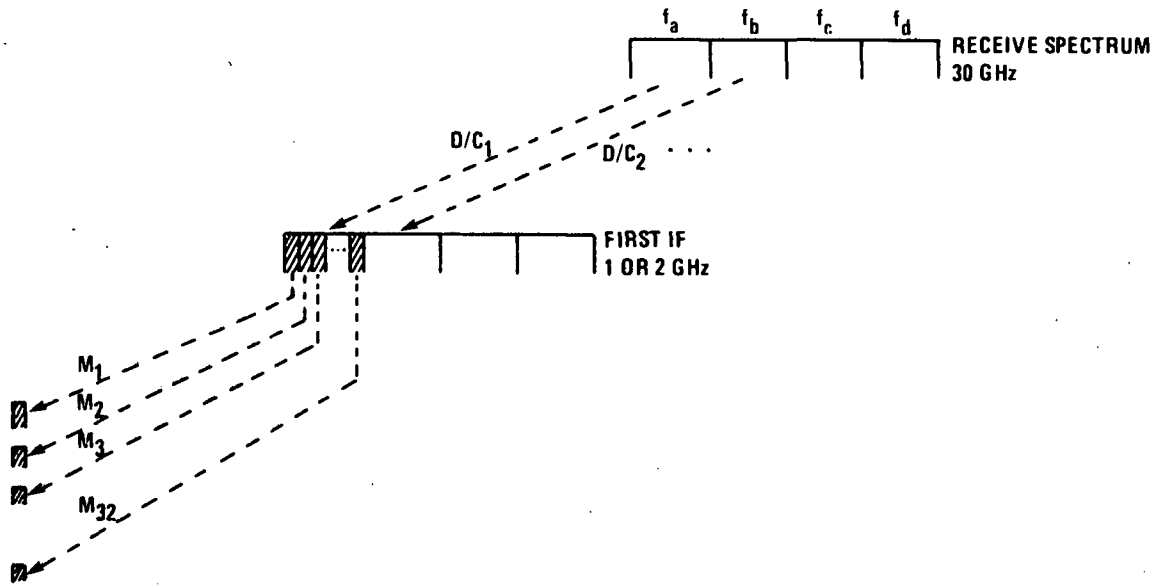

A. THE NECESSARY DOWNCONVERSIONS

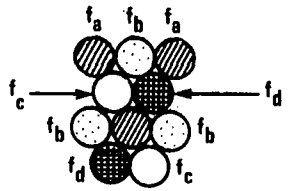

B. A BEAM PATTERN WITH FOUR DISTINCT BANDS (COLORS)

Figure 8-5. Frequency Conversions in the Transponder

The frequency synthesizer must generate 128 local oscillator frequencies for the 1024 receive mixers; these frequencies must be spaced about 8 MHz apart:

$$2(\Delta f/R)R = 2 \times 1.8 \times 1.92 = 7 \text{ MHz}$$

where $(\Delta f/R) = 1.8$ for $(C/I)_x = 33$ dB and multiple shift keying (MSK) modulation, and $R = 1.92$ Mb/s is the uplink burst rate. These frequencies are generated by 128 voltage-controlled oscillators which are phase-locked to a 0.5 MHz reference oscillator. The VCO frequencies range from 125 MHz to 61 MHz. The operation of the synthesizer is outlined in figure 8-6A. The practical realization of the generator for the 2000 MHz LO frequency is shown in figure 8-6B.

8.3 FRAME ORGANIZATION

The frame structure depends on the number of bits in a burst. The message bits of a burst are stored in shift registers on board the satellite. Since the power consumed by shift registers is proportional to their length, the number of message bits in a burst must be minimal. At the same time, the number of message bits must be much larger than the number of synchronization bits in a burst. (Every burst comes from a different source, must be demodulated individually, and therefore needs burst synchronization bits.) Some number of synchronization bits is required to ensure good synchronization. The number of synchronization bits assumed here is 32 and the number of message bits is 128. The latter represents a compromise between the requirement for minimal length shift registers and the desire to keep the burst overhead (defined as the ratio of sync bits to message bits) reasonably small. The burst overhead is quite large, 32/128 = 25%. The throughput equation for such an overhead value is derived in the appendix, table A-11, Case 11A:

$$t_1 + 4t_2 + 0.506\ t_T = 3.445 \times 10^6\ P_{TWT}$$

Solving for $P_{TWT} = 1003$ W, $t_2 = t_1/2.2$, and $t_T = 806$ Mb/s yields

$$t_1 = 1081 \text{ Mb/s},\ t_2 = 492 \text{ Mb/s, and } t_T = 806 \text{ Mb/s}.$$

The number of metropolitan users in an uplink frame is

$$\frac{t_1}{R_v\ N'_{C1}(up)\ N_{B1}} = \frac{1081 \times 10^6}{\left(64 \times 10^3\right) \times 32 \times 22} = 24$$

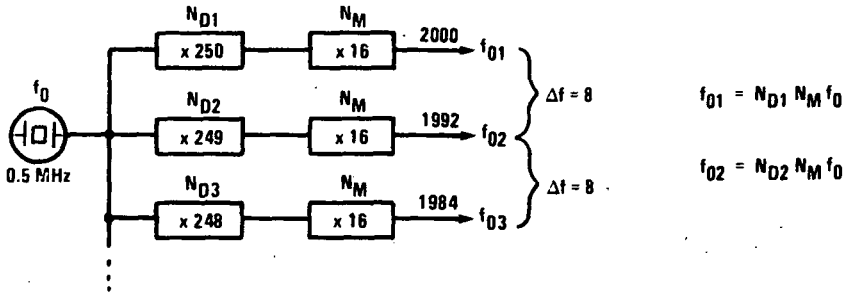

A. PRINCIPLE OF OPERATION OF THE LOCAL OSCILLATOR SYNTHESIZER

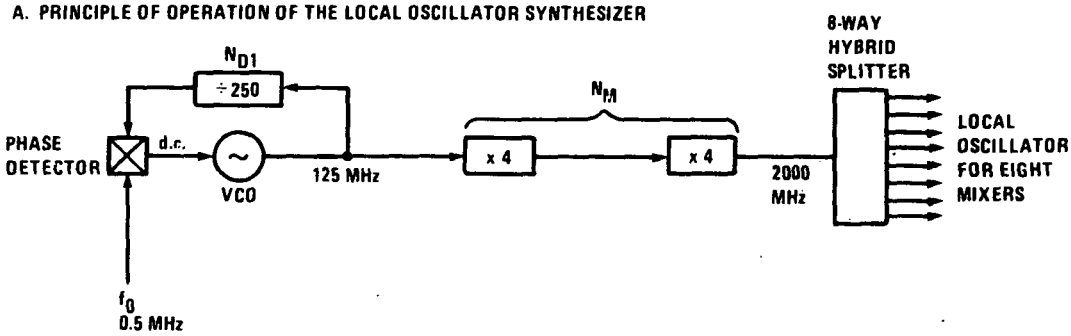

IA-65,132

B. PRACTICAL REALIZATION OF THE 2000 MHz GENERATOR

$$f_{01} - f_{02} = (N_{D1} - N_{D2})\, N_M\, f_0$$

SUPPOSE THAT $\Delta f \triangleq f_{01} - f_{02} = 8$ MHz

ALSO $N_{D1} - N_{D2} = 1$

THEN $f_0 N_M = 8$

IF $N_M = 16$ THEN $f_0 = 0.5$ MHz

$$N_{D1} = \frac{f_{01}}{f_0 N_M} = \frac{2000}{8} = 250$$

$$N_{D2} = \frac{f_{02}}{f_0 N_M} = \frac{1800}{8} = 249 \quad \text{ETC}$$

Figure 8-6. Synthesizer Design

where R_v is the voice data rate (64 kb/s). The number of metropolitan users in a downlink frame is

$$\frac{t_1}{R_v \, N'_{C1}(\text{down}) \, N_{B1}} = \frac{1081 \times 10^6}{\left(64 \times 10^3\right) \times 2 \times 22} = 384$$

The frame length is

$$T = (\#\text{ message bits/burst})/R_v = 128/(64 \times 10^3) = 2 \text{ ms}$$

The uplink burst rate is

$$R_{up} = (\#\text{bits/burst}) \times (\#\text{ bursts/frame})/\text{frame length}$$

$$= \frac{(32 + 128)\,24}{2 \times 10^{-3}} = 1.92 \text{ Mb/s}$$

The downlink burst rate is

$$R_{down} = \frac{32}{2} R_{up} = 30.72 \text{ Mb/s}$$

The uplink and downlink frame organizations are shown in figure 8-7.

8.4 SYSTEM PERFORMANCE

A summary of the system parameters is presented in table 8-1. The low uplink burst rate results in low earth terminal power. Power of 1.4 W can be delivered at 30 GHz by a low-cost, solid-state amplifier.

The estimated values for the weight and power consumption of the transponder are very important in comparing various systems. The weight and power consumption can be estimated by adding these values for every component in the transponder. Although the block diagram gives an idea of the components involved, their exact number can be found only after working out the signal level diagram of the transponder. To begin with, the gain of the transponder must be determined. The gain calculated from figure 8-8 is 124 dB.

The transponder gain and other known parameters (for example, the conversion loss of a downconverter or the gain of a TWT

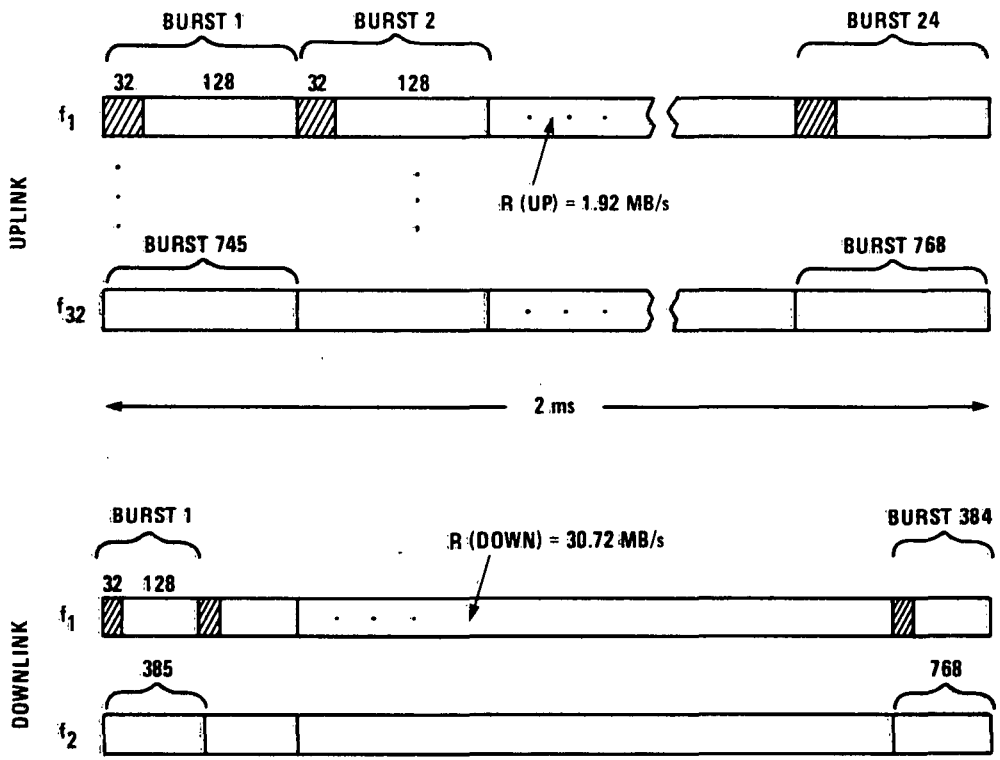

Figure 8-7. Uplink and Downlink Frame Organization

Table 8-1. FR-TDMA System Description

		CPS 1		CPS 2	
		Uplink	Downlink	Uplink	Downlink
Satellite					
Number of Beams		22	22	10	10
Beamwidth	(degrees)	0.35	0.35	0.7	0.7
Number of Carriers Per Beam		32	2	32	2
Noise Temperature	(K)	1500	--	1500	--
Power Amplifier Output	(W)	--	5	--	20
Output Backoff	(dB)	--	0	--	0
Earth Terminals					
Antenna Diameter	(m)	3	3	3	3
Noise Temperature	(K)	--	1000	--	--
Power Amplifier Output	(W)	1.4	--	5.7	--
Output Backoff	(dB)	0	--	0	--
System Parameters					
Bit-Error-Rate		10^{-6}	10^{-6}	10^{-6}	10^{-6}
Required E_b/N_o*	(dB)	13.5	13.5	13.5	13.5
Burst Rate	(Mb/s)	1.92	30.72	1.92	30.72
Rain Margin	(dB)	10	6	10	6
Coding Gain	(dB)	0	5	0	5
System Losses	(dB)	232	220	232	220

*QPSK, including 3 dB implementation loss

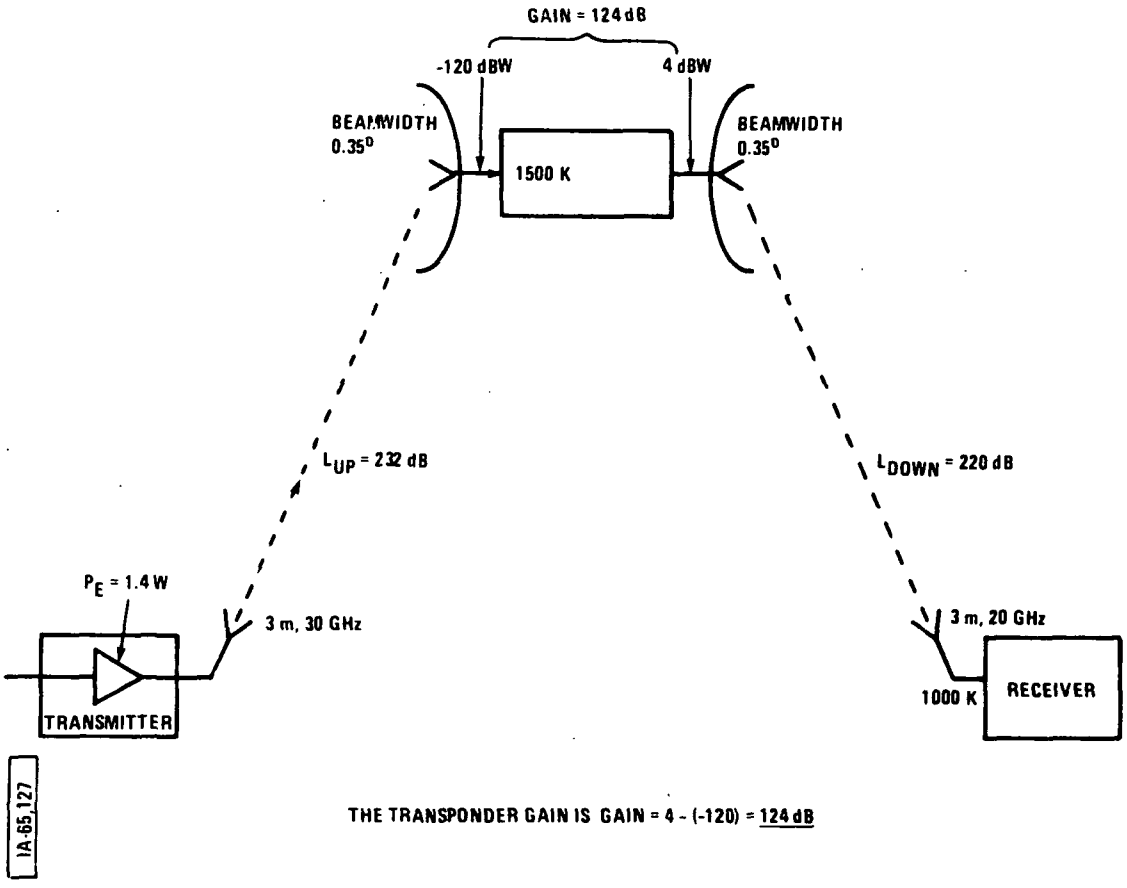

(*) $$P_{E\,1} = \frac{C}{kT}_{up} + R_{up\,1} + k + T_{sat} + B_{E\,1} + L_{up} - G_{E\,1}(tr) - G_{sat}(rec)$$

$$= 13.8 + 10 \log (1.92 \times 10^6) - 228.6 + 10 \log (1500) + 0$$

$$+ 232 - 57 - 53.3 = 1.49 \text{ dBW} = 1.4 \text{ W}$$

(*) $$P_{rec\,1} = P_{E\,1} + G_{E\,1} - L_{up\,1} + G_{sat\,1}$$

$$= 1.49 + 57 - 232 - 53.3 = -120 \text{ dBW} = -90 \text{ dBm}$$

(*) $$P_{sat\,1} = \frac{C}{kT}_{down} + R_{down\,1} + k + T_E + B_{sat} + L_{down} - G_{sat\,1}(tr) - G_{E\,1}(rec)$$

$$= 14.4 + 10 \log (30.72 \times 10^6) - 228.6 + 10 \log (1000) + 0$$

$$+ 220 - 53.3 - 53.4 = 3.97 \text{ dBW per carrier} = 2.5 \text{ W per carrier}$$

(*) The transponder gain is: GAIN = 4 - (-120) = 124 dB

Figure 8-8. Determination of Transponder Gain

amplifier) are combined into a signal level diagram from which the gain of the various amplifiers can be established (see figure 8-9).

Table 8-2 gives a weight and power breakdown for the major components that comprise the CPS transponder. The transponder weight and power consumption are estimated at 2150 lb and 3200 W, respectively.

IA-65,115

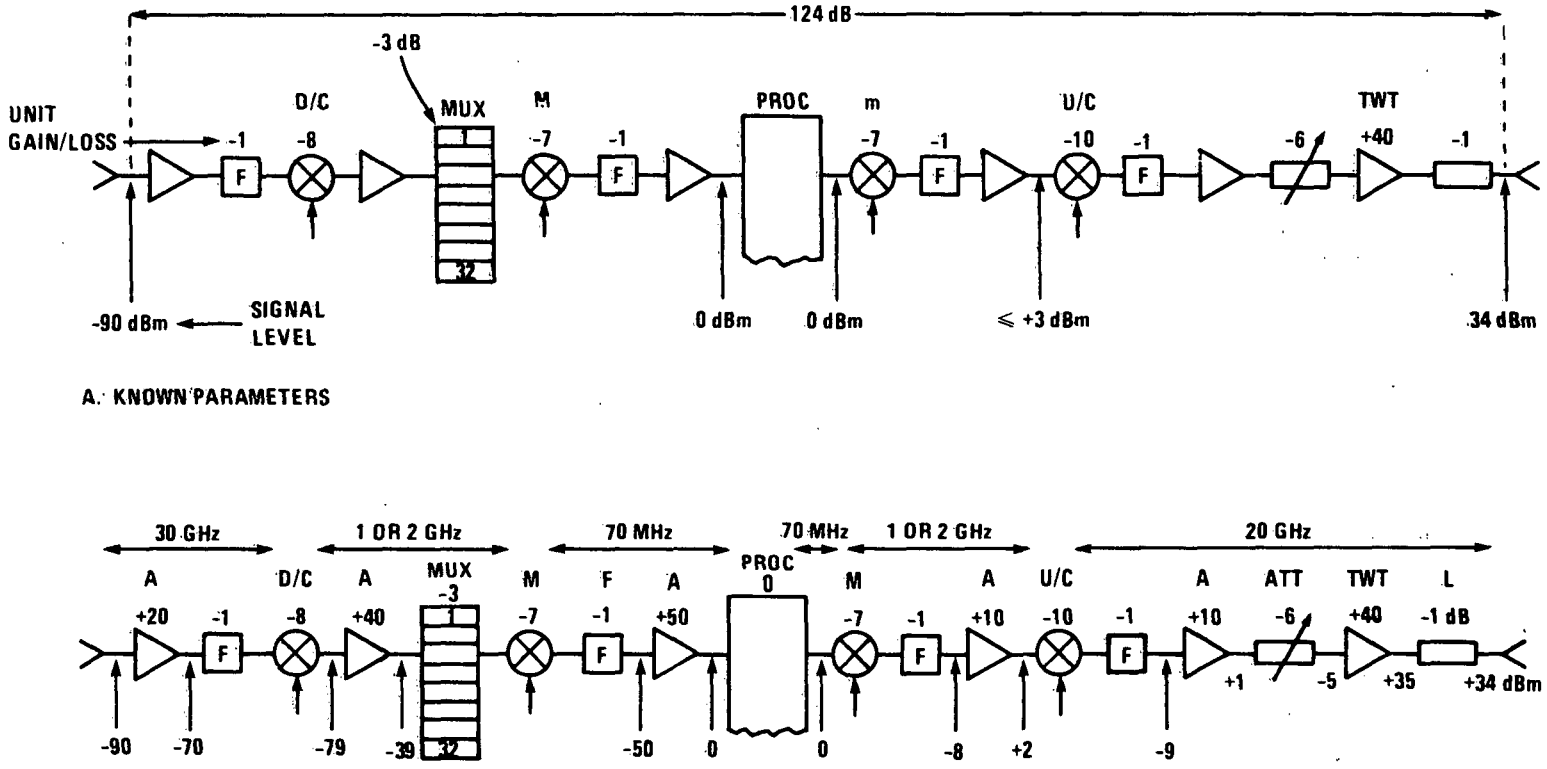

Figure 8-9. Transponder Signal Level and Gain Diagram

Table 8-2. FR-TDMA Transponder Weight and Power Budget

		No. Units	Unit Wt (oz)	Unit Pwr (W)	Weight (oz)	Power (W)
LNA	30 GHz, 20 dB	32	8	1.5	256	48
FILT	30 GHz	32	6	-	192	-
D/C_1	30/2 GHz	32	16	-	512	-
AMPL	2 GHz, 20 dB	2 x 32	6	1.5	384	96
MUX	2 GHz	32	20	-	640	-
D/C_2	2/0.07 GHz	1024	2	-	2048	-
FILT	70 MHz	1024	2	-	2048	-
AMPL	70 MHz, 40 dB	1024	2	-	2048	-
PROC		64	42	12	2688	768
DEMODS		1024	6	0.5	6144	512
MODS		64	32	2	2048	128
U/C_1	0.07/1.5 GHz	64	2	-	128	-
MUX	1.5 GHz	32	20	-	640	-
AMPL	1.5 GHz, 12 dB	32	6	1	192	-
U/C_2	1.5/20 GHz	32	16	-	512	-
FILT	20 GHz	32	6	-	192	-
AMPL	20 GHz, 12 dB	32	8	1.2	256	38
TWT_1	20 GHz, 6.5 W	22	288	19	6336	418
TWT_2	20 GHz, 25 W	10	384	75	3840	750
MULTIPLIERS 1/1500 MHz		136	8	2	1088	272
MULTIPLIERS to 30 & 20 GHz		64	32	2	2048	128
MASTER OSC (redundant)		2	80	5	160	10
					34,400 oz	3200 W
TOTAL WEIGHT					2,150 lb	

SECTION 9

TRUNKING TRANSPONDER

The prime function of the satellite systems described in this report is to provide service for CPS users. However, in order to reduce the CPS system cost, trunking transponders are included in the satellite. Since the trunking terminals use large antennas and very low noise preamplifiers, the trunking service consumes only a small amount of the satellite power.

Comparing a trunking transponder with an FR-TDMA/TDM transponder (see section 8) gives the results shown in table 9-1:

Table 9-1. Trunking vs. CPS Transponders

		Trunking	CPS	CPS/Trunking Ratio
Throughput	(Mb/s)	806	1573	1.95
Transp. Weight	(lb)	523	2150	4.11
Transp. DC Consumption	(W)	480	3200	6.67

If the service charges are proportional to the throughput, while the satellite costs are proportional to the weight or power consumption of the particular service, the trunking users will cover some of the CPS users' satellite expenses.

The trunking users employ large antennas, for example:

$$D_E = 6 \text{ m}$$

where D_E is the terminal antenna diameter, and very low noise preamplifiers; for example, a low-noise amplifier temperature of approximately 150 K, or a system noise temperature, T_E, of

$$T_E = 500 \text{ K}$$

The trunking service therefore has sufficient link margin and does not require processing in the satellite. Routing between the uplink and downlink beams can be accomplished with a switching matrix. The size of the switching matrix equals the number of beams that carry

trunking traffic. Only 16 to 18 large metropolitan centers require trunking service. It is assumed that 16 beams carry trunking traffic; therefore, the matrix size is 16 x 16. A non-processing transponder with a 16 x 16 switching matrix consumes a relatively small amount of power and has a moderate weight, leaving most of the satellite resources for CPS use. The 16 x 16 matrix chosen allows a comparison between several matrix architectures, as explained in section 9.4.

CPS users located in (or near) large metropolitan centers are covered by 22 spot beams (0.35° half-power beamwidth). Some of these beams also cover the 16 metropolitan centers which have trunking traffic; a logical approach would be to use 16 of the 22 CPS beams for trunking purposes also. If the trunking users employ a different frequency band from the CPS band, the two services can be separated easily in the satellite by means of bandpass filters.

9.1 SYSTEM CONSIDERATIONS AND FRAME ORGANIZATION

The trunking data rate assumed is 12.6 Mb/s. Before bursting trunking data towards the satellite, the terminals must add a preamble. The TDM frame is designed with 10% overhead (equal to the ratio of preamble bits to data bits).

The trunking throughput, t_T, must satisfy the requirement that

$$t_T = (\text{integer}) \times (\text{data rate}) \times (\text{number of beams})$$

$$= (\text{integer}) \times (12.6 \times 10^6) \times (16)$$

The integer can be determined by arguing that the prime function of this satellite system is CPS service and allocating more throughput to the CPS than to the trunking service. For example,

$$t_T \simeq 0.5\, t_{CPS}$$

where t_{CPS} is the CPS throughput.

Consider the case in which trunking transponders are added to an FR-TDMA/TDM satellite. As derived in the appendix, such a satellite supports a metropolitan throughput of 1081 Mb/s and a rural throughput of 492 Mb/s; therefore, t_{CPS} = 1573 Mb/s. The above integer is then 4 (that is, four 12.6 Mb/s trunking terminals operate in each of the 16 trunking beams):

$t_T = 4 \times 12.6 \times 16 = 806.4$ Mb/s

$t_T/t_{CPS} = 806.4/1573 = 0.513 \simeq 0.5$

The burst rate, R_T, is:

$R_T = (1 + \alpha)$ (data rate) x (number of users in a beam)

$= (1 + 0.1) \times 12.6 \times 4 = 55.44$ Mb/s

The transponder is transparent to the data stream (non-processing); therefore, the uplink and downlink burst rates are equal.

If the frame length is selected as T = 200 μs, the number of data bits in a burst is

(# data bits) = T(data rate) = (200×10^{-6}) (12.6 x 106)
= 2520

The number of bits in a preamble is

(# preamble bits) = α (# data bits) = 0.1 x 2520 = 252 bits

The frame organization is shown in figure 9-1.

The switching matrix is reconfigured during a guard time.

9.2 TRANSPONDER DESIGN

The receive signals are down-converted to an IF frequency where a high-performance switching matrix can be implemented easily. The 16 IF channels are routed through the matrix and then are up-converted to the transmit band. The design is very straightforward, resulting in relatively low power consumption and weight, leaving much of the satellite resources for the CPS services. A block diagram of the transponder is shown in figure 9-2.

While most of the satellite subsystems are well known and do not require particular attention, the switching matrix is worth considering in some detail.

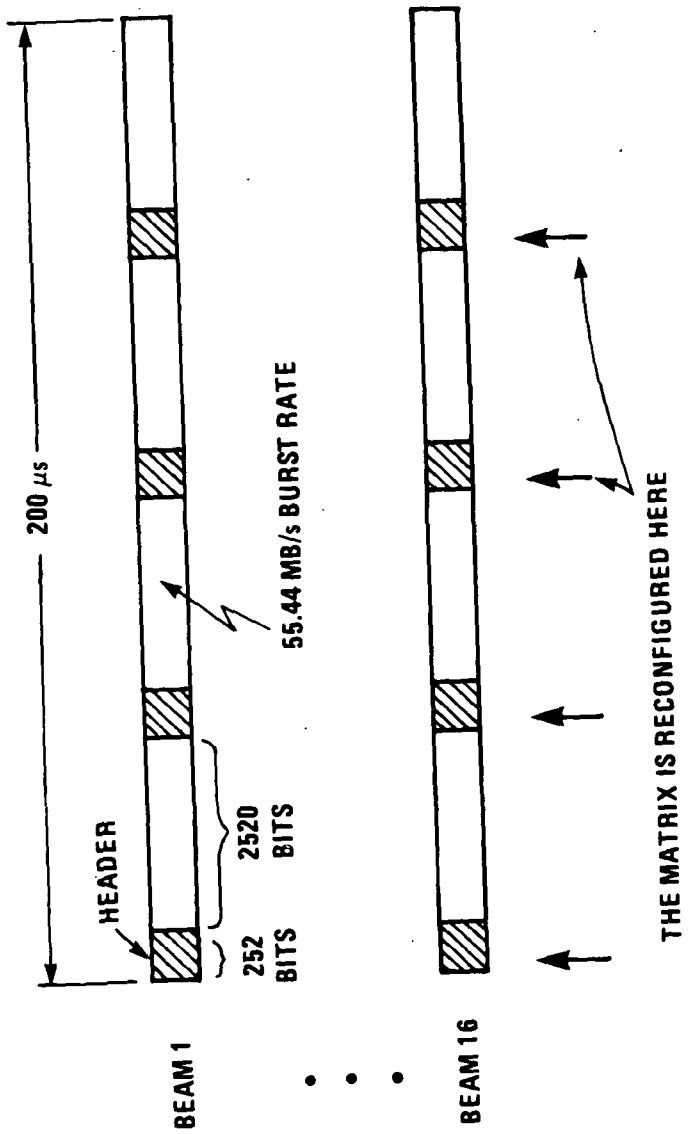

IA-65,123

Figure 9-1. Trunking Frame Organization

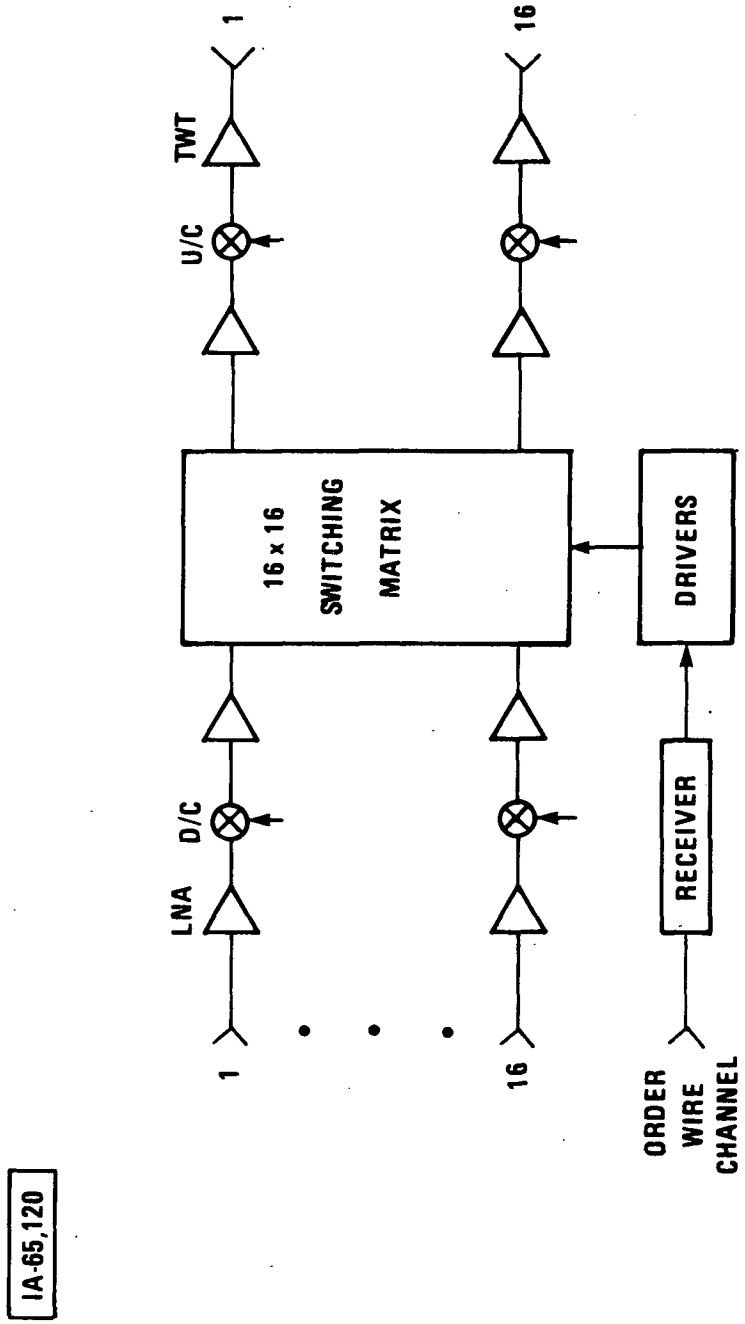

Figure 9-2. Trunking Transponder Block Diagram

9.3 SWITCHING MATRIX

The switching matrix is implemented at a convenient IF band. The IF frequency cannot be too low because of image rejection problems associated with a single down-conversion. One possible choice for the center frequency is 300 MHz, where broadband ultra high frequency (UHF) components (hybrid power-dividers) are readily available. The center frequency can also be chosen at around 1.5 to 2 GHz, where microcomputer integrated circuit (MIC) components would yield a compact low-weight design. The insertion loss associated with the switching matrix must be offset with IF amplifiers. These amplifiers weigh less at 300 MHz and 1.5 GHz than at higher frequencies. Also, at frequencies much higher than 1.5 GHz, a sufficient "isolation" of the OFF branches of the matrix is hard to achieve. It is assumed here that the center frequency of the IF band lies around 1.5 GHz. The bandwidth that the switching matrix must pass is relatively narrow:

$$2 \times (\text{burst rate}) \times (\text{bandwidth/burst rate}) \simeq 200 \text{ MHz}$$

and can easily be accommodated by broadband UHF devices or at 1.5 GHz ($\Delta f/f = 0.13$ is very small) by the MIC devices.

Three matrix architectures are discussed in some detail next.

9.3.1 Switch Matrix Architecture

The switch matrix consists of single-pole N-throw diode switches where N is the matrix size. Figure 9-3 shows a 3 x 3 matrix, which consists of six single-pole 3-throw switches. Although the connections between the switches appear quite involved, they become disentangled if all input switches are arranged in parallel planes and all output switches are arranged in planes perpendicular to the input switches. A large size single-pole N-throw diode switch is difficult to implement because of the proximity of the diodes; in such a case the switch can be implemented by connecting smaller size switches in cascade. Figure 9-4 shows a 1 x 16 switch which is built from one 1 x 4 input switch and four 1 x 4 output switches. Depending on the isolation requirements, each arm may contain from one to more than three diodes; the 1 x 4 switch shown in figure 9-4 uses three diodes per arm. If one diode per arm is used, the total number of diodes in a 16 x 16 matrix is (16 + 4) x 16 x 2 = 640. The isolation from an input port of the matrix to an undesirable output port appears sufficient (over 60 dB) with one diode per arm. Note that the probability that not a single diode will fail is exponentially proportional to the number of diodes; therefore the number of diodes

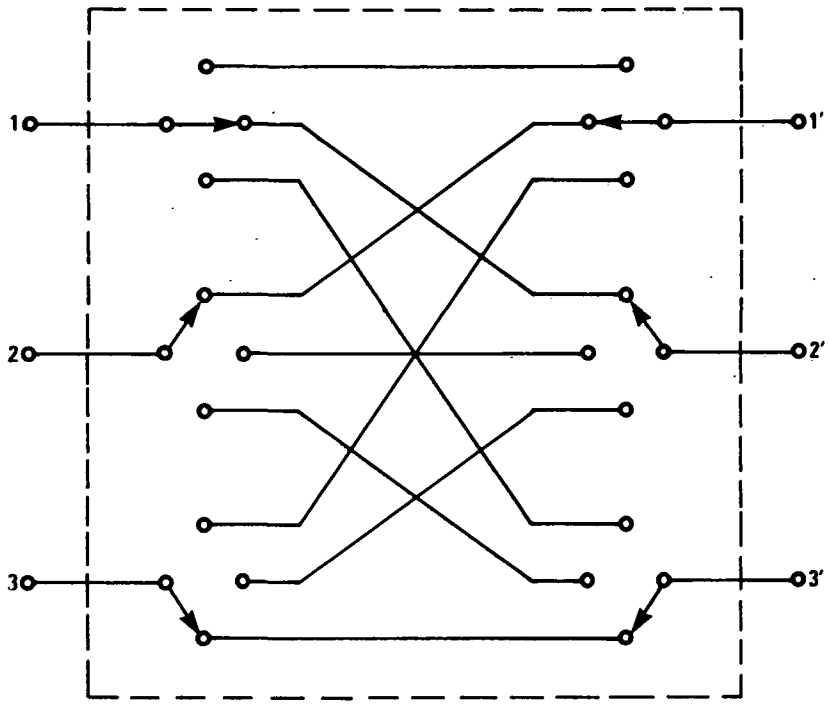

A. 3 x 3 SWITCH MATRIX

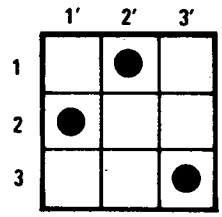

B. CONNECTIVITY MATRIX

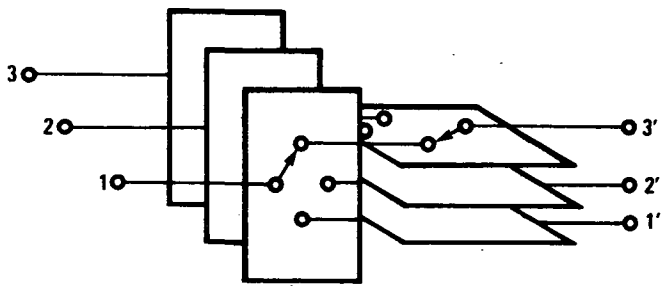

C. PRACTICAL IMPLEMENTATION TECHNIQUE

IA-65,168

Figure 9-3. Switch Matrix and Its Implementation

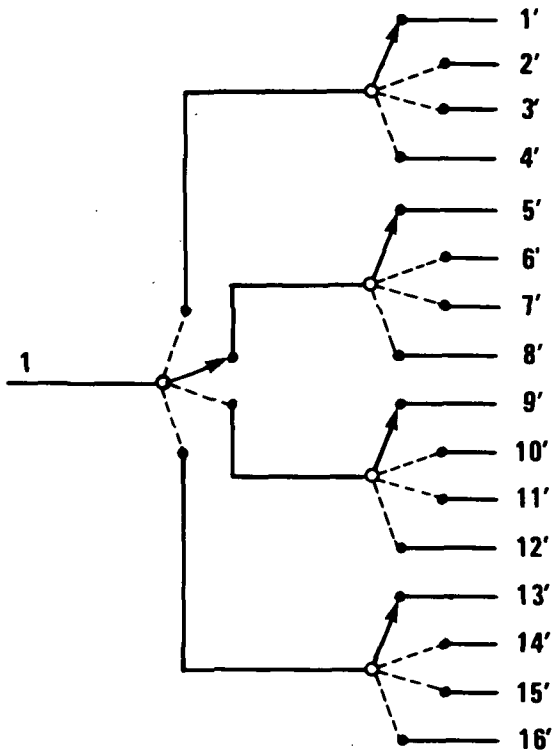

A. SCHEMATIC OF A SINGLE-POLE SIXTEEN-THROW SWITCH

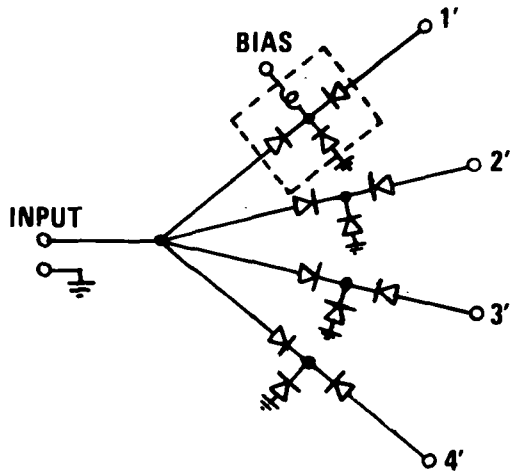

IA-65,119

B. IMPLEMENTATION OF A SINGLE-POLE FOUR-THROW SWITCH (3 DIODES PER ARM)

Figure 9-4. Multipole Diode Switches

must be minimal. The advantages of the switch-matrix are: (a) low insertion loss, (b) good input match, and (c) the fact that the matrix size is not restricted to power-of-2 numbers. No significant disadvantages can be cited for this matrix architecture.

9.3.2 Splitter Matrix Architecture

The splitter matrix consists of N-way power splitters and single-pole single-throw diode switches, where N is the matrix size. Figure 9-5 shows a 3 x 3 splitter matrix. It consists of six 3-way splitters and $(3)^2 = 9$ diode switches. Similar to the previous architecture, the input and output splitters are arranged in perpendicular planes in order to disentangle the connections between them. The splitters are usually implemented with 2-way hybrid junctions which are cascaded in a tree structure to obtain an N-way splitter. This leads to power-of-2 splitters; the arrangement for a 16-way splitter is shown in figure 9-6. The outputs of the eight splitters in column 4 are connected to the diode switches. Only one of the 16 diode switches is ON at a time, the remaining 15 diode switches are OFF. The splitters in column 4 must therefore be of the quadrature (90^o) type in order to provide a good input match under such loading. The splitters in columns 1, 2, and 3 must be the in-phase type for a good input match.

The ideal insertion loss of a 16-way splitter is 10 log (16) = 12 dB. Some 3 dB of implementation loss may be expected, for a total loss of 15 dB. The insertion loss of the matrix equals the sum of the input splitter loss, the diode-switch loss, and the output combiner loss, which is in the order of 15 + 1 + 15 = 31 dB. This insertion loss must be offset with IF amplifiers, a serious drawback of this architecture.

The diode-switches must contain at least two diodes (see figure 9-5B) in order to provide sufficient isolation; therefore, the total number of diodes for a 16 x 16 matrix is $2(16)^2 = 512$. Compare this number with the 614 diodes needed in a switch matrix architecture.

The advantage of the splitter matrix is the lower number of diodes. The disadvantages are (a) the high insertion loss and (b) the fact that the matrix size is restricted to a power-of-2. Another matrix size is possible but it involves a penalty of increased insertion loss. For example, a 17 x 17 switch can be built with 32-way splitters whose unused ports are properly loaded; the ideal insertion loss however will be 2[10 log (32)] = 30 dB and not 2[10 log (17)] = 25 dB.

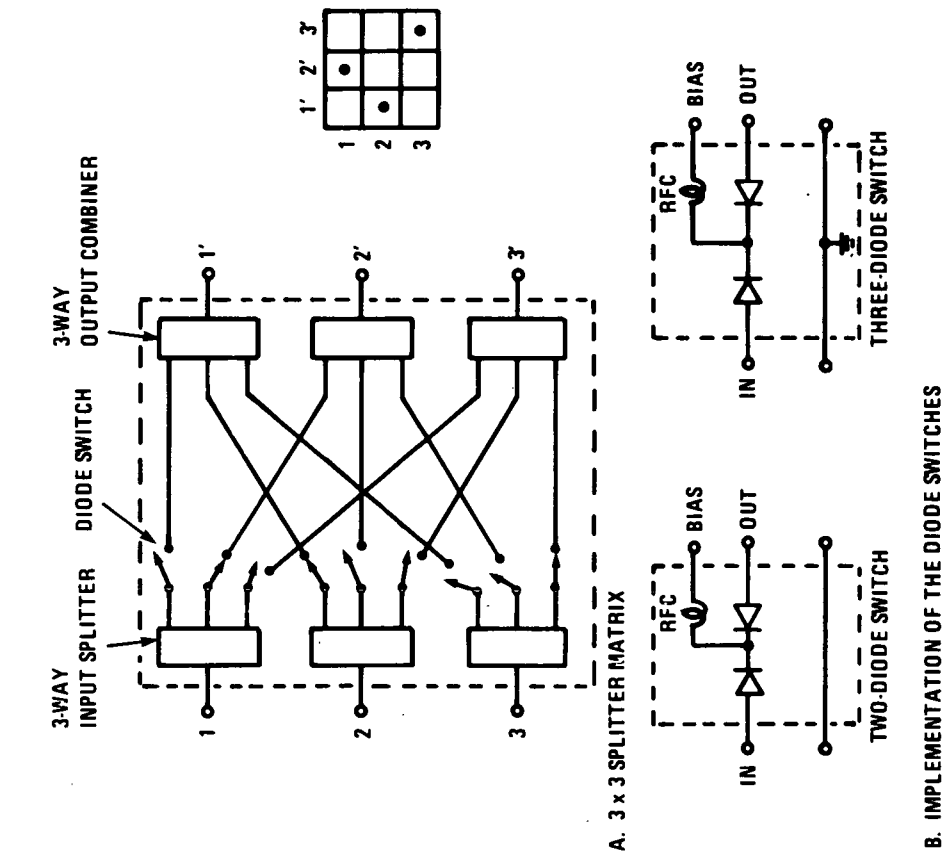

IA-65,133

Figure 9-5. Simple Splitter Matrix

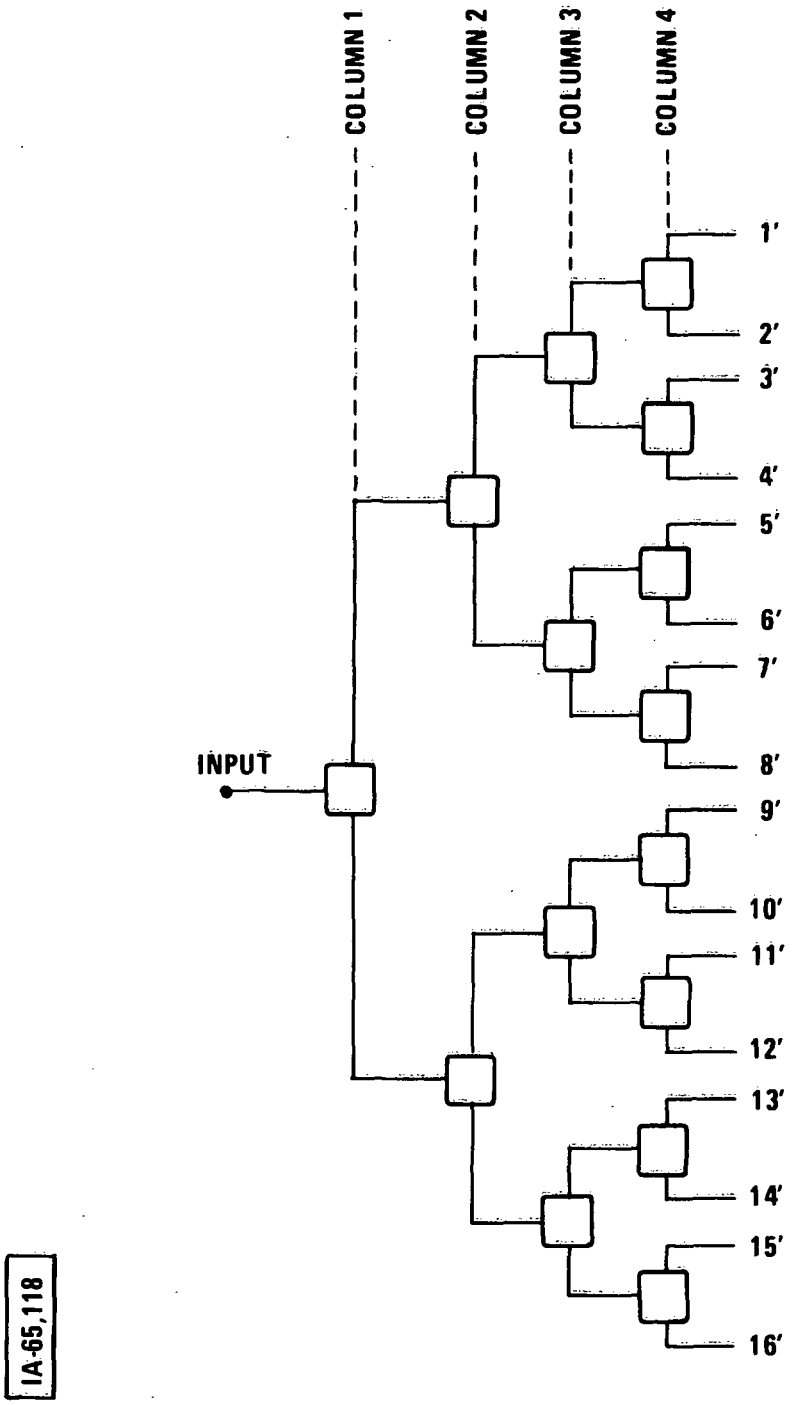

Figure 9-6. Schematic of a 16-Way Splitter

9.3.3 Rearrangeable-Elements Matrix

The most commonly encountered rearrangeable-elements matrices consist of building blocks called β-elements that function as reversing switches; see figure 9-7. A non-redundant 16 x 16 matrix consists of 49 β-elements. A single-redundant 16 x 16 matrix consists of 57 β-elements; see figure 9-8. Since each β-element consists of eight diodes (figure 9-7B), the total number of diodes in a redundant 16 x 16 matrix is 8 x 57 = 456. Notice that this represents not only the smallest number of diodes of all three architectures but also corresponds to a redundant operation. The reliability of a rearrangeable-element matrix is the highest of the three architectures.

The advantages of a rearrangeable-elements matrix are: (a) the low number of diodes and drivers is relatively low, consequently, reliability is high; (b) redundant operation is easy to achieve by adding a few β-elements; and (c) medium scale integration (MSI) technology can be applied easily, increasing the reliability further. The disadvantages are: (a) the entire matrix must be reconfigured even if only a single path must be altered; (b) if a diode fails, the faulty β-element can be traced and by-passed only with a special test procedure; (c) the redundant configuration is applicable only to power-of-2 matrix sizes; and (d) amplitude imbalance results from the fact that some paths in the matrix pass through more β-elements than other paths. In the redundant configuration, the amplitude imbalance equals the loss of one β-element.

Table 9-2 provides a comparison between the various matrix architectures.

Table 9-2. Comparison of Matrix Architectures (16 x 16)

	Switch (non-redundant)	Splitter (non-redundant)	Rearrangeable (redundant)
Number of Diodes	640	512	456
Number of Drivers	64	256	57
Insertion Loss (dB)	8	31	16 max/14 min
Isolation (dB)	80	60	40 per β-el.
Probab. of Survival (in 5 years)	0.571	0.260	0.846

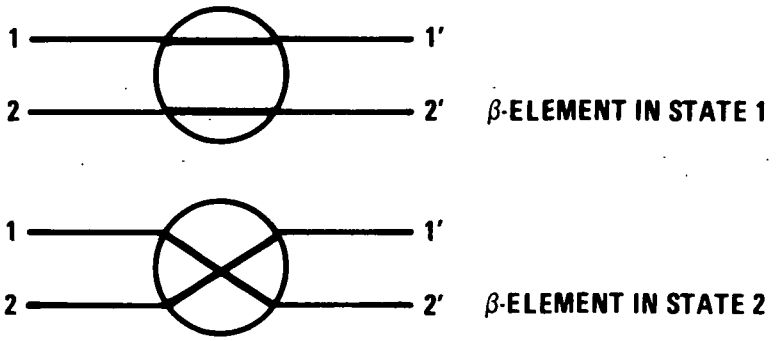

A. THE TWO STATES OF A β-ELEMENT

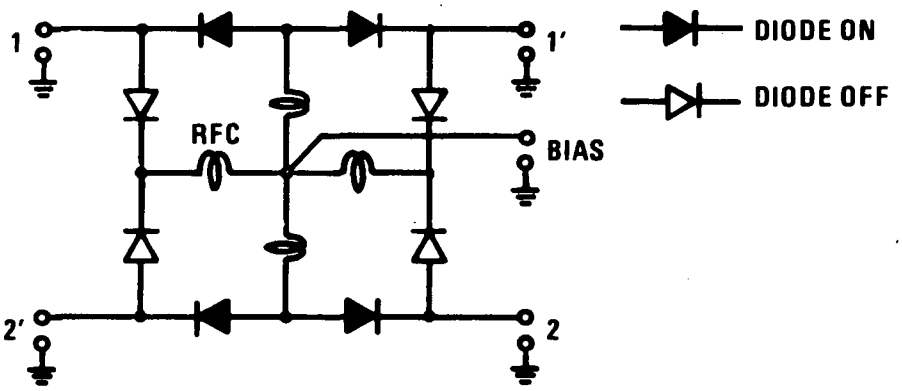

B. PRACTICAL IMPLEMENTATION OF A β-ELEMENT

IA-65,117

Figure 9-7. The β-Element

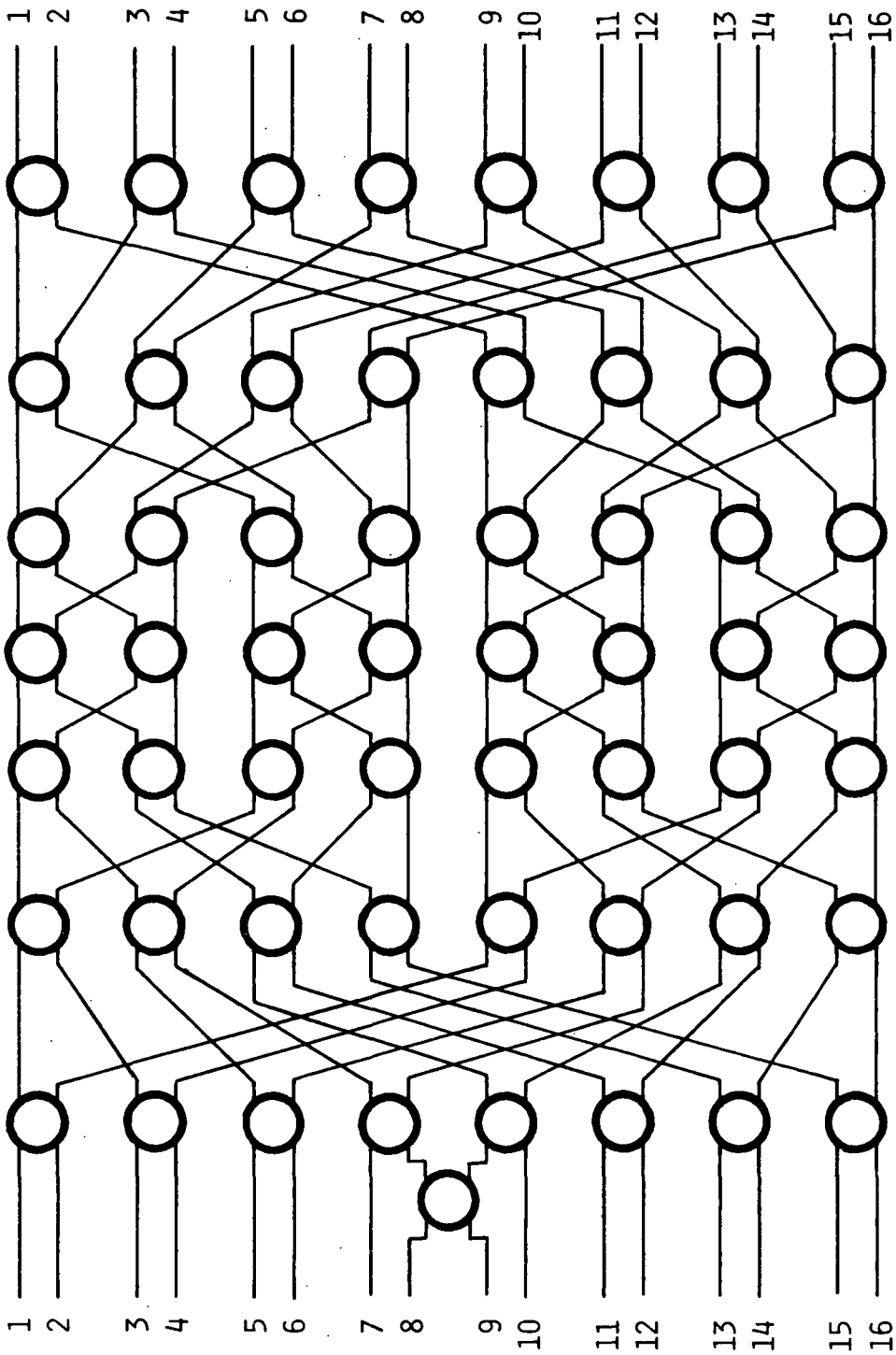

Figure 9-8. Redundant 16 x 16 Rearrangeable Network Matrix

Note: Survival of a non-redundant matrix means that all diodes and drivers survive. Survival of a single-redundant matrix means that all diodes and drivers survive, or that all but one of the diodes and drivers survive.

The probability of survival for a non-redundant switch matrix and splitter matrix is calculated from the formula

$$\exp\left[-(\text{number of diodes})\,\lambda_1 t - (\text{number of drivers})\,\lambda_2 t\right]$$

where $\lambda_1 = 10$ failures/10^9 hours for a PIN diode and $\lambda_2 = 100$ failures/10^9 hours for a driver.

The probability of survival of a single redundant 16 x 16 rearrangeable matrix is calculated from the formula

$$(p^8 r)^{57} + 57\left[p^8 s + (8p^7 q + 12\,p^6 q^2 + 8p^5 q^3 + 2p^4 q^4)(r + 0.5s)\right](p^8 r)^{56}$$

where $p = \epsilon^{-\lambda_1 t}$, $q = 1 - p$, $r = \epsilon^{-\lambda_2 t}$ and $s = 1-r$.

These figures for the probability of survival are for comparison only. They can be improved by providing redundancy in the matrix; however, this is outside the scope of the present work.

9.4 SYSTEM PERFORMANCE

A summary of the system parameters is presented in table 9-3. The relatively large uplink burst rate requires large earth terminal power. Presently such power levels cannot be furnished by solid state amplifiers at 30 Ghz.

The weight and power consumption of the trunking transponder can be estimated from the weight and power consumption of the individual building blocks. The number of these building blocks can be established with reference to figure 9-9, which shows the signal level and gain distribution in the transponder. The gain (and thus the number) of various amplifiers can be determined from this figure. Table 9-4 provides a weight and power consumption breakdown for the major building blocks.

Table 9-3. Summary of the Trunking Parameters

Satellite		
Number of Beams		16
Beamdwidth	(degrees)	0.35
Number of Carriers Per Beam		1
Power Amplifier Output	(W)	29
Output Backoff	(dB)	0
Transponder Gain	(dB)	105
Earth Terminal		
Antenna Diameter	(m)	6
Noise Temperature	(K)	500
Power Amplifier Output	(W)	2.6
Output Backoff	(dB)	0
System Parameters		
Bit-Error-Rate		10^{-6}
Required E_b/N_o	(dB)	13.5
Data Rate	(Mb/s)	12.6
Burst Rate	(Mb/s)	55.44
Rain Margin (up/down)	(dB)	10/6
Systems Losses (up/down)	(dB)	232/225

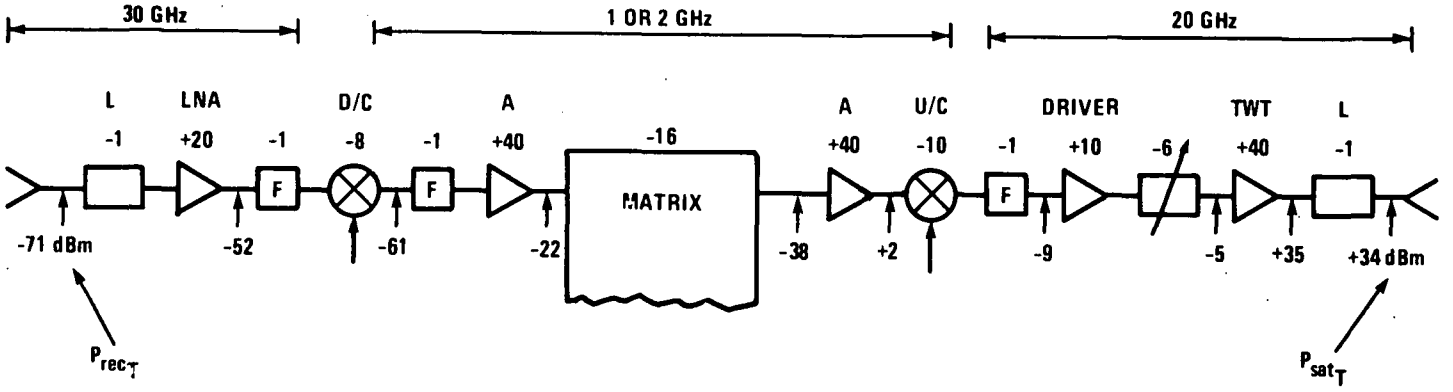

(*) $P_{ET} = \frac{C}{kT}_{up} + R_T + k + T_{sat} + B_{ET} + L_{up} - G_{ET}(tr) - G_{sat}(rec)$

$= 18.3 + 10 \log (55.44 \times 10^6) - 228.6 + 10 \log (1500) + 0$

$+ 232 - 63 - 53.3 = 14.6 \text{ dBW} = 29 \text{ W}$

(*) $P_{rec\,T} = P_{ET} + G_{ET}(tr) - L_{up} + G_{sat}(rec)$

$= 14.6 + 63 - 232 + 53.3 = -101.1 \text{ dBW}$

(*) $P_{sat\,T} = \frac{C}{kT}_{down} + R_T + k + T_E + B_{sat} + L_{down} - G_{sat}(tr) - G_E(rec)$

$= 16.0 + 10 \log (55.44 \times 10^6) - 228.6 + 10 \log (500) + 0$

$+ 225 - 53.3 - 59.4 = 4.1 \text{ dBW} = 2.6 \text{ W}$

The gain of the trunking transponder is:

(*) GAIN = 4.1 - (-101.1) = 105.2 dB

Figure 9-9. Transponder Signal Level and Gain Diagram

Table 9-4. *Trunking Transponder Weight and Power Budget*

Component	No. Units	Unit Weight (oz)	Unit Power (W)	Weight (oz)	Power (W)
LNA, 30 GHz, 20 dB	16	8	1.5	128	24
Filter, 30 GHz	16	6	--	96	--
D/C, 30/2 GHz	16	16	--	256	--
Filter, 2 GHz	16		--	128	--
Amplifier, 2 GHz, 20 dB	32	6	1.5	192	48
Matrix (β -Element)	57	2	0.12	114	7
Diode Drivers	57	3	1.2	171	68
Amplifier, 2 GHz, 20 dB	32	6	1.5	192	48
U/C, 2/20 GHz	16	16	--	256	--
Filter, 20 GHz	16	6	--	96	--
Amplifier, 20 GHz, 10 dB	16	8	1.2	128	19
TWTA, 20 GHz, 3 W	16	384	10	5568	160
Multipliers	32	32	3	1024	96
Master Osc. (redundant)	2	80	5	20	10
				8369 oz	480 W
Total Weight				=523 lb	

SECTION 10

COST COMPARISON STUDY

The CPS space segment cost for each conceptual satellite design is estimated by a simple cost model based on weight and power consumption. The terminal cost is estimated by the model discussed in detail in MTR-8311, page 165.

A comparison of satellite weight and power for the four systems is shown in table 10-1. The satellite weight is estimated by a subsystem components count, using a complexity multiplier. This complexity multiplier varies from 1 to 1.3 in the four systems. The trunking transponders share the satellites, but add only 500 lb to the weight and 500 W to the DC power consumption. This is less than 20% of the CPS weight and 15% of the CPS power consumption. The trunking transponders share the satellite cost in some (undefined) proportion to their throughput capacity, weight, and power consumption. Since this sharing is not a clearly defined issue at this time of the study, only the CPS segment cost and its impact are considered.

10.1 SATELLITE COST

The space segment cost consists of two parts: R&D cost and satellite hardware cost, including launch fee. The cost calculation assumes for simplicity that each system comprises only two satellites: one operational and one spare. The satellite average weight, shown in table 10-1, is applied to equations (10.1) and (10.2) to compute the satellite R&D cost and hardware cost (in millions of dollars).

$$C_{NRE} = 0.016\ W_C^{1.16} \tag{10.1}$$

$$C_{SU} = 0.031\ W_C^{0.93} \tag{10.2}$$

Where C_{NRE} is the non-recurring engineering cost, C_{SU} is the first unit cost, and W_C is the communications related average weight (in lbs).

In order to derive the total system cost for each of the four access modes, the terminal costs need to be estimated by the aid of a conceptual terminal design. The estimated satellite costs based on the above principles are shown in table 10-1.

Table 10-1. Satellite Cost Estimates

	FR-TDMA	SR-FDMA	SS-TDMA	PR-TDMA
Comm. Related Weight+	3762 lb	3615 lb	3660 lb	3707 lb
Avg Wt	4514 lb	3615 lb	4172 lb	5004 lb
R&D Cost	$277.6 M	$214.5 M	$253.3 M	$312.3 M
Production Cost	$ 77.6 M	$ 63.2 M	$ 72.1 M	$ 85.5 M
Quantity	2	2	2	2
Launch Cost	$ 35 M	$ 35 M	$ 35 M	$ 35 M
Total Cost	$467.8 M	$376.0 M	$432.5 M	$519 M
Satellite Cost/T_1	$.240M/$T_1$	$.259M/$T_1$	$.230M/$T_1$	$.276M/$T_1$
Satellite Efficiency	1.75W/Mb/s	1.68W/Mb/s	1.58W/Mb/s	2.1W/Mb/s

+Communications Related Weight includes the items listed and is a term defined for purposes of this report. It should not be confused with conventionally employed "communications payload" or "satellite dry weight".

10.2 TERMINAL COST

A common design of the terminals use a 3.0 m dish antenna and 1000 K receiver noise temperature. The terminals, whenever possible, are non-redundant single thread designs; however, some redundancy was introduced in the SS-TDMA system terminals, as described later. The terminal cost calculation using cost modeling and computer analysis is described in detail by MTR-8311, pages 165 to 170.

10.2.1 SR-FDMA Terminal

The SR-FDMA terminal is designed with four up-converters and down-converters in order to provide simultaneous routing by means of frequency selection to different geographical locations. This mode of operation requires fairly inexpensive modems (1 Mb/s), relatively inexpensive transmitters (1 to 2 W), but rather expensive frequency synthesizers. If a single up-converter were used this would be the lowest cost terminal. The detailed cost breakdown is shown in table 10-2 along with some projected production costs. The production cost is estimated by the cost model for a production quantity of 100, with conventional waveguide technology. If larger quantities are involved (over 1000) this cost will not be reduced substantially due to the labor-intensive operation. Different technology like MIC or MMIC would change the cost relationship at the expense of performance and related specifications. The solid-state transmitter at 2 to 3 W power level is far less expensive than the TWT (about $5K to 10K). The cost of the antenna is $35K without tracking and is common to all systems. Finally, integration, test, quality control, overhead costs are included.

In summary, this terminal is costly because of the four simultaneous uplink and downlink carriers needed for the individual addressing mode.

10.2.2 FR-TDMA Terminal

The FR-TDMA terminal has the lowest cost design among the four alternatives, despite the fairly high modem ($35K) and synthesizer costs. Since the uplink burst rate is 2.5 Mb/s and the downlink is 36 Mb/s, the modem cost splits unevenly (80% for demodulation and 20% for modulation). By using frequency hopping, only a single carrier must be generated at a time; therefore, only one up-converter and one down-converter are required. The solid state transmitter for CPS_1 (2 W HPA) and the traveling wave tube amplifier (TWTA) for CPS_2 (10^1 W HPA) contribute to the low terminal cost. The

total terminal cost is substantially lower than that of the other systems because of the single up/down converters. Frequency hopping synthesizers are not expensive and are presently available, provided they are not fast hopping. The remainder of the cost elements are the same (antenna, LNA, overhead) as for the other systems. Not included in the analysis are expenses related to system time and frequency synchronization. It is assumed that these expenses will not alter the cost estimates signficantly.

10.2.3 SS-TDMA Terminal

The SS-TDMA terminal is fairly complex and requires a considerable cost estimating effort. The antenna cost is the same as before but the transmitter cost is nearly doubled relative to the SR-FDMA or FR-TDMA systems due to the relatively high uplink burst rate (18 Mb/s). Solid-state power amplifiers are not expected to operate in this power range even by 1990. The modem cost is moderate ($35K) because the 18 Mb/s burst rate is not considered beyond the state-of-the-art. Since the adaptive rain compensation mode requires a special carrier frequency, each terminal must have two up-converters and two down-converters, one for each frequency. This increases the hardware cost significantly and consequently the terminal cost.

The frequency synthesizer is less complex than in an FDMA terminal and is therefore less costly. The frequency and time standard, on the other hand, is more expensive due to synchronization accuracy requirements. The detailed cost breakdown is shown in table 10-2. The final production cost of such a TDMA terminal would be in the $500K range, not including installation. Note that a single-frequency TDMA terminal would cost about 25% less than quoted above. Coding and decoding at a 18 Mb/s burst rate is not trivial and requires high-speed digital technology with a fairly large number of chips. The FEC coding equipment alone would cost well over $20K. Data and voice multiplexing/equipment are not included in the above cost estimate.

10.2.4 PR-TDMA Terminal

The PR-TDMA terminal design is very similar to the SS-TDMA concept. The terminal operates with a 3.0 m antenna system, and includes TWTA transmitters at 10 W for CPS_1, and at 20 W for CPS_2. The dual-frequency operation for uplink service in this system also requires two up- and down-converters per terminal, a significant cost contribution. The largest cost increase in comparison to SS-TDMA comes from the modem cost of operating at a 72 Mb/s downlink

Table 10-2. Terminal Cost Analysis

ITEM	FR-TDMA	SR-FDMA	SS-TDMA	PR-TDMA
Antenna D = 3.0 m	$ 35K	$ 35K	$ 35K	$ 35K
LNA	$ 10K	$ 10K	$ 10K	$ 10K
Transmitter	$ 20K	$ 20K	$ 40K	$ 40K
CPS_2	$ 40K	$ 40K	$ 40K	
Modem + FEC	$ 35K	$ 20K	$ 35K	$ 90K
Up-Converter	$ 35K(1)	$ 25K(4)	$ 35K(2)	$ 35K(2)
Down-Converter	$ 35K(1)	$ 25K(4)	$ 35K(2)	$ 35K(2)
Frequency Synthesizer	$ 20K	$ 10K	$ 5K	$ 5K
Frequency Standard	$ 15K	$ 10K	$ 15K	$ 15K
Total Hardware	$205K	$305K	$280K	$335K
Overhead	$374 K	$555K	$510 K	$610 K
Total 1st Unit	$580K	$860K	$790K	$945K
Production Cost				
N = 100 X = 95%	$460K	$685K	$630K	$753K
N = 1000 X = 95%	$390K	$578K	$530K (397)	$634K

rate. Since modem cost is mainly related to synchronization circuit requirements, the cost of the modem was estimated at $90K (this includes a 18 Mb/s modulator). The remaining terminal subsystems like the frequency synthesizer, and frequency and time standard are the same as in the SS-TDMA terminal. The total terminal production cost, $630K, is the highest among the four systems mainly due to the high modem cost. However, if two downlink carriers with 36 Mb/s each supported CPS traffic in a beam, the terminal cost would be about the same ($550K) as the SS-TDMA terminal. The details of major subsystem cost breakdown for these terminals are shown in table 10-2. The terminal cost does not include installation and multiplex equipment.

10.3 SYSTEM COST COMPARISON RESULTS

The anticipated cost of the space segment and ground segment is summarized in table 10-3. The ground segment cost is defined as about 80% to 85% of the total system cost. The system cost factor (efficiency) is the ratio of the total cost to the system capacity in megabits per second and is shown in table 10-4 for each of the four systems. The FR-TDMA system has the lowest cost factor of $1.26 M per Mb/s, closely followed by the SS-TDMA system ($1.42 M per Mb/s). The two other systems, SR-FDMA and PR-TDMA have an equally high cost factor of $1.70 M per Mb/s for different reasons. The cost factor of the SR-FDMA is high because of the low system capacity. For PR-TDMA, the cost factor is high because of the high terminal cost. The trunking transponders share the satellite and its cost in a certain proportion to their throughput capacity weight and power consumption. However, in this comparison only the CPS space segment cost is considered. The ratio of the space segment cost to the number of satellites yields a single spacecraft cost. The satellite cost then is apportioned among the transponders to provide the transponder cost.

The capacities of the CPS_1 and CPS_2 transponders are not equal; however, in this study an average capacity per transponder is assumed for both services. The ratio of the transponder cost to its throughput capacity provides information about the cost to the user per megabit per second. The total system cost per megabit per second can be expressed as follows:

$$\text{System cost per Mb/s} = \frac{\text{Satellite Cost}}{\text{No. Transponders}} \frac{1}{K} + \frac{\text{Earth Terminal Cost}}{N}$$

Table 10-3. Total System Cost Comparison Results

ITEM	FR-TDMA	SR-FDMA	SS-TDMA	PR-TDMA
Space Segment	$ 468M	$ 376M	$ 432M	$ 519M
No. CPS_1 E. Terminal	2816	1980	2970	2970
Cost/E. Terminal	$ 390K	$ 578K	$ 530K	$ 634K
No. CPS_2 E. Terminal	2558	900	1310	1350
Cost/E. Terminal	$ 426K	$ 615K	$ 530K	$ 645K
Total Terminal Cost	$2,188M	$1,698M	$2,268M	$2,754M
Total System Cost	$2,656M	$2,074M	$2,700M	$3,273M
System Cost Factor (CPS Only)	$1.26M/Mb/s	$1.70M/Mb/s	$1.42M/Mb/s	$1.72M/Mb/s
CPS T_1 Rate	$1.94M	$2.62M	$2.19M	$2.65M

Table 10-4. Total System Cost Comparison Study

	FR-TDMA	SR-FDMA	SS-TDMA	PR-TDMA
No. Transponders				
CPS_1	22	22	44	22
CPS_2	10	10	10	10
Traffic Capacity				
CPS_1	65.6 Mb/s	45.8 Mb/s	34.56 Mb/s	65 Mb/s
CPS_2	65.6 Mb/s	22.9 Mb/s	36.0 Mb/s	34.5 Mb/s
Total Satellite Cost CPS Only				
CPS_1 (2/3)	$278M	$217.0M	$254.3M	$311.3M
CPS_2 (1/3)	$139M	$108.5M	$127.2M	$155.6M
Transponders Cost				
CPS_1	$15.8M	$ 12.3M	$ 7.22M	$ 17.7M
CPS_2	$17.4M	$ 13.5M	$15.90M	$ 19.5M
For 7 Years Life Per Year at T_1 Rate				
CPS_1	$0.106M	$0.118M	$0.092M	$0.112M
CPS_2	$0.116M	$0.260M	$0.194M	$0.248M
Terminal Cost/Year				
1/3 T_1 CPS_1	$55.7K	$82.6K	$75.7K	$90.6K
1/6 T_2 CPS_2	$60.9K	$87.8K	$75.7K	$92.1K
Total Cost/Year = Term + Sat for T_1 Rate				
CPS_1	$273.1K	$365.7K	$319.1K	$383.7K
CPS_2	$481.0	$787.1	$648.3	$800.8
	(298.7K)	(523.5K)	(421.1K)	(524.4K)
Total Cost/Year Per Satellite Voice Ch. 64kb				
CPS_1	$11.4K	$15.2K	$13.3K	$16.0K
CPS_2	$20.0K	$32.8K	$27.0K	$33.3K
	($12.5K)	($21.8K)	($17.5K)	($21.8K)

where

K = satellite transponder capacity in Mb/s

N = earth terminal capacity in Mb/s

The terminal segment cost per voice channel should be a fraction (20% to 40%) of the space segment cost per voice channel. Then the cost of the satellite per voice channel will determine the system cost efficiency and the number of voice channels that could be economically supported by the terminal. In a well balanced cost relationship, a minimum cost for the satellite or transponder (per voice channel) leads to a low system cost (per voice channel). The goal of the system economics is to keep the space and ground segment cost per voice channel in balance.

To optimize the system cost, maximum capacity access modes (processing, coding, etc.) high gain satellite beams, a large DC solar array, and a large number of transponders are required. Some of these conclusions exclude the FDMA/FDM non-processing satellite system as a cost effective candidate.

In summary, to find the most economical system on a per voice channel basis, the following procedure must be used:

1. Define each system and design the proper satellite.

2. Calculate the throughput capacity for each system.

3. Calculate individually each satellite communications payload weight and required DC power.

4. Calculate from a cost model the single satellite cost.

5. Compute the single transponder cost by CPS_1 and CPS_2 apportionment of the satellite for each service according to its capacity.

6. Select an acceptable cost ratio (per voice channel) between space and ground segment.

7. Design an earth terminal for each system at minimum cost.

The Satellite-Routed FDMA/FDM scheme has the lowest system cost and the least throughput capacity of the systems in this study. Its system cost per voice channel is the highest among the four systems and its terminal cost is relatively high due to the multicarrier operation used for routing. The Frequency-Routed TDMA system has

the lowest terminal cost, a high satellite capacity, and relatively low cost per voice channel. The Satellite-Switched TDMA system is the most cost-effective system per voice channel among the four systems because it has a relatively low uplink burst rate, partial processing in the satellite, and high throughput capacity. The Processor-Routed TDMA/TDM design is not as cost-effective a system per voice channel because of its complex, full-processing satellite, high downlink burst rate, and high terminal cost.

Large, complex, processing satellites are heavy, expensive, and also require expensive terminals at 30/20 GHz operation. The complex and expensive terminals are only economical if a large number of users are serviced by a single terminal. Providing individual addressing schemes for a large community of small users is a complex task both in the frequency domain (FDMA) and the time domain (TDMA). The terminal cost is dominated by the high microwave components cost and by the modem cost (in a high burst rate system). The economics call for more than eight voice channels per terminal and the idea of a small and inexpensive terminal does not appear to be feasible in the 30/20 GHz band today, even when the system throughput capacity is substantially reduced.

SECTION 11

CONCLUSIONS

This section summarizes the major conclusions of the report. Detailed discussions of these points can be found in the main body of the report.

A satellite system for CPS communications involves thousands of earth terminals; therefore, the ground segment cost essentially determines the system cost. Reduction of the terminal cost requires low-cost transmitters and modems and moderate size antennas.

Low-cost transmitters can be achieved with solid-state amplifiers. Output power of up to 2 W can be obtained at 30 GHz with presently available technology. This low power will suffice for closing the link only with a low uplink transmission rate. Such a low rate is characteristic of FDMA systems and multicarrier TDM systems.

The modem cost is proportional to the burst rate. Therefore, low cost modems can be used only in FDMA and multicarrier TDMA systems.

A CPS terminal antenna size of about 3 m is a reasonable compromise between gain and cost. A larger size antenna requires satellite tracking capabilities and is expensive.

Processing on board the satellite is beneficial for the system performance. For instance, processing isolates the uplink and downlink noise contributions. It also allows system flexibilities which are not possible in a non-processing system. For example, processing allows the system to operate with many uplink carriers and only one or two downlink carriers. The small number of downlink carriers enables the satellite TWT amplifier to operate near saturation. However, a processing satellite consumes a large amount of DC power and is heavy.

Processing in the satellite provides a link improvement which can be used as part of the required rain margin. Thus, only part of the rain margin must be obtained by terminal transmitter over-design. Experimental data show that only a small portion of CONUS experiences heavy rain and therefore only some of the CPS users need the processing advantage. If most of the CPS users are routed by means of non-processing (low power consuming) transponders and a few

are routed by means of processing (high power consuming) transponders, the satellite resources can be utilized more efficiently.

High-gain multibeam satellite antennas reduce the satellite power requirements and allow reuse of the frequency band. Scanning beams result in a high-burst-rate operation and are, therefore, incompatible with the low-cost terminal requirement. A large number of fixed beams require a large number of transponders; this leads to a heavy satellite that consumes a large amount of DC power. On the other hand, a small number of spot beams cover only a restricted area. Thus, a careful selection of 0.35° beams that cover only the large metropolitan centers and 0.7° beams that cover rural areas appears to be a reasonable compromise.

The analysis of costs indicates that the postulated scenario of small earth terminals which service a number of large users and signal routing to individual users cannot be implemented inexpensively. Increasing the number of satellites from one to two appears to be more cost efficient. Partial processing, for only those users that experience rain attenuation, and a Frequency-Routed TDMA system can be combined to provide less expensive operation. Such a combination deserves further study.

BIBLIOGRAPHY

Berk, G., P. F. Christopher, M. Hoffman, P. N. Jean, E. Rotholz, B. E. White, "Final Technical Report; On-Board Processing for Future Satellite Communications Systems: Satellite-Routed FDMA," MTR 8311, NASA/LeRC C-49029-D, Bedford, MA: The MITRE Corp., May 1981.

Berk, G., P. N. Jean, E. Rotholz, B. E. White, "An FDMA System Concept for 30/20 GHz High Capacity Domestic Satellite Service," 9th AIAA Communications Satellite Systems Conference, San Diego, CA, March 7-11, 1982.

Crane, R. K., "Prediction of Attenuation by Rain," Concord, MA: Environmental Research and Technology, Inc., August 1979.

Dill, G. D. and G. C. Jenkins, "TDMA in the Dow Jones and Company, Inc. Satellite Communications Network," National Telecommunications Conference, Houston, TX, May 1980.

Foldes, P., "Ka-Band Multiband Contiguous Coverage Satellite Antenna for the USA," 8th AIAA Communications Satellite Systems Conference, Orlando, FL, April 1980.

Ford Aerospace, "Concepts for 18/30 GHz Communication System Study," NASA Contract NAS3-21362, Vol. I, Final Report, Palo Alto, CA: Ford Aerospace Corp., November 1979.

Gabbard, O. G. and P. Kaul, "Time Division Multiple Access," Proceedings of EASCON '74, Fall, 1974, pp. 179-184.

Jean, P. N. and W. R. Neal, "An Architectural Design of an FDMA/TDM Baseband Processor for 20/30 GHz Satellite Communications System," International Telemetering Conference Proceedings, San Diego, CA, 1981.

Katz, J. L., H. Hoffman, S. L. Kota, J. M. Ruddy, B. E. White, "Final Report: Application of Advanced On-Board Processing Concepts to Future Satellite Communications Systems," MTR-3787, Vol I, Bedford, MA: The MITRE Corp., June 1979.

Spielker, J., "Digital Communications by Satellite," Englewood Cliffs, NJ: Prentice-Hall, 1977.

APPENDIX

SYSTEM THROUGHPUT STUDY

Page Intentionally Left Blank

TABLE OF CONTENTS

LIST OF ILLUSTRATIONS

LIST OF TABLES

SYSTEM THROUGHPUT STUDY

This appendix presents a throughput study for several power limited systems for Customer Premise Service (CPS).

A.1 AVAILABLE DC POWER

The power generated by a solar-cell array of reasonable size and weight is estimated to be less than 5000 W. This power can be apportioned among the satellite subsystems as shown in table A-1. About 1000 W can be allocated to supply the traveling wave tube (TWT) amplifiers in a processing satellite. This TWT power, P_{TWT}, determines the system throughput. A well planned system that operates in the 20/30 GHz band is not bandwidth limited because the multibeam operation permits frequency reuse of the 2.5 GHz bandwidth.

Table A-1. Sample Apportionment of Satellite DC Power

	CPS Processing Satellite (W)	CPS Non-Processing Satellite (W)
TWT Amplifiers	1000	2000
Processor/Switch	2000	1000
Remaining Functions	1500	1500
Trunking Transponder	500	500
Total	5000	5000

A.2 THROUGHPUT DEFINITION

The throughput is the system capacity summed over all beams, expressed in bits per second (b/s). This definition uses the message bit rate rather than the total bit rate. In time division multiplex (TDM) systems, some of the bits carry header information and the total number of transmitted bits is larger than the number of message bits. Frequency division multiplex (FDM) systems, on the other hand, do not require header bits. Thus, to provide a fair comparison between these systems, they are evaluated on the basis of the message bits they can support. The ratio of header bits to message bits is defined as overhead. The overhead is zero in FDM systems and from 10% to 25% in the various TDM systems that are described in this report.

A.3 THROUGHPUT DERIVATION

The throughput is calculated by using the downlink power budget. The expression for the throughput is obtained by adding the DC power, P_{DC}, consumed by all TWT amplifiers:

$$P_{TWT} = P_{DC}\ (\text{all metropolitan TWT}) + P_{DC}\ (\text{all rural TWT}) + P_{DC}\ (\text{all trunking TWT})$$

$$P_{DC}\ (\text{all metropolitan TWT}) = \frac{1}{\eta_1} P_{RF}\ (\text{all metropolitan TWT})$$

where

η_1 is the DC/RF efficiency of the metropolitan TWT amplifiers

P_{RF} is the radio frequency (RF) power generated by all TWT amplifiers

P_{RF} (all metropolitan TWT) = $N_{B1}\ N'_{C1}\ p_{RF1}$

N_{B1} is the number of the metropolitan beams, and

N'_{C1} is the number of carriers in a metropolitan beam.

p_1 is the RF power per carrier

Thus,

$$P_{TWT} = \frac{N_{B1}N'_{C1}\ p_1}{\eta_1} + \frac{N_{B2}N'_{C2}p_2}{\eta_2} + \frac{N_{BT}N'_{CT}p_T}{\eta_T}$$

The RF power per carrier, p_i, is

$$p_i = \frac{\left(\frac{C}{kT}\right)_{down\ i}\ R_{down\ i}\ k\ T_{Ei}\ L_{down\ i}}{G_{sat\ i}\ (tr)\ G_{Ei}\ (rec)} \qquad i = 1, 2, T$$

where

(C/kT) is the carrier-to-thermal noise ratio

R is the transmission rate

T is the system noise temperature

L is the transmission loss and

G is the antenna gain

Thus,

$$P_{TWT} = \left(N_{B1}N'_{C1}R_{down\ 1}\right)\frac{\beta_1}{G_{sat\ 1}} + \left(N_{B2}N'_{C2}\ R_{down\ 2}\right)\frac{\beta_2}{G_{sat\ 2}} + \left(N_{BT}N'_{CT}\ R_{down\ T}\right)\frac{\beta_T}{G_{sat\ T}}$$

where β_i is a constant,

$$\beta_i = \frac{\left(\frac{C}{kT}\right)_{down\ i}\ kT_{Ei}\ L_{down\ i}}{\eta_i\ G_{Ei}\ (rec)} \qquad (A.1)$$

Note that $(N_{Bi}\ N'_{Ci}\ R_{down\ i})$ is equal to the throughput for service i, t_i, in an FDM system (where there is no overhead). In a TDM system, the burst rate is larger than the message rate, so that

$$(N_{Bi}\ N'_{Ci}\ R_{down\ i}) = (1+\alpha_i)\ t_i \qquad i = 1,2,T \tag{A.2}$$

and α_i is the overhead for service i,

$$\alpha_i \triangleq \frac{\text{number of header bits}}{\text{number of message bits}} \tag{A.3}$$

$$P_{TWT} = \frac{(1+\alpha_1)\beta_1}{G_{sat\ 1}} t_1 + \frac{(1+\alpha_2)\beta_2}{G_{sat\ 2}} t_2 + \frac{(1+\alpha_T)\beta_T}{G_{sat\ T}} t_T \tag{A.4}$$

or in a general form

$$t_1 + at_2 + bt_T = c\ P_{TWT} \tag{A.5}$$

where a, b, and c are constants that depend on the accessing mode. Equation (A.5) is referred to as the <u>throughput equation</u>.

A.4 ASSUMPTIONS ABOUT THE SYSTEM PARAMETERS

The downlink transmission loss appears in the expressions for P_{RF} (per carrier) and β_i. The transmission loss (downlink or uplink) consists of four components: free space loss, rain attenuation, edge of coverage loss, and miscellaneous losses. The links are designed with a rain margin of 6 dB for the downlink and 10 dB for the uplink. Such a rain margin corresponds to a 99.5% link availability for most of the continental United States (CONUS). The rain margin can be reduced by using coding. During rain storms, the transmit and receive CPS terminals switch to rate-1/2 coding/decoding which provides a 5 dB downlink coding gain. If the CPS

transponder decodes/encodes the uplink signal, then a 5 dB coding gain can be applied to the uplink rain margin. Thus, for CPS users

$$L_{down} = L(\text{free space}) + [L(\text{rain margin}) - G(\text{coding})] + L(\text{edge of cov}) + L(\text{miscellaneous})$$
$$= 210 + [\,6 - 5] + 4 + 5 = 220 \text{ dB} \quad (A.6)$$

$$L_{up} = 213 + [10 - 5] + 4 + 5 = 227 \text{ dB} \quad (A.7)$$
for decoding/encoding transponders

$$L_{up} = 213 + [10 - 0] + 4 + 5 = 232 \text{ dB} \quad (A.8)$$
for non-decoding/encoding transponders

The trunking stations use larger antennas, low-noise receivers (and possibly diversity reception), and have no need to resort to coding in order to combat rain attenuation. For the trunking users

$$L_{down} = 210 + [6 - 0] + 4 + 5 = 225 \text{ dB} \quad (A.9)$$

$$L_{up} = 213 + [10 - 0] + 4 + 5 = 232 \text{ dB} \quad (A.10)$$

The earth terminal antenna gain, G_E, appears in the expressions for p_{RF} (per carrier) and β_i. A large antenna gain means low terminal transmit power (inexpensive transmitter) as well as reduced demand from the satellite transmitter (low DC consumption). However, a large gain antenna must track the satellite. Also, a very large size antenna cannot always be physically accommodated in the customer premises. For all these reasons, an antenna diameter of 3 m is selected as a reasonable compromise for the CPS users. An antenna diameter of 6 m is chosen for the trunking users. Standard formulas are used for calculating G_E:

$$G_E = 0.55 \left(\frac{\pi D_E}{\lambda}\right)^2 \quad (A.11)$$

where D_E is the antenna diameter and λ is the wavelength.

The satellite antenna gain is determined from the half-power beamwidth. The metropolitan CPS and the trunking users are serviced by 0.35^o beams, while the rural CPS users are serviced by 0.7^o beams. The antenna gain is related to the half-power beamwidth, θ , by the following expression:

$$G_{sat} = \frac{26600}{\theta^2} \qquad (A.12)$$

where θ is in degrees.

Table A-2 presents the parameters for the three services.

Table A-2. System Parameters

	Metropolitan CPS	Rural CPS	Trunking Users
Satellite			
Number of Beams	22	10	16
Beamwidth (degrees)	0.35	0.70	0.35
Antenna Gain (dB)	53.3	47.3	53.3
Noise Temperature (K)	1500	1500	1500
Earth Terminals			
Antenna Diamter (m)	3	3	6
Transmit Ant. Gain (dB)	57.0	57.0	63.0
Receive Ant. Gain (dB)	53.4	53.4	59.4
Noise Temperature (K)	1000	1000	500

The DC/RF efficiency for the traveling wave tube which appears in the expressions for p_{RF} and β_i depends on the output backoff and is given in table A-3.

Table A-3. TWT Efficiency

Output Backoff (dB)	TWT Alone (%)	TWT and Power Supply (%)
0	40	35
5	30	25
7	28	23

The backoff value depends on the amount of noise that is allocated to intermodulation (see section A.6.1) and the accessing mode.

Expressing β_i in decibels (indicated by an asterisk at the left) results in the following:

$$(*) \quad \beta_1 = (C/kT)_{down\ 1} + k + T_{E1} + L_{down\ 1} - \eta_1 - G_{E1}(rec)$$

$$(*) \quad \beta_1 = (C/kT)_{down\ 1} - 228.6 + 10\log(1000) + 200 - \eta_1 - 53.4$$
$$= (C/kT)_{down\ 1} - \eta_1 - 32 \qquad (A.13)$$

$$(*) \quad \beta_2 = \beta_1 \qquad (A.14)$$

$$(*) \quad \beta_T = (C/kT)_{down\ T} - 228.6 + 10\log(500) + 225 - \eta_T - 59.4$$
$$= (C/kT)_{down\ T} - \eta_T - 36 \qquad (A.15)$$

A.5 CASES STUDIED

The coefficients a, b, and c in the throughput equation can be determined if α_i and β_i are known. The coefficient β_i can be calculated from the above equations if the downlink carrier-to-thermal noise density ratios are known. The latter depend on the interferences in the system, which in turn depend on the accessing mode. Several combinations of accessing modes for the CPS and trunking users were investigated; see table A-4.

Table A-4. Cases Studied

Case #	CPS			Trunking		
	Uplink	Downlink	Processing	Uplink	Downlink	Processing
1	FDMA	FDM	NO	FDMA	FDM	NO
2	FDMA	FDM	NO	HY	HY	NO
3	FDMA	FDM	YES	FDMA	FDM	NO
4	FDMA	FDM	YES	TDMA	TDM	NO
5	FDMA	FDM	YES	HY	HY	NO
6	FDMA	HY	YES	HY	HY	NO
7	FDMA	HY	YES	TDMA	TDM	NO
8	FDMA	TDM	YES	TDMA	TDM	NO
9	HY	HY	YES	HY	HY	NO
10	HY	HY	YES	TDMA	TDM	NO
11	HY	TDM	YES	TDMA	TDM	NO
12	TDMA	TDM	YES	TDMA	TDM	NO
13	FDMA	FDM	NO	TDMA	TDM	NO

In table A-4, TDM designates a system in which all the users in a beam operate on the same carrier frequency but are multiplexed in time. Since the burst rate in a pure TDM system is very high (expensive transmitters and modems), two carriers can be used in every beam; half of the users in the beam operate on one of the carriers and the other half operate on the second carrier. The TWT amplifiers in the satellite amplify only two carriers and can operate at saturation with negligible intermodulation interference generated. HY designates a hybrid multiplexing scheme that uses more than two carriers. All users operating on a given carrier are multiplexed in time. Figure A-1 illustrates a case in which the uplink uses an HY accessing mode with four carriers per beam and the downlink uses TDM with one carrier per beam. "Processing" indicates that the uplink signal is demodulated in the satellite, the bit stream is reshaped, and the signal is modulated for a downlink transmission. The uplink noise does not add to the downlink noise in a processing satellite. The accessing mode for the uplink may be different from the downlink in such a satellite. Processing satellites are suitable for TDM and HY accessing modes but are not suitable in FDM systems because of the large number of demodulators/ modulators required. (The number equals the number of active users, which could be 30,000.)

Consider Cases 1 and 3, where FDM is employed by the CPS and the trunking users: $\alpha_1 = \alpha_2 = \alpha_T = 0$ (no overhead), and $G_{sat1}\ (0.35^{o}) = G_{satT}\ (0.35^{o}) = 4\ G_{sat2}\ (0.7^{o})$ from equation (A.12). Then equation (A.4) becomes

$$P_{TWT} = \frac{\beta_1 t_1}{G_{sat\ 1}} + \frac{\beta_2 t_2}{G_{sat\ 2}} + \frac{\beta_T t_T}{G_{sat\ T}}$$

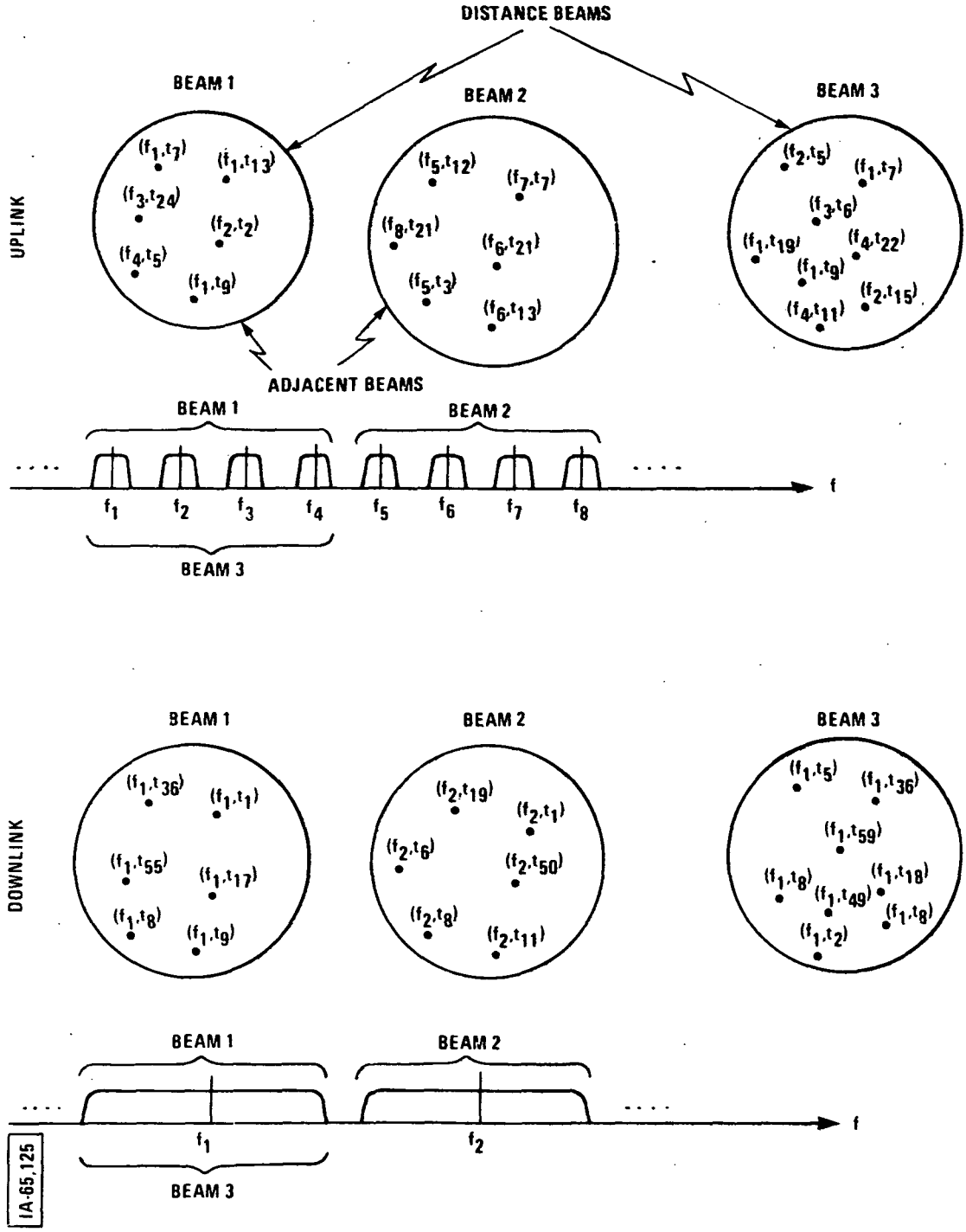

Figure A-1. Hybrid Uplink and TDM Downlink

Thus, the throughput equation for Cases 1 and 3 is

$$t_1 + 4t_2 + \left(\frac{\beta_T}{\beta_1}\right) t_T = \frac{G_{sat\ 1}}{\beta_1} P_{TWT} \tag{A.16}$$

Similarly, it can be shown that the throughput equations for the remaining cases are as follows:

Cases 2, 4, 5, and 13:

$$t_1 + 4t_2 + \left(1 + \alpha_T\right)\left(\frac{\beta_T}{\beta_1}\right) t_T = \frac{G_{sat\ 1}}{\beta_1} P_{TWT} \tag{A.17}$$

Cases 6, 7, 8, 9, 10, 11, and 12:

$$t_1 + 4t_2 + \frac{\left(1 + \alpha_T\right)}{\left(1 + \alpha_1\right)}\left(\frac{\beta_T}{\beta_1}\right) t_T = -\frac{G_{sat\ 1}}{\left(1 + \alpha_1\right)\beta_1} P_{TWT} \tag{A.18}$$

A.6 NOISE BUDGET

The throughput equations can be evaluated if the β_i values are determined; this requires a knowledge of the downlink carrier-to-thermal noise density ratio, $(C/kT)_{down}$. Thermal noise is one of several interferences that constitute total system noise. In a non-processing satellite, the total noise consists of the following seven components:

1. Earth terminal intermodulation
2. Uplink co-channel interference
3. Uplink thermal noise
4. Cross-channel interference
5. Satellite intermodulation
6. Downlink co-channel interference
7. Downlink thermal noise

The carrier-to-noise density ratios associated with these noise contributions are related by the following noise budget expression:

$$\frac{1}{\left(\frac{E_b}{N_o}\right)} = \frac{1}{\left(\frac{C}{IM}\right)_E} + \frac{1}{\left(\frac{C}{I}\right)_{co\ up}} + \frac{1}{\left(\frac{C}{kT}\right)_{up}} + \frac{1}{\left(\frac{C}{I}\right)_x}$$

$$+ \frac{1}{\left(\frac{C}{IM}\right)_{sat}} + \frac{1}{\left(\frac{C}{I}\right)_{co\ down}} + \frac{1}{\left(\frac{C}{kT}\right)_{down}} \qquad \text{(A.19)}$$

In a processing satellite, the noise can be divided into two groups

Uplink Noise	Downlink Noise
1. Earth terminal intermodulation	1. Satellite intermodulation
2. Uplink co-channel interference	2. Downlink co-channel interference
3. Cross-channel interference	3. Cross-channel interference
4. Uplink thermal noise	4. Downlink thermal noise

The carrier-to-noise density ratios associated with these noise contributions are related by the following noise-budget expressions:

$$\frac{1}{\left(\frac{E_b}{N_o}\right)} = \frac{1}{\left(\frac{C}{IM}\right)_E} + \frac{1}{\left(\frac{C}{I}\right)_{co\ up}} + \frac{1}{\left(\frac{C}{I}\right)_x} + \frac{1}{\left(\frac{C}{kT}\right)_{up}}$$

$$\frac{1}{\left(\frac{E_b}{N_o}\right)} = \frac{1}{\left(\frac{C}{IM}\right)_{sat}} + \frac{1}{\left(\frac{C}{I}\right)_{co\ down}} + \frac{1}{\left(\frac{C}{I}\right)_x} + \frac{1}{\left(\frac{C}{kT}\right)_{down}} \qquad \text{(A.20)}$$

The quantity of interest is $(C/kT)_{down}$. The system throughput is large if the coefficient c in the throughput equation, eq.(A.5), is large. However, $c \propto 1/\beta_1 \propto 1/(C/kT)_{down}$; hence, a small $(C/kT)_{down}$ is required for a large throughput. The noise budget equations show that $(C/kT)_{down}$ can approach the system E_b/N_o value only for large values of the remaining carrier-to-interference ratios.

The E_b/N_o value used in this report is 13.5 dBHz (11 dBHz for a bit error rate of 10^{-6} and 2.5 dB for implementation loss). This value ensures sufficient quality for data and voice communications.

A.6.1 Intermodulation Noise

The carrier-to-intermodulation ratio (C/IM) depends on the number of carriers that drive the power amplifier and on the output backoff. The C/IM for a single carrier (pure TDM) is infinite. It is assumed here that C/IM is quite large for two carriers even if the power amplifier operates at saturation. If the beams support several carriers, the carriers can be divided (by means of filters) into groups of two and each group can be amplified separately; see figure A-2. Some residual intermodulation can be anticipated; therefore, in HY systems, the assumed C/IM at saturation is 24 dB. FDM systems have hundreds of carriers in every beam. The satellite TWT must operate at backoff in order to reduce the intermodulation noise. The relation between backoff and C/IM is given in table A-5.

The amount of backoff can be calculated by optimizing the system performance. To illustrate this optimization, consider a processing satellite in which the carrier-to-interference ratio for the co-channel and the cross-channel interference in the downlink is 27 dB each.

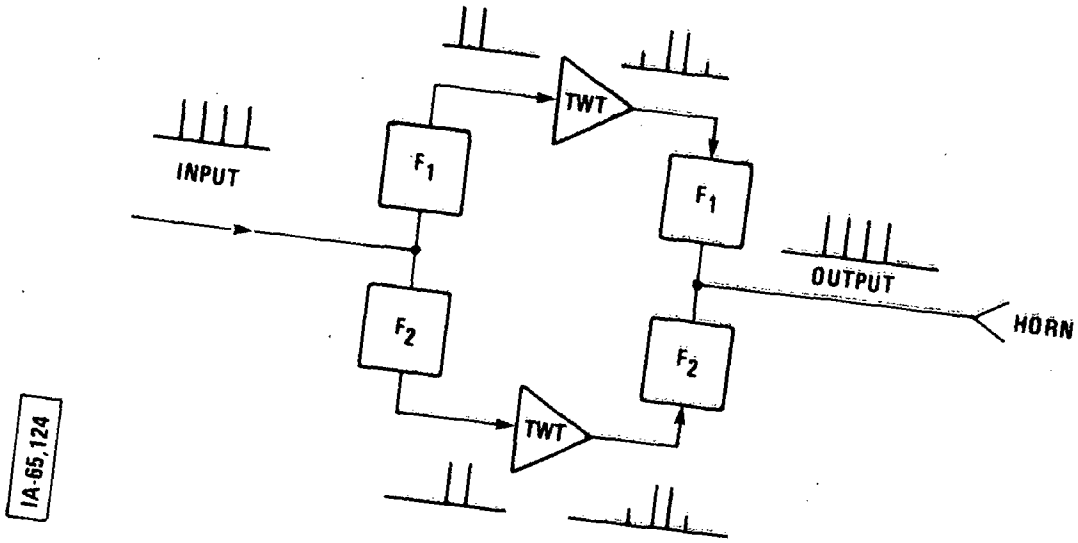

Figure A-2. Simple Intermodulation Reduction Scheme

Table A-5. C/IM Versus Output Backoff

Output Backoff (dB)	C/IM (dB)
5	16
6	18
7	20
8	22
9	24

$$\frac{1}{\left(\frac{E_b}{N_o}\right)} = \frac{1}{\left(\frac{C}{IM}\right)_{sat}} + \frac{1}{\left(\frac{C}{I}\right)_{co\ down}} + \frac{1}{\left(\frac{C}{I}\right)_{x}} + \frac{1}{\left(\frac{C}{kT}\right)_{down}}$$

$$\frac{1}{\left(\frac{C}{kT}\right)_{down}} = \frac{1}{\left(\frac{E_b}{N_o}\right)} - \left[\frac{1}{\left(\frac{C}{I}\right)_{co}} + \frac{1}{\left(\frac{C}{I}\right)_{x}}\right] - \frac{1}{\left(\frac{C}{IM}\right)_{sat}}$$

$$-13.5\ dB \quad -27\ dB \quad -27\ dB$$

$(C/kT)_{down}$ is tabulated versus $(C/IM)_{sat}$ in table A-6. As C/IM increases, $(C/kT)_{down}$ decreases. However $(C/IM)_{sat}$ increases only at the expense of increased backoff, i.e., reduced downlink power. The optimum $(C/IM)_{sat}$ (and also the optimum backoff) corresponds to the minimum of the function [C/kT + backoff] in dB. In this specific example, $(C/IM)_{opt} \simeq 19$ dB and the optimum backoff $\simeq 6.5$ dB.

Table A-6. Optimization of C/IM for Best System Performance

$(C/IM)_{sat}$ (dB)	Output Backoff (dB)	$(C/kT)_{down}$ (dB)	$(C/kT)_{down}$+Backoff (dB)	
17	5.5	16.8	22.3	
18	6.0	16.0	22.0	
19	6.5	15.5	22.0	opt.
20	7.0	15.1	22.1	
21	7.5	14.8	22.3	
22	8.0	14.6	22.6	

A.6.2 Co-Channel Interference

A multibeam satellite system conserves the frequency spectrum by allowing beams that are sufficiently separated to operate in the same frequency band. Even widely separated beams spill some energy into beams of the same band. Figure A-3 illustrates the co-channel interference. Beams 1 through 6 use the same frequency band, designated as f_1. If beam 1 is the desirable beam, the remaining beams are interfering. Of these, beam 6 is too far from beam 1 and can be ignored. Thus, in a typical situation, four beams cause co-channel interference.

$$\left(\frac{C}{I}\right)_{co} \simeq \frac{1}{4} \text{ (isolation between two beams)} \qquad \text{(A.21)}$$

The definition of "isolation" used here is illustrated in figure A-4.

If the desirable beam experiences rain attenuation, while the interfering beams do not, then

$$(*) \quad \left(\frac{C}{I}\right)_{co} = \text{(isolation)} - 6 - \text{(rain attenuation)} \qquad \text{(A.22)}$$

It is assumed here that the same band is assigned to beams that are isolated by at least 36 dB. Assume further a 3 dB residual rain attenuation (after the earth terminal has attempted to compensate for the rain); then

$$(*) \quad \left(\frac{C}{I}\right)_{co} = 36 - 6 - 3 = 27 \text{ dB} \qquad \text{(A.23)}$$

The number of carriers in a beam does not affect the above figure.

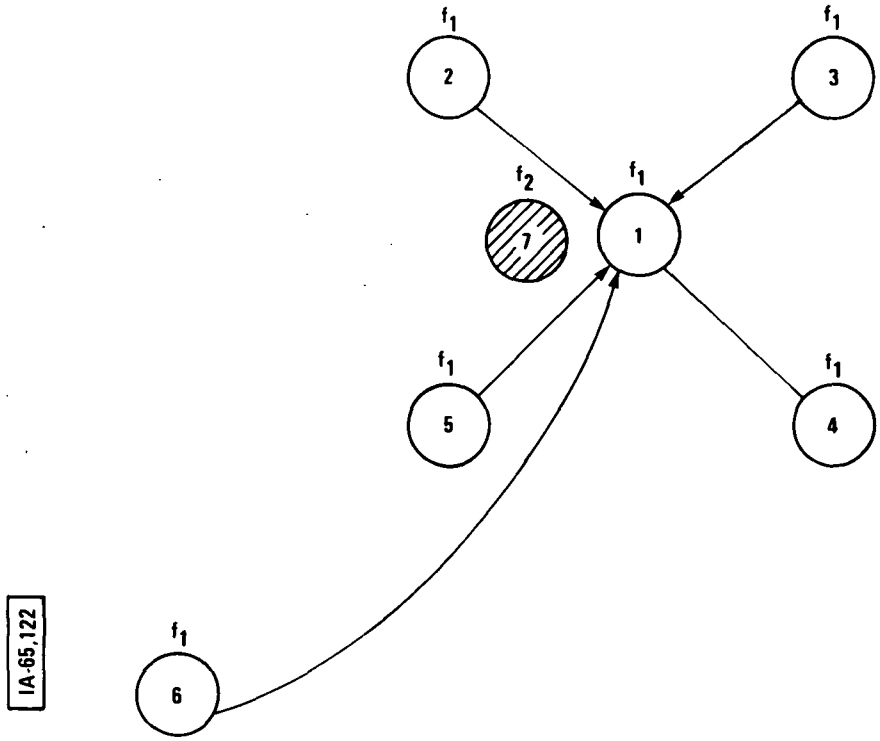

Figure A-3. Beam Topology for Co-Channel Interference Calculation

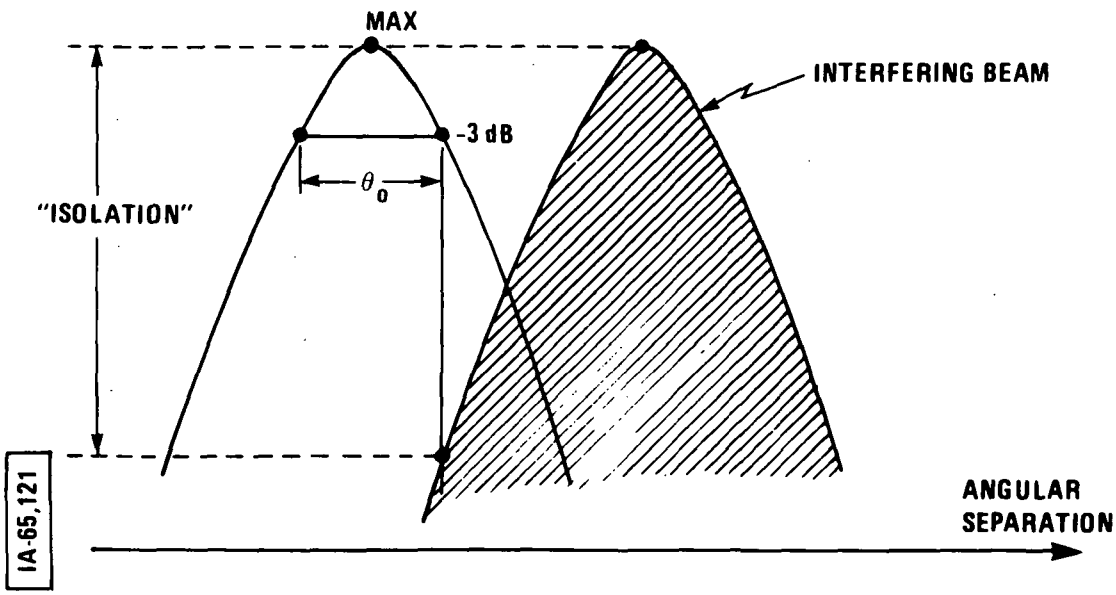

Figure A-4. Definition of Isolation

A.6.3 Cross-Channel Interference

Adjacent channels in the same beam interfere with each other due to energy spreading of modulated signals. The amount of interference between two adjacent channels is designated as H. The interference depends on the modulation scheme and the spacing between the carriers, $\Delta f/R$, where R is the bit rate. H versus $\Delta f/R$ for various modulation schemes is plotted in figure A-5. When a channel is surrounded by two adjacent channels, the amount of interference doubles, 2H; see figure A-6. More than two adjacent channels increase the interference to slightly more than 2H; thus

$$\left(\frac{C}{I}\right)_x = \infty \qquad \text{a single channel} \tag{A.24}$$

$$\left(\frac{C}{I}\right)_x = \frac{1}{H} \qquad \text{one adjacent channel} \tag{A.25}$$

$$\left(\frac{C}{I}\right)_x = \frac{1}{2H} \qquad \text{two or more adjacent channels} \tag{A.26}$$

If the desired channel experiences rain attenuation, while the adjacent channels do not, then

$$(*) \quad \left(\frac{C}{I}\right)_x = \frac{1}{H} - 3 - (\text{rain attenuation}) \tag{A.27}$$

Assume a 3 dB "residual" attenuation; then

$$(*) \quad \left(\frac{C}{I}\right)_x = \frac{1}{H} - 3 - 3 = \frac{1}{H} - 6 \text{ dB} \tag{A.28}$$

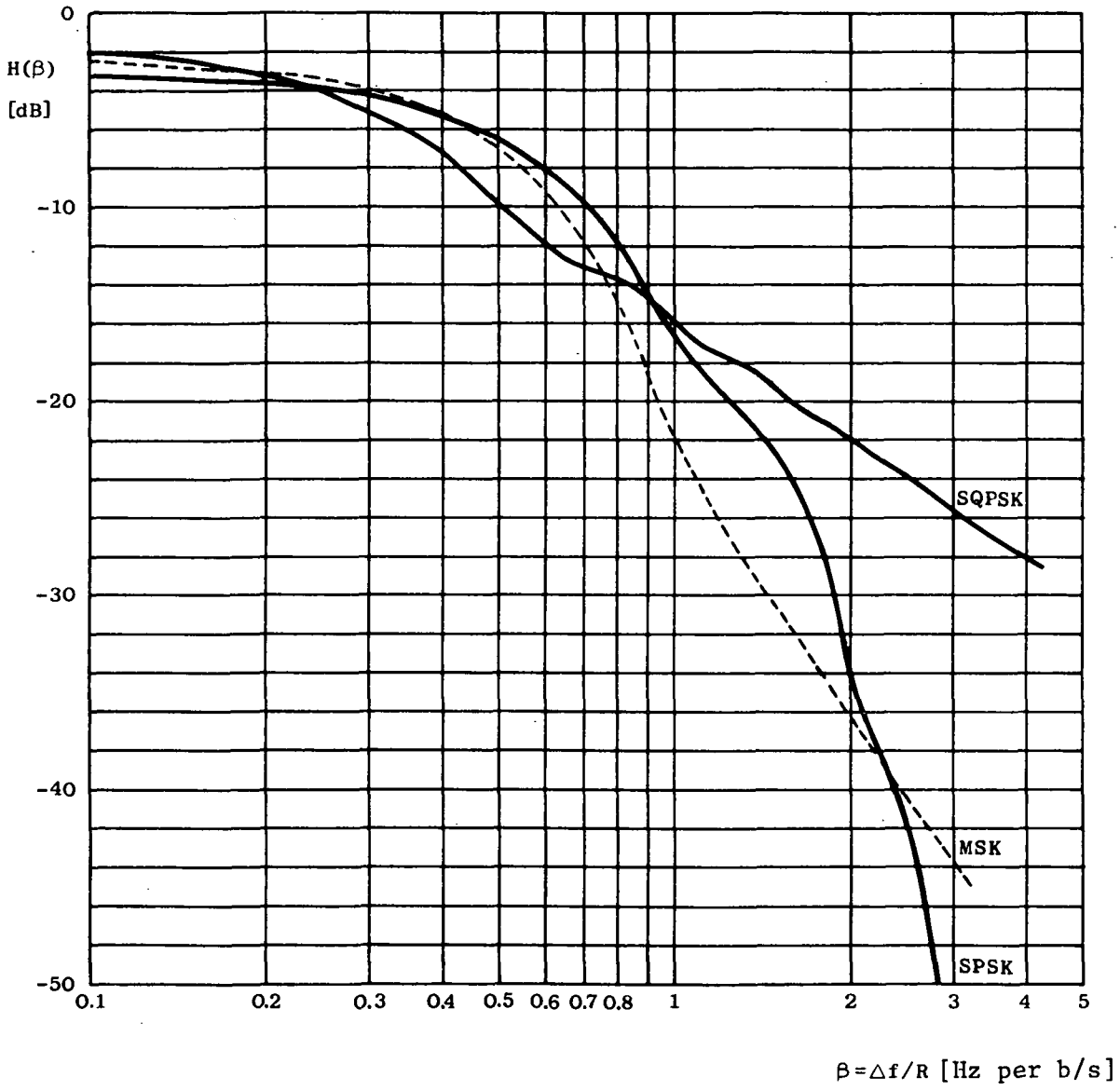

Figure A-5. Cross-Channel Interference Between Two Adjacent Channels

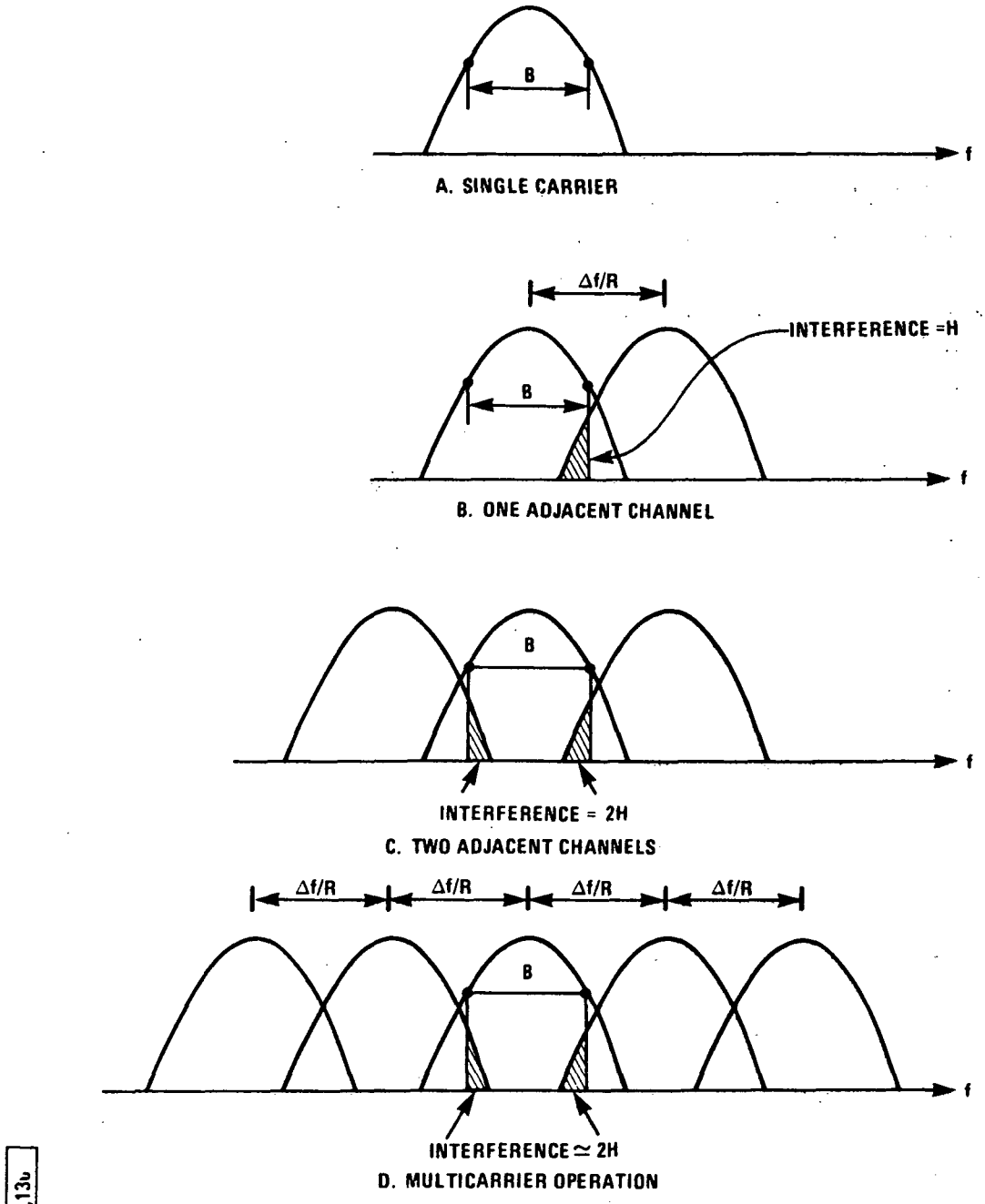

Figure A-6. Cross-Channel Interference in a Beam

For a multiple shift keyed (MSK) modulation and $\Delta f/R = 1.8$, $1/H = 33$ dB from figure A-5, so that $(C/I)_x = 33 - 6 = 27$ dB (3 dB residual rain and two or more adjacent channels). If the spacing between the carriers is reduced or if the modulation scheme is not MSK, then $(C/I)_x$ is smaller than 27 dB.

A.6.4 Noise Summary

The carrier-to-noise density ratios for intermodulation, co-channel, and cross-channel interference are summarized in table A-7 as a function of the number of carriers per beam.

Table A-7. C/I For Various Accessing Schemes

		(C/IM) (dB)	Backoff (dB)	$(C/I)_{co}$ (dB)	$(C/I)_x$ (dB)
Single carrier	(TDM)	∞	0	27	∞
Two carriers	(TDM)	∞	0	27	30
4 to 6 carriers	(HY)	24	0	27	27
Multiple carriers	(FDM)	*	variable	27	27

* Depends on the backoff (optimized)

where

$(C/I)_{co}$ includes a 3 dB residual rain attenuation and

$(C/I)_x$ is for MSK with $\Delta f/R = 1.8$ and includes a 3 dB residual rain attenuation.

Applying these results to the 13 cases in table A-4 yields the results listed in table A-8. In the non-processing cases,

Table A-8. Noise Distribution

CASE	LINK	CPS						TRUNKING					
		ACCESS	$\frac{E_b}{N_0}$	$\frac{C}{kT}$	$\frac{C}{IM}$	$\frac{C}{I}_{co}$	$\frac{C}{I}_{x}$	ACCESS	$\frac{E_b}{N_0}$	$\frac{C}{kT}$	$\frac{C}{IM}$	$\frac{C}{I}_{co}$	$\frac{C}{I}_{x}$
1	down up	FDMA FDM	13.5 -	18.5 20.8	19 24	27 27	27	FDMA FDM	13.5 -	17.8 20.1	19 ∞	27 27	27
2	down up	FDMA FDM	13.5 -	18.5 20.8	19 24	27 27	27	HY HY	13.5 -	16.6 18.9	24 ∞	27 27	27
3	down up	FDMA FDM	13.5 13.5	16.0 14.4	18 24	27 27	27 27	FDMA FDM	13.5 -	17.8 20.1	19 ∞	27 27	27
4	down up	FDMA FDM	13.5 13.5	16.0 14.4	18 24	27 27	27 27	TDMA TDM	13.5 -	16.0 18.3	∞ ∞	27 27	30
5	down up	FDMA FDM	13.5 13.5	16.0 14.4	18 24	27 27	27 27	HY HY	13.5 -	16.6 18.9	24 ∞	27 27	27
6	down up	FDMA HY	13.5 13.5	16.0 13.9	18 ∞	27 27	27 27	HY HY	13.5 -	16.6 18.9	24 ∞	27 27	27
7	down up	FDMA HY	13.5 13.5	16.0 13.9	18 ∞	27 27	27 27	TDMA TDM	13.5 -	16.0 18.3	∞ ∞	27 27	30

Table A-8. Noise Distribution (Continued)

CASE	LINK	CPS						TRUNKING					
		ACCESS	$\frac{E_b}{N_0}$	$\frac{C}{kT}$	$\frac{C}{IM}$	$\frac{C}{I}_{co}$	$\frac{C}{I}_{x}$	ACCESS	$\frac{E_b}{N_0}$	$\frac{C}{kT}$	$\frac{C}{IM}$	$\frac{C}{I}_{co}$	$\frac{C}{I}_{x}$
8	down up	FDMA TDM	13.5 13.5	16.0 13.8	18 ∞	27 27	27 30	TDMA TDM	13.5 -	16.0 18.3	∞ ∞	27 27	30
9	down up	HY HY	13.5 13.5	14.4 13.9	24 ∞	27 27	27 27	HY HY	13.5 -	16.6 18.9	24 ∞	27 27	27
10	down up	HY HY	13.5 13.5	14.4 13.9	24 ∞	27 27	27 27	TDMA TDM	13.5 -	16.0 18.3	∞ ∞	27 27	30
11	down up	HY TDM	13.5 13.5	14.4 13.8	24 ∞	27 27	27 30	TDMA TDM	13.5 -	16.0 18.3	∞ ∞	27 27	30
12	down up	TDMA TDM	13.5 13.5	14.2 13.8	24 ∞	27 27	30 30	TDMA TDM	13.5 -	16.0 18.3	∞ ∞	27 27	30
13	down up	TDMA TDM	13.5 13.5	14.2 13.8	24 ∞	27 27	30 30	TDMA TDM	13.5 -	16.0 18.3	∞ ∞	27 27	30

$(C/kT)_{down}$ cannot be separated from $(C/kT)_{up}$ unless some assumptions are made about their relationship.

If we define

$$\frac{(C/kT)_{down}\,(C/kT)_{up}}{(C/kT)_{down} + (C/kT)_{up}} \triangleq x$$

then, it is assumed that

(*) $$\left(\frac{C}{kT}\right)_{down} = x + 2 \text{ dB}$$

$$\left(\frac{C}{kT}\right)_{up} = \frac{(C/kT)_{down}\,x}{(C/kT)_{down} - x}$$

For example, in a non-processing FDM system in which $(C/IM)_E = 24$ dB (arbitrarily assumed), $(C/IM)_{sat} = 19$ dB (optimized), $(C/I)_{co\ up} = 27$ dB, the noise budget equation (19) gives

$$\frac{(C/kT)_{down}\,(C/kT)_{up}}{(C/kT)_{down} + (C/kT)_{up}} = 16.5 \text{ dB}$$

This is apportioned as

$$(C/kT)_{down} = 16.5 + 2 = 18.5 \text{ dB}$$

and

$$(C/kT)_{up} = 20.8 \text{ dB}$$

These values apply for the CPS users in Case 1 and are shown in table A-8.

A.7 NUMERICAL THROUGHPUT EQUATIONS

Numerical values for the coefficients of the throughput equations can be obtained by first assuming values for the TDM overhead, α, and then evaluating the constants β_i. The latter requires a knowledge of $(C/kT)_{down}$, which is available from table A-8, and the satellite TWT efficiency. The efficiency depends on the TWT backoff, as shown in table A-3. The backoff for the downlink is 0 dB for TDM and HY and is optimized (see section A.6.1) for FDM. The TWT efficiency for the various cases is given in table A-9.

The constants α_1, α_2 and α_T are evaluated by using equations (A.13), (A.14), and (A.15) and are listed in table A-10.

The throughput equations for cases 1 through 13 are listed in table A-11. These are based on a TDM overhead of about 10%, which is considered quite reasonable. An additional case, 11A, which applies to the FR-TDMA system described in section 8, is included. The throughput equation for case 11A is calculated for a 25% overhead.

A.8 SOLUTION OF THE THROUGHPUT EQUATIONS

The throughput equation for a particular case involves four unknowns: t_1, t_2, t_T, and P_{TWT}. P_{TWT} is assumed close to 1000 W for a processing satellite and 2000 W for a non-processing one. To solve the throughput equation, some relations between t_1, t_2, and t_T must be assumed. The following considerations are adopted here:

Table A-9. TWT Backoff and DC/RF Efficiency for the Various Cases

Case	TWT_1 Backoff (dB)	TWT_1 Efficiency (%)	TWT_T Backoff (dB)	TWT_T Efficiency (%)
1	6.5	23	6.5	23
2	6.5	23	0	35
3	6	24	6.5	23
4	6	24	0	35
5	6	24	0	35
6	6	24	0	35
7	6	24	0	35
8	6	24	0	35
9	0	35	0	35
10	0	35	0	35
11	0	35	0	35
12	0	35	0	35
13	6.5	23	0	35

Table A-10. Constants α_1, α_2, and α_T for the Various Cases

Case	$\alpha_1 = \alpha_2$ (dB)	α_T (dB)
1	-7.117	-11.817
2	-7.117	-14.841
3	-9.802	-11.817
4	-9.802	-15.441
5	-9.802	-14.841
6	-9.802	-14.841
7	-9.802	-15.441
8	-9.802	-15.44
9	-13.041	-14.841
10	-13.041	-15.441
11	-13.041	-15.441
12	-13.241	-15.441
13	-7.117	-15.441

Table A-11. Throughput Equations

Case 1	$t_1 + 4t_2 + 0.339\ t_T = 1.101 \times 10^6\ P_{TWT}$
Case 2	$t_1 + 4t_2 + 0.187\ t_T = 1.101 \times 10^6\ P_{TWT}$
Case 3	$t_1 + 4t_2 + 0.339\ t_T = 2.043 \times 10^6\ P_{TWT}$
Case 4	$t_1 + 4t_2 + 0.300\ t_T = 2.043 \times 10^6\ P_{TWT}$
Case 5	$t_1 + 4t_2 + 0.345\ t_T = 2.043 \times 10^6\ P_{TWT}$
Case 6	$t_1 + 4t_2 + 0.313\ t_T = 1.857 \times 10^6\ P_{TWT}$
Case 7	$t_1 + 4t_2 + 0.273\ t_T = 1.857 \times 10^6\ P_{TWT}$
Case 8	$t_1 + 4t_2 + 0.273\ t_T = 1.857 \times 10^6\ P_{TWT}$
Case 9	$t_1 + 4t_2 + 0.661\ t_T = 3.915 \times 10^6\ P_{TWT}$
Case 10	$t_1 + 4t_2 + 0.575\ t_T = 3.915 \times 10^6\ P_{TWT}$
Case 11	$t_1 + 4t_2 + 0.575\ t_T = 3.915 \times 10^6\ P_{TWT}$
Case 11A	$t_1 + 4t_2 + 0.506\ t_T = 3.445 \times 10^6\ P_{TWT}$
Case 12	$t_1 + 4t_2 + 0.603\ t_T = 4.099 \times 10^6\ P_{TWT}$
Case 13	$t_1 + 4t_2 + 0.162\ t_T = 1.101 \times 10^6\ P_{TWT}$

The dimension of t is b/s, the dimension of P_{TWT} is watts.
$\alpha_1 = \alpha_2 = 0.1$, $\alpha_T = 0.1$ for all cases except Case 11A.
$\alpha_1 = \alpha_2 = 0.1$, $\alpha_T = 0.25$ for Case 11A.

1. Since the satellite's prime function is to service CPS users, the trunking throughput supported by the satellite is assumed to be equal to approximately one-half the CPS throughput,

$$t_T \simeq 0.5\ t_{CPS} = 0.5(t_1 + t_2) \qquad \text{(A.29)}$$

2. Trunking throughput must be an integer multiple of 12.6Mb/s which is the lowest trunking data rate.

3. Rural CPS traffic probably represents 20 to 25% of the metropolitan throughput. This presumption can be obtained in two ways:

a.

Metrop. CPS	Rural CPS
$N_{B1} = 22$	$N_{B2} = 10$
$N'_{C1} = c_1$	$N'_{C2} = c_1/2$
$R_1 = r_1$	$R_2 = r_1$

b.

Metrop. CPS	Rural CPs
$N_{B1} = 22$	$N_{B2} = 10$
$N'_{C1} = c_1$	$N'_{C2} = c_1$
$R_1 = r_1$	$R_2 = r_1/2$

(A.30)

$$\frac{t_1}{t_2} = \frac{22\ c_1 r_1}{10\left(c_1/2\right) r_1} = 4.4 \qquad \frac{t_1}{t_2} = \frac{22\ c_1 r_1}{10\ c_1\left(r_1/2\right)} = 4.4$$

In certain systems, for example in FR-TDMA (see section 8), the number of carriers in all beams must be the same, $N'_{C1} = N'_{C2}$, and the burst rates in all beams must be the same, $R_1 = R_2$. In such a case,

$$t_1 = (22/10)\ t_2 = 2.2\ t_2 \qquad \text{(A.31)}$$

The throughput equations are solved with these relations between t_1, t_2, and t_T and the results are listed in table A-12.

Table A-12. Throughputs for the Various Cases

Case	P_{TWT} (W)	t_1 (Mb/s)	t_2 (Mb/s)	t_T (Mb/s)	t_{TOTAL} (Mb/s)
Case 1	2000	1046	238	605	1889
Case 2	2000	1074	244	806	2118
Case 3	1000	963	218	605	1786
Case 4	1000	975	222	605	1802
Case 5	1000	961	218	605	1784
Case 6	1000	874	199	605	1678
Case 7	1000	886	201	605	1692
Case 8	1000	886	201	605	1692
Case 9	1000	1702	387	1008	3097
Case 10	1000	1747	397	1008	3152
Case 11	1000	1747	397	1008	3152
Case 11A	1000	1078	490	806	2374
Case 12	1000	1765	401	1210	3376
Case 13	2000	1085	247	806	2138

In all but Case 11A $t_1/t_2 = 4.4$; in Case 11A $t_1/t_2 = 2.2$.

A.9 SELECTING THE MOST PROMISING CASES

Although throughput equations have been derived for 13 distinct combinations of accessing modes, the various cases cannot be judged on the basis of throughput alone. Terminal and satellite cost and complexity must be considered. Several cases that were selected as the most viable are discussed in detail in the body of this report.

Problems associated with the various cases are assessed below. Cases are ranked on a scale of 1 to 6.

Case 1. Because of the FDM operation, the transmission rate is very low (64 kb/s); therefore, the modems are inexpensive. In spite of backoff operation, the power required from the terminal transmitter is low. The satellite is simple since it does not provide any processing. However, the system throughput is relatively low (less than 2 Gb/s, see table A-11). The overall ranking of this case is 5.

Case 2. Comments for Case 1 apply; the system throughput is slightly higher and there is less interference between CPS and trunking users because of the different accessing modes. (CPS uses FDM and trunking uses TDM.) The ranking is 4.

Case 3 and Cases 4, 5, 6, 7, 8. A processing FDM satellite is very complex; it requires a very large number of demodulators and modulators (some 30,000), while the throughput is still quite small. The ranking of these cases is: unacceptable.

Case 9. The hybrid accessing mode results in a relatively low burst rate (less than 20 Mb/s), relatively low-cost modems, and low-power solid-state transmitters. The hybrid accessing mode for the

trunking service results in low-cost modems and transmitters; however, the transponder is somewhat more complicated, consumes more DC power, and weighs more. The ranking is 3.

Case 10. This case is similar to Case 9 except for a simpler trunking transponder that operates in TDM. The ranking is 2.

Case 11. Like Cases 9 and 10, this is a high-capacity system. The hybrid accessing in the uplink results in low-cost terminals; the TDM in the downlink results in a simpler transponder design. The ranking is 1.

Case 11A. This case is similar to Case 11.

Case 12. This is the highest throughput case; however, the high burst rate (due to TDM operation) results in expensive earth terminals. The ranking is 6.

Case 13. Comments for Case 2 apply here. The ranking is 4.

From the above evaluation, four cases were selected for further detailed studies: Cases 10, 11, 11A and 13. Their important parameters were calculated by using the following formulas, and are summarized in table A-13.

The transmission rate in an FDM system equals the voice rate of 64 kb/s.

The burst rate of TDM and HY systems equals

$$R_i = \frac{\left(1 + \alpha_i\right) t_i}{N_{Bi} N'_{ci}} \qquad (A.32)$$

Table A-13. Important Parameters of the Four Selected Cases

CASE	NAME	LINK	ACCESS	t_{TOT} Mb/s	CPS 1				CPS 2			
					No.of Car/b.	Burst Rate Mb/s	Term. Power W	Through put Mb/s	No.of Car/b.	Burst Rate Mb/s	Term. Power W	Through put Mb/s
10	none	up down	HY HY	3152	4 4	21.838 21.838	5.24 -	1747	4 4	10.919 10.919	10.45 -	397
11	PR-TDM	up down	HY TDM	3152	4 2	21.838 43.675	5.12 -	1747	4 2	10.919 21.838	10.21 -	397
11A	FR-TDM	up down	HY TDM	2374	32 2	1.914 30.625	1.41 -	1078	32 2	1.914 30.625	5.60 -	490
13	SR-FDM	up down	FDMA FDM	2138	1518 1518	0.064 0.064	1.89 -	1085	386 386	0.064 0.064	3.77 -	247

The TDM overhead for Cases 10 and 11 is 10%; for Case 11A it is 25%.
The number of Metropolitan beams is 22; the number of rural beams is 10.
Cases 10 and 11 use processing with decoding/encoding in the satellite.
Case 11A uses processing but not decoding/encoding.
Case 13 does not use processing.

where

α_i is the TDM overhead for service i, i = 1, 2, T

N_{Bi} is the number of beams

N'_{ci} is the number of carriers per beam

The output power of the earth terminal power amplifier, at saturation, is

$$P_{Ei} = \underbrace{\left(\frac{C}{kT}\right)_{up\ i}}_{\text{Table A-8}} + \underbrace{R_{up\ i}}_{\text{Eq. (A.32)}} + k + \underbrace{T_{sat}}_{\text{Table A-2}} + L_{up} + \text{Backoff} - \underbrace{G_{Ei}(tr) - G_{sat\ i}(rec)}_{\text{Table A-2}}$$

L_{up}: Eq. (A.7) or (A.8) or (A.10)

(A.33)

For example, in Case 11A, L_{up} = 232 dB. (See section A.4 for a non-decoding/encoding satellite.)

$$P_{E1} = 13.8 + 10 \log (1.914 \times 10^6) - 228.6 + 10 \log (1500) + 232 + 0 - 57.0 - 53.3 = 1.48 \text{ dBW}$$

$$= 1.41 \text{ W}$$

A.10 THROUGHPUT SUMMARY

This appendix derives the relationship between system throughput and the DC power consumed by the satellite TWT amplifiers for various accessing modes. The relationship is referred to as the throughput equation, and has the general form given by equation (A.5). The set of accessing modes for the CPS and trunking services in the uplink and the downlink defines the study

case. Thirteen cases were considered; their definition is given in table A-4. The throughput equations for the various cases are given by equations (A.16, (A.17), and (A.18). Numerical values for the coefficients of these equations can be obtained by assuming certain system parameters common to all cases and by evaluating the downlink carrier-to-thermal noise density ratio for each particular case. The assumed system parameters (e.g., terminal antenna size, half-power beamwidth, etc.) are listed in table A-2. The downlink carrier-to-thermal noise density ratio is calculated from the noise budget of every case and is given in table A-8. Throughput equations for the various cases are presented in table A-11. Numerical solutions of the throughput equations are given in table A-12.

Four cases were selected as most viable; important system parameters (e.g., burst rate, transmitter power, throughput) were calculated for them and are tabulated in table A-13.

GLOSSARY

AM	amplitude modulation
BER	bit error rate
BFN	beam-forming network
BP	bandpass
BPSK	binary phase shift keying
b/s	bits per second
BW	bandwidth
C/IM	carrier-to-intermodulation ratio
CMOS	complementary metal oxide silicon
CODEC	coder-decoder
CONUS	continental United States
CPS	customer premise service
CW	continuous wave
DAMA	demand assignment multiple access
DCC	Digital Communications Corporation
DOD	Department of Defense
EHF	extremely high frequency
EIRP	effective isotropic radiated power
FDM	frequency division multiplex
FDMA	frequency division multiple access
FEC	forward error correction
FET	field effect transistor

GLOSSARY (Continued)

FR	frequency routed
G/T	gain-to-noise temperature ratio
HPA	high power amplifier
HPBW	half-power beamwidth
IF	intermediate frequency
kb/s	kilobits per second
LNA	low noise amplifier
LO	local oscillator
LSI	large scale integration
MBA	multiple beam antenna
Mb/s	megabits per second
MIC	microwave integrated circuit
MIT	Massachusetts Institute of Technology
MMIC	monolithic microwave integrated circuit
MSI	medium scale integration
MSK	M'ary shift keying
NASA/LeRC	National Aeronautical and Space Administration Lewis Research Center
NCS	network control center
NOSC	Naval Ocean Systems Center
OMT	orthomode transducer
PLL	phase lock loop
PM	phase modulation

GLOSSARY (Concluded)

PPM	permanent positional magnet
PR	processor-routed
QPSK	quarternary phase shift keying
RADC	Rome Air Development Center
R&D	research and development
RF	radio frequency
R/W	read/write
SBS	Satellite Business System
SCC	satellite control center
SCPC	single channel per carrier
SCT	single channel transponder
SR	satellite routed
SR	shift register
SS	satellite switched
TDM	time division multiplex
TDMA	time division multiple access
TTL	transistor-transistor logic
TWT	traveling wave tube
UHF	ultra high frequency
VCO	voltage controlled oscillator

Page Intentionally Left Blank

DISTRIBUTION LIST

INTERNAL

D-10

K. E. McVicar

D-11

J. J. Croke
C. A. Fowler
L. T. Spaney

D-70

W. Zimmer

D-90

E. J. Ferrari
L. R. Jeffery
A. K. Kamal
B. C. Pierstorff

D-91

G. Berk
J. M. Ruddy

D-97

R. Alan
W. T. Brandon (3)
P. F. Christopher
P. D. Engels
W. D. Glenn
J. M. Gutwein
E. Rotholz
R. M. Snow

PROJECT

NASA Lewis Research Center
21000 Brookpark Road
Cleveland, OH 44135

J. O. Rotnem
W. G. Kress
Library (2)
Report Control Office

EXTERNAL

NASA Scientific and Technical
Information Facility
P.O. Box 8757
Balt./Wash. International Airport
MD 21240

Accessioning Dept.

AFAPL/DO
Wright Patterson AFB, OH 45433

E. E. Bailey

DCA/MSO
Defense Communications Agency
Code 800
Washington, D.C. 20305

P. C. Jain

Lincoln Laboratory, MIT
244 Wood Street
Lexington, MA 02173

C. W. Niessen

The Aerospace Corporation
P.O. Box 92957
Los Angeles, CA 90009

F. E. Bond

DISTRIBUTION LIST (Concluded)

Signatron, Inc.
12 Hartwell Avenue
Lexington, MA 02173

B. E. White